

Direction des bibliothèques

AVIS

Ce document a été numérisé par la Division de la gestion des documents et des archives de l'Université de Montréal.

L'auteur a autorisé l'Université de Montréal à reproduire et diffuser, en totalité ou en partie, par quelque moyen que ce soit et sur quelque support que ce soit, et exclusivement à des fins non lucratives d'enseignement et de recherche, des copies de ce mémoire ou de cette thèse.

L'auteur et les coauteurs le cas échéant conservent la propriété du droit d'auteur et des droits moraux qui protègent ce document. Ni la thèse ou le mémoire, ni des extraits substantiels de ce document, ne doivent être imprimés ou autrement reproduits sans l'autorisation de l'auteur.

Afin de se conformer à la Loi canadienne sur la protection des renseignements personnels, quelques formulaires secondaires, coordonnées ou signatures intégrées au texte ont pu être enlevés de ce document. Bien que cela ait pu affecter la pagination, il n'y a aucun contenu manquant.

NOTICE

This document was digitized by the Records Management & Archives Division of Université de Montréal.

The author of this thesis or dissertation has granted a nonexclusive license allowing Université de Montréal to reproduce and publish the document, in part or in whole, and in any format, solely for noncommercial educational and research purposes.

The author and co-authors if applicable retain copyright ownership and moral rights in this document. Neither the whole thesis or dissertation, nor substantial extracts from it, may be printed or otherwise reproduced without the author's permission.

In compliance with the Canadian Privacy Act some supporting forms, contact information or signatures may have been removed from the document. While this may affect the document page count, it does not represent any loss of content from the document.

Université de Montréal

Faculté de pharmacie
Université de Montréal
Grade octroyé le:

4-06-2009

**Pharmacometrics of neuromuscular blocking agents in anesthetized patients and
animals: impact of dose and intravascular mixing phase**

par

Chunlin Chen

Faculté de pharmacie

Thèse présentée à la Faculté des études supérieures
en vue de l'obtention du grade de Philosophiae Doctor
en sciences pharmaceutiques
option pharmacologie

December 2008

© Chunlin Chen, 2008

Université de Montréal
Faculté des études supérieures

Cette thèse intitulée :

Pharmacometrics of neuromuscular blocking agents in anesthetized patients and animals: impact of dose and intravascular mixing phase

présentée par :
Chunlin Chen

a été évaluée par un jury composé des personnes suivantes :

Dr. Julie Ducharme	Président-rapporteur
Dr. France Varin	Directeur de recherche
Dr. Line Labbé	Co-directeur
Dr François Girard	Membre du jury
Dr. Patrick Poulin	Examineur externe
Dr. Sophie Cuvilliez	Représentante du doyen de la FES

Résumé

L'analyse pharmacocinétique/pharmacodynamique (PK/PD) est maintenant universellement reconnue comme un atout en développement du médicament, même si son application majeure demeure en pratique clinique. Les médicaments anesthésiques sont le plus souvent administrés sous forme de bolus intraveineux et par conséquent, sont susceptibles de présenter un début d'action très rapide et une faible marge de sécurité. La concentration dans le compartiment effet correspondant à 50 % de l'effet maximal (EC_{50}) et la constante d'équilibre avec le compartiment effet (k_{e0}) sont deux paramètres-clés qui permettent d'ajuster de manière précise la dose requise pour obtenir l'effet ciblé chez un patient donné. Cependant, leur estimation exacte dépend grandement d'une caractérisation adéquate de la phase de mélange intravasculaire (IVM) lorsque l'effet du médicament survient durant les deux premières minutes suivant l'injection.

Notre laboratoire a déjà rapporté une différence dose-dépendante dans les paramètres PK/PD du cisatracurium, un bloqueur neuromusculaire non dépolarisant, au cours d'études à doses croissantes qui comportaient l'administration d'une dose communément utilisée pour l'intubation (0.075 mg/kg) et des doses plus élevées (jusqu'à 0.3 mg/kg) chez des patients anesthésiés. Des changements significatifs au niveau des EC_{50} et k_{e0} ont été observés. Cependant, l'interprétation de ces résultats demeurait incertaine parce que la phase IVM n'avait pas été caractérisée de manière adéquate durant l'installation de l'effet.

Le premier objectif de cette thèse était de conduire un protocole rigoureusement contrôlé chez le chien anesthésié afin de vérifier si la relation concentration-effet était dose-dépendante. Dans cette étude expérimentale, les changements observés au niveau des paramètres PK/PD après une dose très élevée étaient comparables à ceux rapportés au cours de l'étude clinique et pourraient être attribués à des facteurs physiologiques tels qu'une diffusion restreinte au niveau de la jonction neuromusculaire ou à un artefact de modélisation. Nos résultats indiquent que les paramètres PK/PD obtenus après une dose d'intubation seraient plus fiables lorsqu'on utilise un modèle classique.

Le deuxième objectif était de vérifier si les corrélations *in vitro/in vivo* observées chez l'humain pour le cisatracurium s'appliquaient également chez le chien. L'élimination Hofmann, une voie d'élimination indépendante des capacités intrinsèques des organes d'élimination qui survient au niveau du plasma et des tissus, est en grande partie responsable de l'élimination globale du cisatracurium chez l'humain. Par conséquent, un modèle PK classique qui assumerait une élimination à partir du compartiment central uniquement n'est pas approprié. Chez l'humain, la vitesse d'élimination du cisatracurium à partir du compartiment périphérique est généralement tenue en compte au niveau des modèles PK en substituant sa valeur par la vitesse de dégradation *in vitro* mesurée dans le plasma. Chez le chien, la vitesse d'élimination *in vivo* s'est révélée être de deux fois plus rapide que celle mesurée *in vitro* alors que ces deux vitesses sont semblables chez l'humain. Ces résultats font ressortir les risques inhérents à toute extrapolation entre espèces. Une excrétion biliaire accrue et/ou la présence d'une sécrétion rénale chez le chien sont parmi les mécanismes potentiels qui doivent être explorés.

Notre dernier objectif était de développer un modèle PK qui permettrait une caractérisation précise de la phase IVM pour la plupart des bloqueurs neuromusculaires. Il est bien reconnu que le fait de supposer une entrée instantanée dans le compartiment central après un bolus intraveineux résultera en une caractérisation inadéquate des deux premières minutes. Selon la demi-vie d'élimination du médicament, il pourra en découler un biais négligeable ou important dans l'estimation des paramètres PK importants. Pour cette étude, nous avons utilisé les données recueillies pendant la phase IVM lors d'études cliniques antérieures qui comportaient l'administration d'une dose d'intubation d'atracurium, doxacurium, vécuronium et succinylcholine, sous forme d'un bolus intraveineux. Une fonction d'entrée à distribution de Gauss inversée combinée à un modèle compartimental s'est avérée capable de permettre un lissage adéquat des concentrations plasmatiques obtenues durant la phase IVM et toute la durée de la collecte. Pour tous les bloqueurs neuromusculaires, les estimés moyens du volume apparent de distribution central ont approximé le volume intravasculaire alors que le volume apparent de distribution total ne dépassait pas l'espace extracellulaire. Chez les patients anesthésiés en santé, le temps requis pour atteindre les concentrations maximales ne variait pas de manière significative selon le bloqueur neuromusculaire. Par conséquent, le profil pharmacocinétique immédiat suivant l'injection du bloqueur neuromusculaire ne dépendrait pas du médicament administré mais plutôt de facteurs circulatoires tels que le débit cardiaque.

Mots-clés : Bloqueurs neuromusculaires, cisatracurium, dose-dépendance, phase de mélange intravasculaire, élimination périphérique, pharmacométrie, anesthésie, patients, chiens.

Abstract

Pharmacokinetic/pharmacodynamic (PK/PD) analysis is now widely recognized as an asset in drug development, although its main application remains in clinical practice. Anesthetic drugs are mostly given as intravenous bolus and thus are prone to exhibit a very rapid onset of effect and a low margin of safety. The effect compartment concentration corresponding to 50 % of maximum effect (EC_{50}) and the effect compartment equilibration rate constant (k_{e0}) are key PK/PD parameters that will enable to precisely adjust the dose required to obtain the targeted effect in a given patient. However, its accurate estimation will highly depend on the adequate characterization of the intravascular mixing phase (IVM) when onset of effect occurs during the two first minutes after injection.

Our laboratory has previously reported a dose-dependent change in the PK/PD parameters of cisatracurium, a nondepolarising neuromuscular blocking agent, in a dose-ranging study where a dose commonly used for intubation (0.075 mg/kg) and higher doses (0.3 mg/kg) were administered in anesthetized patients. Significant changes in the EC_{50} (increase) and k_{e0} (decrease) were observed. However, the interpretation of this finding remained unclear because the IVM phase was not adequately characterized during onset of effect.

The first objective of this thesis was to conduct a rigorously controlled protocol in anesthetized dogs to verify if the concentration-effect relationship of cisatracurium is dose-dependent. In this experimental study, changes in PK/PD parameters at very high bolus doses were in agreement with those reported in the clinical study and could be

attributed either to physiological factors such as hindered diffusion at the neuromuscular junction or to modeling artefact. Our results indicate that, when using classic PK/PD models, parameters obtained after an intubating dose of cisatracurium would be more reliable.

The second objective was to verify if the *in vitro* / *in vivo* correlations observed for cisatracurium in humans also applied for dogs. Hofmann elimination, an organ and enzyme-independent elimination pathway occurring in plasma as well as tissues, is mostly responsible for the overall elimination of cisatracurium in humans. Thus, a classic two compartment PK model that assumes elimination only from the central compartment is not appropriate. In humans, peripheral elimination is usually accounted for in the PK models by fixing its value to the *in vitro* degradation rate measured in plasma. In dogs, cisatracurium *in vivo* elimination rate constant was almost twofold faster than its corresponding *in vitro* rate while both rates are similar in humans. This finding re-emphasizes the risk of interspecies extrapolation. Increased biliary excretion and/or presence of renal secretion in dogs are potential mechanisms that need to be further explored.

Our final objective was to develop a PK model that would enable a precise characterization of the IVM phase for most neuromuscular blocking agents. It is well recognized assuming an instantaneous input in the central compartment after an intravenous bolus will result in model misspecification. Depending on the drug terminal half-life, it will result in subtle too large errors in the estimation of major PK parameters. For this study, data collected during the IVM phase in four clinical studies after

administration of an intubating bolus dose of atracurium, doxacurium, vecuronium and succinylcholine were used. The Inverse Gaussian density input function combined with compartmental models proved to provide adequate adjustment to data points collected during both the IVM phase and overall plasma concentration-time profiles. For all neuromuscular blocking agents, mean estimates of apparent central volume of distribution closely approximated the intravascular volume while apparent total body distribution did not exceed the extracellular space. In otherwise healthy anesthetized patients, time to peak concentrations did not differ significantly between neuromuscular blocking agents. Thus, the early pharmacokinetic profile after NMBA injection does not depend on which specific drug is given, but most probably varies in function of circulatory factors such as cardiac output.

Keywords: Non depolarizing neuromuscular blocking agent, cisatracurium, dose-dependency, intravascular mixing phase, peripheral elimination, pharmacometrics, anesthesia, patients, dogs .

Table of Content

Résumé	iii
Abstract	vi
Table of Content	ix
List of Tables	xiii
List of Figures	xv
Acknowledgements	xx
Dedication	xxii
1. Neuromuscular pharmacology and physiology	3
1.1 Neuromuscular junction	3
1.1.1 Anatomy of neuromuscular junction	4
1.1.1.1 The presynaptic region	4
1.1.1.2 The synaptic space	5
1.1.1.3 The postsynaptic region	5
1.1.2 Physiology of neuromuscular transmission	7
1.1.3 Margin of safety of neuromuscular transmission	9
1.2 Monitoring of neuromuscular function	10
1.2.1 Methods of evaluating neuromuscular transmission	11
1.2.2 Site of stimulation	11
1.2.3 Stimulation patterns	12
1.2.3.1 Single twitch stimulation	12
1.2.3.2 Train-of-four stimulation	12
1.3 Classification of neuromuscular blocking agents	14
1.3.1 Depolarizing neuromuscular blocking agents	14
1.3.1.1 Mechanism of action	14
1.3.1.1.1 Desensitization block	15
1.3.1.1.2 Phase II block	15
1.3.1.2 Pharmacokinetics	16
1.3.1.3 Pharmacodynamics	17
1.3.2 Nondepolarizing neuromuscular blocking agents	18
1.3.2.1 Mechanism of action	18

1.3.2.1.1 Competitive mechanisms of neuromuscular block	18
1.3.2.1.2 Noncompetitive mechanisms of neuromuscular block	19
1.3.2.2 Pharmacokinetics	20
1.3.2.3 Pharmacodynamics	23
1.3.2.2.1 Factors affecting the onset of neuromuscular blockade	25
1.3.2.2.2 Factors affecting the duration of neuromuscular blockade	27
2. Design NMBAs pharmacokinetic/pharmacodynamic study	29
3. Pharmacokinetic and pharmacodynamic modeling of NMBAs	32
3.1 Individually based pharmacokinetic/pharmacodynamic analysis	32
3.1.1 Individually based pharmacokinetic models	32
3.1.1.1 Noncompartmental pharmacokinetic models	32
3.1.1.3 Recirculatory pharmacokinetic models	36
3.1.2 Individually-based pharmacokinetic/pharmacodynamic models	37
3.1.2.1 Parametric PK/PD models	37
3.1.2.2 Nonparametric PK/PD models	38
3.2 Population-based pharmacokinetic/pharmacodynamic analysis	40
3.2.1 Standard two-stage approach	41
3.2.2 The mixed effect modeling approach	42
3.2.2.1 Model definition	44
3.2.2.1.1 Base model development	44
3.2.2.1.1.1. Structure of the PK/PD model	44
3.2.2.1.1.2. Inter-individual variability	45
3.2.2.1.1.3. Intra-individual variability	46
3.2.2.1.1.4. Inter-occasion variability	47
3.2.2.1.2 Covariate model development	48
3.2.2.1.3 Estimation method	52
3.2.2.1.4 Model building criteria	54
3.2.2.1.5 Model Validation	54
4. Interspecies extrapolation	56
4.1 Physiological models	56
4.2 Allometry	57

4.1.1 Interspecies scaling of clearance.....	58
4.1.1.1 Prediction of human renal clearance based on GFR values	59
4.1.1.2 Prediction of human clearance for biliary excretion of drugs	61
5. Cisatracurium	62
5.1 Chemical Structure.....	62
5.2 Pharmacokinetics	62
5.3 Pharmacodynamics	69
5.4 Pharmacokinetic-Pharmacodynamic Relationship.....	72
6. Research objectives	75
7. Manuscrit No. 1: Dose-dependency of PK/PD parameters after Intravenous bolus doses of cisatracurium	76
8. Manuscrit No. 2: Studies on the pharmacokinetics of cisatracurium in anesthetized dogs: <i>In vitro- In vivo</i> correlations.....	117
9. Manuscrit No. 3: Modeling of the Intravascular Mixing Phase of Neuromuscular Blocking Agents Following Intravenous Bolus Injection.....	142
10. Discussion	171
10.1 Dose-dependency of PK/PD parameters after intravenous bolus doses of cisatracurium.....	171
10.2 Pharmacokinetics of cisatracurium in anesthetized dogs: <i>In vitro-In vivo</i> correlations.....	175
10.3 Modeling of the intravascular mixing phase of neuromuscular blocking agents following intravenous bolus injection.....	179
11. Conclusion.....	182
Reference	184
APPENDIX I	193
APPENDIX II	194

List of Tables

Table 1. Nondepolarizing muscle relaxants pharmacokinetic parameters.....	22
Table 2. Neuromuscular blocking agents pharmacodynamic parameters.....	24
Table 3. Changes in estimated apparent volume of distribution of model drugs according to basic assumptions made during PK modeling.....	35
Table 4. Cisatracurium pharmacokinetic parameters.....	66
Table 5. Cisatracurium pharmacodynamic parameters.....	71
Table 6. Cisatracurium pharmacokinetic/pharmacodynamic parameters.....	74

Manuscript No. 1

Table 1. Physiological parameters during baseline and at onset time in pentobarbital anaesthetized dogs after sequential administration of two doses of cisatracurium	102
Table 2. Study time flow.	103
Table 3. Pharmacodynamic parameters in pentobarbital anaesthetized dogs after sequential administration of two doses of cisatracurium.	104
Table 4. Pharmacokinetic parameters in pentobarbital anaesthetized dogs after sequential administration of two doses of cisatracurium.	105
Table 5. NONMEM Objective Function Values (-2 log Likelihood) obtained during stepwise exploration of dose impact on PK/PD parameters.....	106
Table 6. PK/PD parameters in pentobarbital anaesthetized dogs after sequential administration of two doses of cisatracurium.....	107

Manuscript No. 2

Table 1. Exit-site-independent pharmacokinetic parameters of cisatracurium in pentobarbital anesthetized dogs.....	136
Table 2. Exit-site-dependent pharmacokinetic parameters of cisatracurium in pentobarbital anesthetized dogs.....	137
Table 3. Comparison of cisatracurium pharmacokinetic parameters in humans and dogs...	

.....138

Manuscrit No. 3

Table 1. Patient demographic data and anesthetic procedure for doxacurium,
vecuronium, atracurium and succinylcholine 161

Table 2. Mean doxacurium, vecuronium, atracurium and succinylcholine
pharmacokinetic parameters 162

List of Figures

Figure 1. Anatomical structure of the neuromuscular junction.....	3
Figure 2. Structure of the motor endplate nicotinic acetylcholine receptor in side view (left) and plan view (right)	7
Figure 3. Margin of safety of neuromuscular transmission	10
Figure 4. Effects of neuromuscular blocking agents on the single-twitch and train-of- four response.	13
Figure 5. Example of an empirical 2-compartment pharmacokinetic model.....	34
Figure 6. Structural formula of cisatracurium besylate.....	62
Figure 7. Proposed metabolic elimination pathways for cisatracurium besylate in human plasma.	64

Manuscript No. 1

Figure 1. Mean dose-normalized cisatracurium concentrations <i>versus</i> time for pentobarbital anaesthetized dogs after a dose of 0.15 mg kg ⁻¹ (black triangles) and 0.6 mg kg ⁻¹ (white circles).....	109
Figure 2. Individual mean dose-normalized cisatracurium plasma concentrations for the first minute after administration of 0.15 mg kg ⁻¹ (panel A) and 0.6 mg kg ⁻¹ (panel B) to pentobarbital anaesthetized dogs.....	110
Figure 3. Mean dose-normalized cisatracurium effect compartment concentrations <i>versus</i> time after a dose of 0.15 mg kg ⁻¹ (black triangles) and 0.6 mg k ⁻¹ (white ircles).111	111
Figure 4. Hysteresis curves (panel A) and Sigmoid Emax curves (panel B) derived for dog #1. 0.15 mg kg ⁻¹ dose (dashed line) and 0.6mg kg ⁻¹ dose (solid line).....	112
Figure 5. Collapsed hysteresis curves for a low dose (panel A) and high dose (panel B) for dog #1.....	113
Figure 6. Intraindividual comparison of PK/PD parameters obtained for each dose of cisatracurium.....	114
Figure 7. Temporal profiling of observed (black circles) <i>vs</i> simulated effect (solid line) after an i.v. bolus dose of 6 x ED ₉₅ of cisatracurium.....	115
Figure 8. Temporal profiling of observed (black circles) <i>vs</i> predicted effect (solid line) after an i.v. bolus dose of 1.5 x ED ₉₅ of cisatracurium.....	116

Manuscript No. 2

Figure1. Individual dose-normalized cisatracurium plasma concentration-time curves.140

Figure2. Linear regression of the temperature versus the *in vitro* speed of degradation

($K_{in vitro}$).....141

Manuscript No. 3

Figure 1. Schematic presentation of the proposed pharmacokinetic model.....165

Figure 2. Individual dose-normalized doxacurium, vecuronium, atracurium and succinylcholine plasma concentrations versus time curves in anesthetized patients.....166

Figure 3. Individual predicted (solid line) and observed (closed circle) dose-normalized doxacurium (A), vecuronium (B), atracurium (C) and succinylcholine (D) plasma concentrations versus time curves in anesthetized patients.....167

Figure 4. Predicted (solid line) and observed (closed circle) mean dose-normalized doxacurium (A), vecuronium (B), atracurium (C) and succinylcholine (D) plasma concentrations versus time curves in anesthetized patients.....168

Figure 5. Predicted (solid line) and observed (closed circle) individual dose-normalized succinylcholine plasma concentrations versus time curves in anesthetized patients using single (A) or two (B) IG density functions.....169

Figure 6. Simulated (solid line) and observed (closed circle) midazolam dose-normalized plasma concentration versus time curves obtained in two patients using mean NMBAs parameters (A and B) or optimized values (C and D) for the IG input function.....170

List of Abbreviations

ACh	Acetylcholine
AChE	Acetylcholinesterase
AChR	Acetylcholine receptors
AIC	Akaike Information Criterion
ASA	American Society of Anesthesiologists
AUC	Area under the plasma concentration-time curve
BrW	Brain weight
C_e	Drug concentration in effect compartment
C_p	Plasma concentration
CL	Total body clearance
C_{max}	Maximum plasma concentration
E	Effect
EC ₅₀	Effect compartment concentration of drug at 50% effect
ED ₉₅	95% effective dose
F_u	Un-bound fraction of drug in plasma
GAE	General allometric equation
GFR	Glomerular filtration rate
	The slope factor of sigmoid curve
HPLC	High Performance Liquid Chromatography
ICG	Indocyanine green
IV	Intravenous

IIV	Inter individual variability
IOV	Inter occasion variability
k_{e0}	Equilibrium rate constant between plasma concentration and effect
$k_{in\ vitro}$	The <i>rate</i> of <i>in vitro</i> disappearance
k_{10}	Elimination rate constant for the first compartment
k_{12}	Transfer rate constant from the first to the second compartment
k_{21}	Transfer rate constant from the second to the first compartment
k_{20}	Elimination rate constant for the second compartment
k_{e0}	Equilibrium rate constant between plasma concentration and effect compartment
LBF	Liver blood flow
MEM	Mixed effect modeling
MI	Multiple imputation
MLBF	Monkey liver blood flow
MLP	Maximum life-span potential
N_2O	Nitrous oxide
nm	Nanometer
NMJ	Neuromuscular Junction
PD	Pharmacodynamics
OBJ	Objective function
OFV	Objective function value
PK	Pharmacokinetics
PK/PD	Pharmacokinetics-Pharmacodynamics

R _{tot}	Total concentration of receptors
ROE	Rule of exponents
t	Time
T _{1/2}	Elimination rate constant half-life
TOF	Train-of-four stimulation
TS	Two stage
UDGPT	Uridine diphosphate glucuronyltransferase
URM	Unbound receptor model
V ₁	Apparent volume of distribution in the central compartment
V ₂	Apparent volume of distribution in the peripheral compartment
V _{d_{ss}}	Apparent volume of distribution at steady state

Acknowledgements

First and foremost I would like to extend my deep appreciation and gratitude to the people who made this work possible, have encouraged and helped me over the years.

I would like to sincerely thank my advisor, Dr. France Varin who gave me the opportunity to work in her laboratory and for guidance on my thesis project. Her limitless experience in Pharmacokinetic-Pharmacodynamic modeling and her zeal to succeed have provided me with an invaluable educational experience. I would like also to my deepest appreciation and gratitude to my codirector, Dr Line Labbé, for her guidance throughout my doctoral research.

I thank Drs. Fahima Nekka and Dr Robert Tardif, who gave me such needed advice and encouragement for the formation of the ideas and aiding in successful completion of my thesis. I would like to thank Dr. Nobuharu Yamaguchi and Ms. Sanae Yamaguchi for their help with the animal experiments. I would like also to my appreciation to my thesis advisory committee, Dr François Girard and Dr Patrick Poulin, who reviewed my thesis.

The value of the special relationships I have experienced in my areas here is beyond estimation. The caring and friendly nature of the people in the lab (Sybil Robertson, Francois Gaudreault, Anne Nguyen Quynh-Nhu) will always be greatly appreciated. I would also like to heartfelt thank to Ms. Johanne Couture for her superb technical support, as well as keeping the lab running smoothly.

Thanks to my family, who always believed in me, supported me and served as my grounding force. Thank you, my Mom and Dad, for teaching me patience and fairness. Thanks to my wife, for her love, understanding, sacrifices and continuing support through the entire study period.

I would like to thank all the Faculty, staff and graduate students of Faculté de Pharmacie for making these years at the Université de Montréal an exceptional experience for me.

Dedication

This Thesis is dedicated to:

Professor France Varin:

Preface

The delay in equilibration between drug concentration in plasma and biophase is, for anesthetics, clinically significant and worth characterizing. (Beaufort et al. 1999; Shafer et al. 1989; Swerdlow and Holley 1987) Pharmacokinetic/pharmacodynamic (PK/PD) modeling is the mathematical description of the relationship between the pharmacokinetics (plasma concentration *vs* time profile) and pharmacodynamics (observed effect *vs* time profile) of a drug. It allows characterization of the time-dependent aspects of the equilibrium between plasma concentration and effect under non-steady-conditions. (Sheiner et al. 1979)

Intravenous anesthesia is concerned with proper use of drugs to achieve the desired effects during the induction of anesthesia, during surgery, and in the early postoperative period. The main drug classes used during induction of general anesthesia are the hypnotics, the analgesics, and the neuromuscular blocking agents (NMBAs).

In the past two decades, the continuing emergence of PK/PD modeling gave some insight on the concentration-effect relationship of NMBAs and thereby helped the clinician in understanding the underlying mechanism of the physiological processes. The application of quantitative modeling in PK and PD enables the clinician to use rationally the anesthetics and, hence, to provide more benefit to patients undergoing anesthesia. (Gambus and Troconiz 2001)

The objectives of this thesis were to enhance knowledge and understanding of the impact of methodological factors during the establishment of the concentration-effect relationship of the neuromuscular blocking agents in anesthetized patients and animals.

Chapter 1 of this thesis gives an overview of neuromuscular pharmacology and physiology, including neuromuscular junction, monitoring of the neuromuscular function and classified neuromuscular blocking drugs. In Chapter 2, chemical structure, pharmacokinetics-pharmacodynamics previous reported studies of NMBAs are reviewed. Chapter 3 overviews the PK/PD model building strategies applied to neuromuscular blocking agents such as individual approach and population approach. In Chapter 4, different interspecies scaling approaches are described. Chapter 5 reviewed model drug (cisatracurium) chemical structure, pharmacokinetics/pharmacodynamics and reported studies. Chapter 6 described research objectives. The experimental work carried out is presented in the form of publications and manuscripts in Chapters 7 to 9 followed by an overall discussion in Chapter 10.

1. Neuromuscular pharmacology and physiology

1.1 Neuromuscular junction

Skeletal muscle contraction is a complex process, originating at the neuromuscular junction (NMJ). The NMJ is the chemical synapse that lies between the terminal ends of motor neuron and skeletal muscle fibers. The unique structure and functional organization of this synapse allows for the process of transmitting an electrical impulse from a motor axon to the muscle fiber it innervates. The NMJ consists of three basic components (Fig. 1): (a) the presynaptic region, consisting of a terminal branch of a motor axon (the nerve terminal) in which the neurotransmitter is synthesized, stored, and released; (b) the synaptic basal lamina that occupies the synaptic cleft; and (c) the postsynaptic membrane which contains the receptor for the neurotransmitter. (Meriggioli et al. 2004)

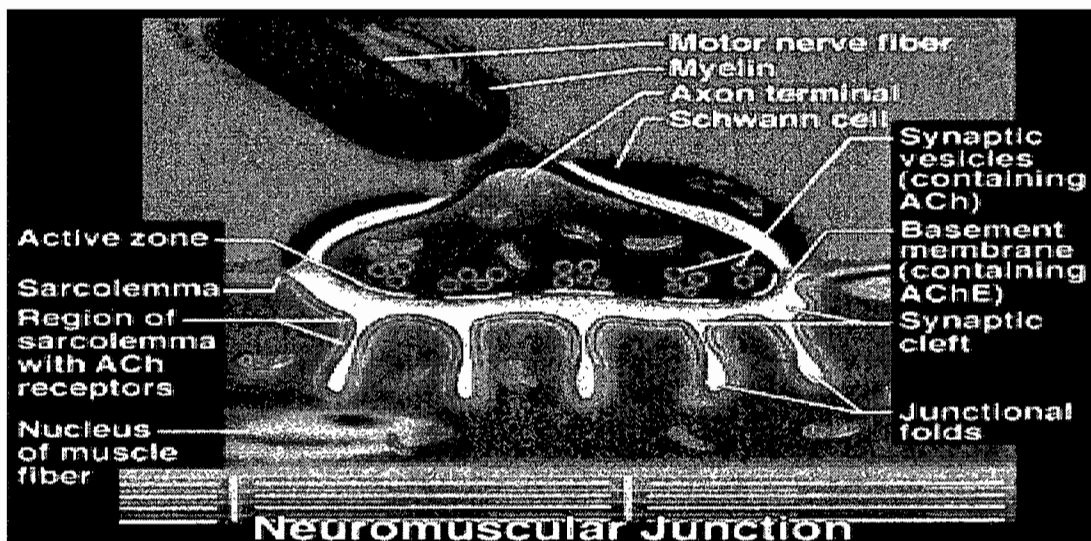


Figure 1. Anatomical structure of the neuromuscular junction

<http://abdellab.sunderland.ac.uk/Lectures/Pharmacology/ANSdoc/cholinergic10.html>

1.1.1 Anatomy of neuromuscular junction

1.1.1.1 The presynaptic region

The hallmark ultrastructural features of the nerve terminal are the synaptic vesicle, about 50 nm in diameter, and all proteins of the nerve terminal function directly or indirectly supporting synaptic vesicle function. (Hughes et al. 2006; Vincent 1992) The vesicles filled with acetylcholine (ACh) are clustered particularly within electron-dense regions of the cytoplasm adjacent to the presynaptic membrane. These “active zones”, opposite to the postsynaptic folds, are thought to be the sites of ACh release. There are about a thousand such active zones at each nerve ending. (Ceccarelli and Hurlbut 1980)

ACh is synthesized in the cytoplasm of the nerve terminal from acetyl CoA and choline in a reaction catalysed by the soluble enzyme choline acetyltransferase. (Tucek 1984) It is packaged in the vesicles and released into the synaptic cleft upon arrival of a nerve impulse. Each vesicle contains from nearly 8 000 to 13 000 ACh molecules, termed the “quanta”. Release of ACh into the synaptic cleft by a nerve stimulus requires calcium; the process is called stimulus-secretion coupling. Calcium influx occurs through voltage-gated calcium channels that are located near the release sites. The entry of calcium triggers the fusion of the vesicle with the presynaptic nerve cell membrane. (Protti et al. 1996) Subsequently, the contents of the vesicles are released into the synaptic cleft by exocytosis. Some of the ACh molecules bind to the ACh receptors (AChRs) on the postsynaptic membrane while the rest is rapidly hydrolysed by the acetylcholinesterase (AChE) present in the synaptic cleft. The choline thus formed is taken back up into the

terminal by a high-affinity uptake system, making it available for resynthesis of ACh. (Jahn and Sudhof 1994; Vincent and Wray 1992).

1.1.1.2 The synaptic space

The synaptic space is located between the presynaptic nerve terminal membrane and the postsynaptic muscle membrane. It consists of a primary cleft and a number of secondary clefts. The primary cleft is the space that separates presynaptic nerve membrane from the postsynaptic junctional folds. It is approximately 50 nm wide and its length is equal to the presynaptic basal membrane. It has no lateral boundaries and, therefore, it communicates with the extracellular space. ACh is released into this space before it acts on the AChR. The short expanse of the primary synaptic cleft allows AChRs to reside very near the ACh release sites so that diffusion time across the cleft is short. The secondary cleft is the space between the junctional folds on the postsynaptic membrane and communicates with the primary cleft. Acetylcholinesterase is most highly concentrated in the secondary cleft. It hydrolyses ACh to terminate neuromuscular transmission. (Meriggioli et al. 2004)

1.1.1.3 The postsynaptic region

The postsynaptic region is a specialized area of the muscle fiber membrane that is also known as the endplate. The motor endplate membrane is thrown into folds (secondary cleft), with the AChRs organized in discrete clusters located on the shoulders of those folds. (Daniel 1975) These postsynaptic junctional folds increase its surface area by up to eight times. (Vincent and Wray 1992) Because the junction folds are separated by the

secondary synaptic clefts, this organization also increases the volume of the synaptic space. The density of the folding is much more extensive at the endplate compared to the extra junctional membrane. The vast majority of AChRs are concentrated on the crests of the junction folds at a density of approximately 10,000 sites/ μm^2 , each of them is inserted through the phospholipids bilayer of the motor endplate membrane. (Meriggioli et al. 2004)

On closer examination of motor endplate, nicotinic membranes of AChRs are cylindrical, membrane-spanning glycoproteins with a central cation channel. (Fig. 2) Each functional molecule contains five homologous subunits in the mammalian adult: two α subunits (MW = 40,000 Da) which have the same amino acid sequence, one β subunit, one δ subunit, and one ϵ subunit. The receptor found early in fetal development and after denervation has a γ subunit replacing the ϵ subunit. (Mishina M 1986) Each of the α subunits carries a single acetylcholine binding region on its extracellular surface. They also bind other agonists, toxins, (Lee 1972) and reversible antagonists, such as nondepolarizing neuromuscular blocking drugs (Kistler 1982). Although the two α subunits have the same amino acid sequence, they reside in different environments. One α subunit has the β and the ϵ adjacent to it, whereas the other is surrounded by the δ and the ϵ subunits. This results in the properties of the two sites being different. (Evers and Mervyn 2004)

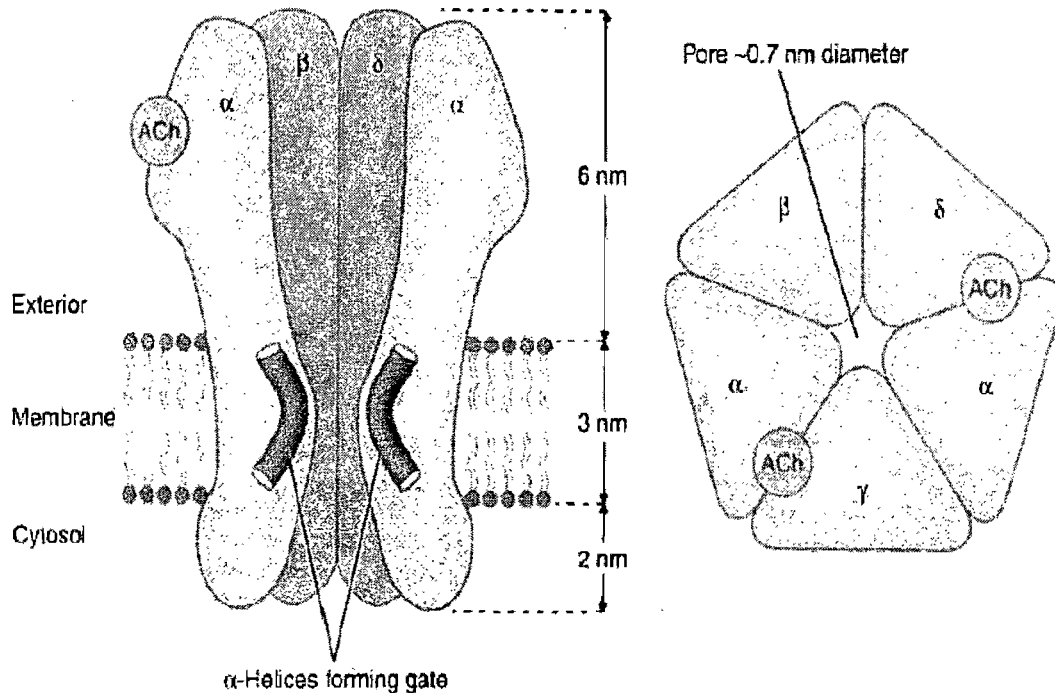


Figure 2. Structure of the motor endplate nicotinic acetylcholine receptor in side view (left) and plan view (right)

(Rang 2003)

When two ACh (or other agonist) molecules simultaneously attach to ACh binding sites on the α subunits, one on each, which produces conformational changes, the channel between the receptors is opened for a very short period, about 1 ms. (Guy 1984) This allows movement of cations such as Na^+ , K^+ , Ca^+ and Mg^+ along their concentration gradients. The main change is influx of Na^+ ions, the endplate current, followed by efflux of K^+ ions. (Aitkenhead 2007)

1.1.2 Physiology of neuromuscular transmission

ACh is released from the presynaptic membrane either spontaneously or as a result of a nerve impulse. Released ACh diffuses across the synaptic cleft and binds to the two α

subunits of the nicotinic cholinergic receptor on the postsynaptic membrane of the skeletal muscle fiber. The remaining three subunits (β , δ and ϵ) of the nicotinic receptor influence the conformational changes induced by ACh binding to the two α subunits. As explained above, a change in the membrane permeability to ions causes a decline in the membrane resting potential, producing skeletal muscle contraction. This change in the membrane resting potential occurs due to sufficient movement of Na^+ to reduce intracellular negativity (depolarization). As the action potential is propagated, Ca^{2+} is released from the sarcoplasmic reticulum that, in return, results in activation of myosin-adenosine triphosphate and excitation contraction coupling of the myofilaments (i.e., muscle contraction). (Evers and Mervyn 2004)

Spontaneous release of ACh involves contents from a single vesicle, giving rise to a low amplitude depolarisation of the muscle membrane miniature endplate potentials. Following a nerve impulse, a large number of vesicles release ACh in “quanta”. This produces a large depolarisation, “endplate potential” (EPP) of the muscle membrane, leading to a propagated action potential and muscle contraction. During repeated nerve stimulations, the amount of ACh released progressively decreases after the initial few stimuli, the so-called “synaptic rundown”. Under normal conditions, the amplitude of the EPP is more than necessary to trigger an action potential. Several factors may influence its amplitude including the amount of ACh released, and the number and integrity of the AChRs, among others.(Vincent et al. 2000)

1.1.3 Margin of safety of neuromuscular transmission

The existence of a safety margin of neuromuscular transmission was firstly pointed out by Paton and Waud in 1967, (Paton and Waud 1967) who reported the existence of high density of receptors at the neuromuscular junction. Under normal conditions the amount of ACh released is abundant, and the number of AChRs activated is much larger than the number needed to initiate a muscle action potential. (Paton and Waud 1967) Approximately 75% of the AChRs must be blocked by an antagonist (neuromuscular blocker) before any effect (fade) can be seen during the administration of neuromuscular blockers. At least 95% receptor occupancy is necessary for complete suppression of twitch. (Booij 1997) There is thus a large margin of safety both in the prejunctional (AChR activation) and postjunctional components of neuromuscular blocking agents. (Paton and Waud 1967)

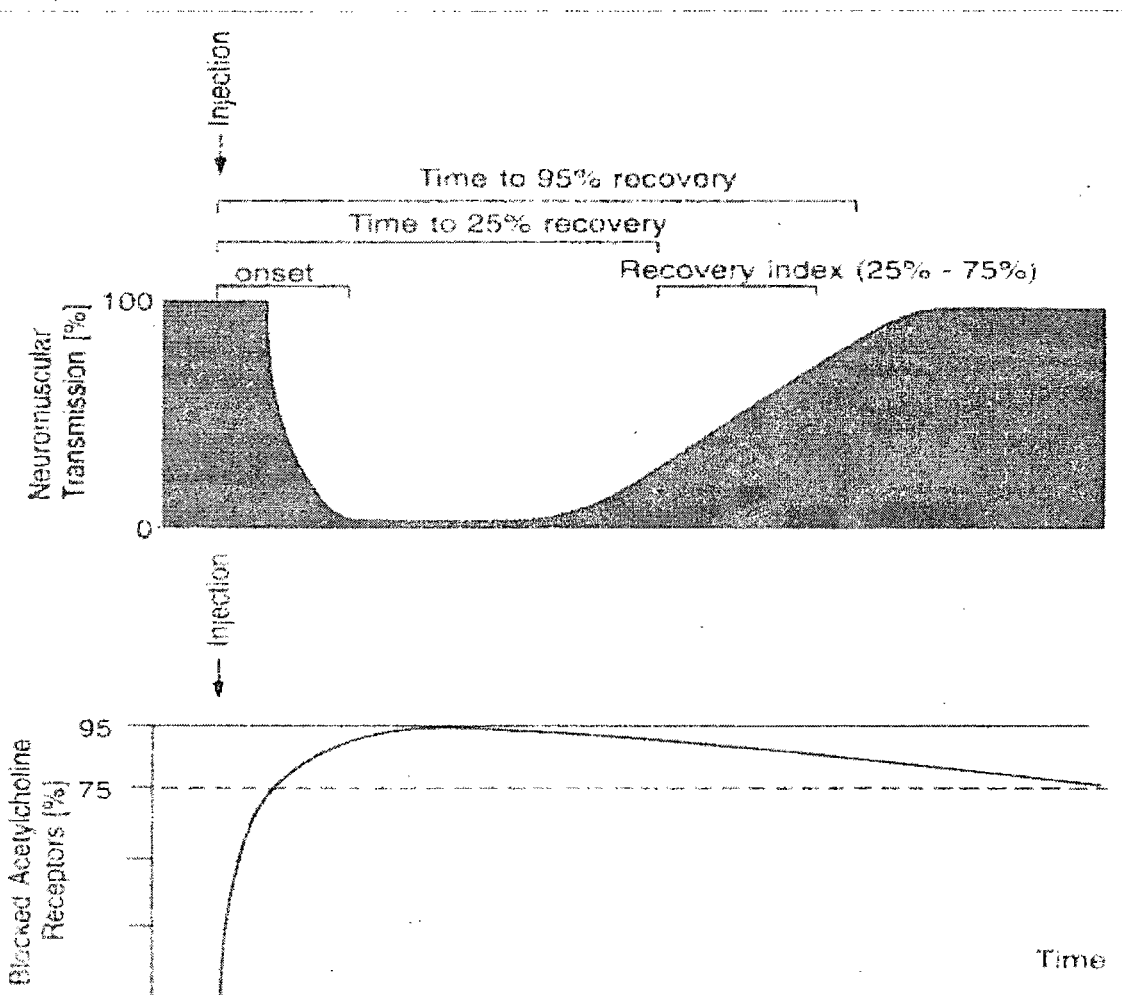


Figure 3. Margin of safety of neuromuscular transmission

(Evers and Mervyn 2004)

1.2 Monitoring of neuromuscular function

The “therapeutic window” of NMBAs is narrow because of the high margin of safety of the neuromuscular junction. Moreover, the response to the same dose of relaxant is quite variable and unpredictable in the population at large. Therefore, the degree of neuromuscular blockade must be assessed frequently and carefully. (Bevan 1988)

1.2.1 Methods of evaluating neuromuscular transmission

Compared to tactile or visual appreciation of the response of the muscle, quantitative monitoring is the most reliable one. It can be done with electromyography (EMG), mechanomyography (MMG) and accelerography. There is a difference in the response obtained with these different methods of quantitation of the response. (Engbaek and Roed 1992; Kopman 1985) With nondepolarizers the MMG is more depressed than the EMG; with succinylcholine the opposite is seen. (Harper et al. 1986; Katz 1973) With accelerography there is, in comparison to MMG, an underestimation during onset of block and an overestimation during recovery. (Harper et al. 1994) Both EMG and MMG are influenced by temperature. (Smith and Booth 1994)

1.2.2 Site of stimulation

The choice of the site of neurostimulation depends on several factors. In a practical sense, however, accessibility to a superficial nerve intraoperatively is most important. In the evaluation of a neuromuscular blockade, stimulation of the ulnar or median nerve near the wrist is especially appropriate. Not only are these nerves most of the time easily accessible for stimulation, but also a good correlation exists between the response of the muscle innervated by them, and the ability of the patient to breath spontaneously. Also different muscle groups have different sensitivities to neuromuscular blocking agents, therefore; results obtained for one muscle cannot be extrapolated automatically to other muscles. (Donati et al. 1990)

1.2.3 Stimulation patterns

There are many available patterns of neurostimulation, such as single twitch, train-of-four, tetanus, and double burst. The selection of patterns of nerve stimulation depends on the particular clinical setting. The most often used stimulation patterns will be described.

1.2.3.1 Single twitch stimulation

An electrical pulse is delivered at 0.1-0.15 Hz and the ratio of the evoked twitch compared with that before muscle relaxation gives a crude indication of neuromuscular blockade (Fig. 3). When 75% of the AChRs on the postsynaptic membrane of the neuromuscular junction are occupied by a NMBA, twitch magnitude starts to decrease. When there is 100% drug occupation, no twitch is elicited.

1.2.3.2 Train-of-four stimulation

The train-of-four stimulation (TOF) is the most frequently used stimulation pattern. Four stimuli are given at a frequency of 2 Hz, potentially eliciting 4 twitches (T1–T4). The ratio T4:T1 indicates the degree of neuromuscular block. Non-depolarizing NMBAs produce a decrease in magnitude of the first twitch compared with a pre-relaxant stimulus, and a progressive reduction in magnitude of T1–T4. The number of elicited twitches indicates the degree of receptor occupancy. Disappearance of T4, T3, T2, T1 corresponds to 75%, 80%, 90% and 100% occupancy. With recovery of neuromuscular function the twitches appear in the reverse order. Depolarizing NMBAs react differently to the peripheral nerve stimulation. They produce equal but reduced twitches in response

to single twitch and TOF stimulation (the T4:T1 is 1), reduced but sustained contraction with tetanic stimulation, but do not demonstrate either tetanic fade or post-tetanic facilitation.

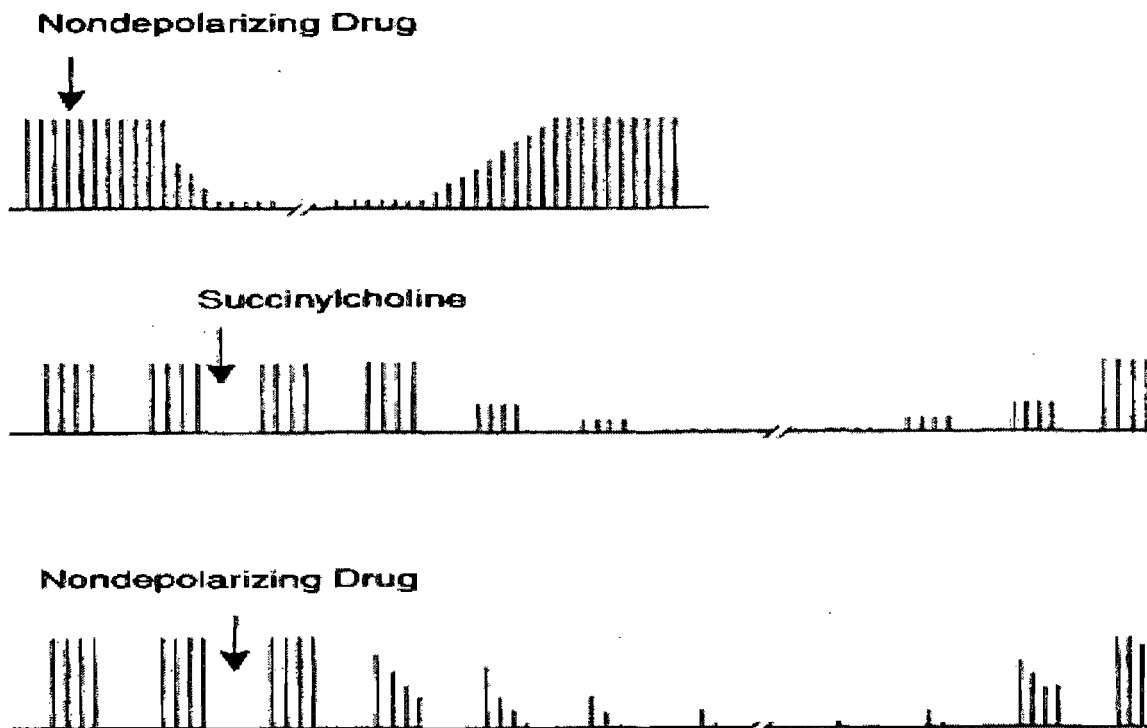


Figure 4. Effects of neuromuscular blocking agents on the single-twitch and train-of-four response.

The top tracing depicts the effect of a nondepolarizing neuromuscular blocking agent on the single-twitch response. A depolarizing agent (succinylcholine) would have the same effect on single-twitch response. The middle tracing depicts the effect of succinylcholine on train-of-four response characterized by a similar decrease (no fade) in the magnitude of the four-twitch response. The lower tracing depicts the contrasting effects of a nondepolarizing agent on train-of-four responses characterized by a decrease in the magnitude of the four-twitch response. (Stoelting and Hillier 2006)

1.3 Classification of neuromuscular blocking agents

Analogous to ACh, all NMBAs have at least one quaternary nitrogen group ($N^+(CH_3)_3$) that binds to the α subunit of the nicotinic receptor. Many NMBAs (e.g. succinylcholine) contain two quaternary ammonium cations. These bisquaternary amines are more potent than monoquaternary amines (e.g. rocuronium), which have only one permanent quaternary cation and one tertiary amine. However, at physiological pH, and especially in acidic conditions, the tertiary amine can become protonated and therefore positively charged, increasing the potency of monoquaternary NMBAs. The two quaternary ammonium groups are separated by a bridging structure that is lipophilic and varies in size. The bridging structure varies with different series of NMBAs and is a major determinant of their potency.

According to the different mechanism of action, the neuromuscular blockers are classified as depolarizing or nondepolarizing.

1.3.1 Depolarizing neuromuscular blocking agents

1.3.1.1 Mechanism of action

Depolarizing drugs, such as succinylcholine, are agonists at AChRs. Succinylcholine consists of two ACh molecules joined through the acetate methyl groups. The two quaternary ammonium radicals, $N^+(CH_3)_3$, have the capacity to bind to each of the α units of the postsynaptic ACh receptor, altering its structural conformation and opening the ion channel, and act like ACh to depolarize the junction. (Aitkenhead 2007) Unlike ACh, which is instantly destroyed by AChE, the depolarizing agents are not susceptible

to hydrolysis by the AChE. They persist at high concentrations in the synaptic cleft. They remain attached to the receptor for a relatively longer time, providing a constant stimulation of the receptor. The depolarizing agents first cause the sodium channel associated with the nicotinic receptors to open, which results in depolarization of the receptors (phase I). This causes a transient twitching of the muscle, termed fasciculation. The continued binding of the depolarizing agent renders the receptor incapable of transmitting further impulses. With time, prolonged exposure of the neuromuscular junction to succinylcholine can result in (i) desensitization block or (ii) Phase II block.

1.3.1.1.1 Desensitization block

The desensitized state is one in which ACh can bind to the receptor but cannot activate (open) the channel. Receptors are in a constant state of transition between resting and desensitized states, whether or not agonists are present. Agonists do promote the transition to a desensitized state or trap receptors in that state, as desensitized receptors have a high affinity for them. (Appiah-Ankam 2004)

Normally, ACh is hydrolysed so rapidly that it has no potential for causing desensitization. Desensitization block may be a safety mechanism that prevents an excessive muscle response to extreme neural stimulation.

1.3.1.1.2 Phase II block

Phase II block is a complex phenomenon and differs from desensitization block. It occurs not only after high single or cumulative doses of a depolarizing muscle relaxant, but also after normal doses of succinylcholine during lack or functional inefficiency of

pseudocholinesterases. (Evers and Mervyn 2004) After the initial depolarization, the membrane potential gradually returns towards the resting state, even though the neuromuscular junction is still exposed to the drug. Neurotransmission remains blocked throughout. The exact mechanism underlying a phase II block remains unclear. It is probably due to interference with presynaptic AChRs. (Bowman 1980) Clinically, the block is characterized by fade of the train-of-four twitch response, titanic fade and post-tetanic potentiation.

1.3.1.2 Pharmacokinetics

Succinylcholine is poorly absorbed from the gastrointestinal tract. After IV administration, succinylcholine is distributed in the extracellular fluid and rapidly reaches its site of action at the motor endplate of the neuromuscular junction. Up to 10% of a succinylcholine dose is excreted unchanged in the urine. The remainder is rapidly hydrolyzed by plasma pseudocholinesterases to succinylmonocholine and choline. Because pseudocholinesterases exist in plasma but not at the neuromuscular junction (unlike acetylcholinesterase, the enzyme that degrades ACh), succinylcholine is not metabolized at the neuromuscular junction. Thus the action of succinylcholine terminates as its plasma concentration decreases and it diffuses from the neuromuscular junction into plasma.

Following an IV dose of 1 or 2 mg/kg, succinylcholine, the mean values for clearance for both doses (700 and $250 \text{ ml} \cdot \text{min}^{-1} \cdot \text{kg}^{-1}$, respectively), (Hoshi 1993) were 7-20 times as large as those observed in the Roy *et al* study (Roy *et al* 2002) ($37 \text{ ml} \cdot \text{min}^{-1} \cdot \text{kg}^{-1}$). Consequently, the elimination half-life of succinylcholine (16.6 and 11.7 s,

respectively) was only 30% of that observed in Roy *et al* study. The discrepancy is potentially the result of a lack of sensitivity of the analytical method in the former study.

1.3.1.3 Pharmacodynamics

The ED₉₅ of succinylcholine at the adductor muscle function varies with the types of anesthesia. During opiate-thiopental-nitrous oxide (N₂O) anesthesia, the ED₉₅ of succinylcholine is approximately 0.3 mg/kg; (Smith et al 1988) whereas it is increased to 0.5 mg / kg without N₂O. (Szalados et al 1990)

Perfect intubating conditions are achieved with 1mg/kg I.V. succinylcholine by about 60 to 90 seconds, (Cullen. 1971; Blitt et al 1981) although this may be delayed by a slow circulation time. (Harrison and Junius 1972) The clinical duration is about 5 – 10 min. (Roy et al, 2002; Scott and Goat 1982) The extremely brief duration of action of succinylcholine is primarily due to its rapid hydrolysis by pseudocholinesterases, enzymes mostly found in the liver and plasma. Pseudocholinesterases have an enormous capacity to hydrolyze succinylcholine at a very rapid rate such that only a small fraction of the original intravenous dose actually reaches the neuromuscular junction. The neuromuscular block of succinylcholine is terminated by its diffusion away from the neuromuscular junction back into the circulation. Pseudocholinesterases, therefore, influence the onset and duration of action of succinylcholine by controlling the rate at which the drug is hydrolyzed before and after it reaches the neuromuscular junction. Factors that have been described as lowering pseudocholinesterases concentration are either decreased availability, inhibition or genetic polymorphism of pseudocholinesterases. Low levels of normal pseudocholinesterase generally do not

prolong succinylcholine block to a clinically significant degree; this occurs only when normal pseudocholinesterase activity is reduced by at least 75% (normal, 4.9 to 12 IU/ml). The difference among normal, atypical, and abnormal pseudocholinesterase variants is shown in the laboratory with compounds (e.g., dibucaine, fluoride) that inhibit benzoylcholine hydrolysis pseudocholinesterase. The most common forms of abnormal pseudocholinesterase are the dibucaine-resistant and atypical variants (Eu Ea and Ea Ea, respectively). Other forms of pseudocholinesterase include fluoride-resistant variants and a “silent” variant that shows neither dibucaine nor fluoride induced inhibition. (Evers and Mervyn 2004)

1.3.2 Nondepolarizing neuromuscular blocking agents

Nondepolarizing NMBAs are either aminosteroidal compounds (pancuronium, vecuronium, rocuronium) or benzyloquinolinium compounds (atracurium, cisatracurium, mivacurium, doxacurium). According to the duration of action, nondepolarizing neuromuscular blocking drugs are classified as: short-acting agents, including mivacurium; intermediate-duration drugs, including rocuronium, vecuronium, atracurium; and long-acting agents, including pancuronium and doxacurium.

1.3.2.1 Mechanism of action

1.3.2.1.1 Competitive mechanisms of neuromuscular block

Nondepolarizing NMBAs function as competitive antagonists. The principal action of nondepolarizing agents is to prevent depolarization of endplate. Nondepolarizing agents

bind to the α subunit of the ACh and prevent the binding of ACh, but they are incapable of inducing the conformational change necessary for ion channel opening. (Evers and Mervyn 2004) Therefore, the membrane will not be depolarized because no current will flow through it. As a result, no endplate potential is produced to open neighboring sodium channel to elicit a muscle action potential. A dynamic equilibrium exists between the interaction of ACh and nondepolarizing agent, which favors either ACh or non-depolarizing agents, depending on concentrations within the active biophase. The probability of binding is solely dependent on the concentration of each ligand present at the neuromuscular junction and their affinity for the receptor. (Evers and Mervyn 2004)

1.3.2.1.2 Noncompetitive mechanisms of neuromuscular block

Nondepolarizing NMBAs, like the depolarizing drugs, also exhibit desensitization block. They bind tightly to desensitized receptors and can trap them in these states. This is a noncompetitive block. When more receptors are in the desensitized state, the margin of safety of transmission is reduced. (Appiah-Ankam 2004)

Beside desensitization block, ion-channel block occurs, in which some drugs block the flow of ions through the AChRs. There are two types of ion-channel block: open or closed. During closed-channel block, the drug molecules occupy the mouth of the receptors. During open-channel block, the molecules enter and obstruct the ACh receptor channel only after it is opened by ACh binding. NMBAs cause open-channel block when present in high concentration. It is not likely that open-channel block is of greater importance in clinical practice, but it may explain why it is difficult to antagonize profound neuromuscular block. It may also play a role in interactions of

NMBAs and steroids, local anesthetics, antibiotics, calcium-channel blockers or inhalation anesthetics. (Appiah-Ankam 2004)

1.3.2.2 Pharmacokinetics

The pharmacokinetic parameters of nondepolarizing muscle relaxants are listed in Table 1. Because nondepolarizing muscle relaxants are highly ionized, water-soluble drugs, their volume of distribution is mostly limited to the extracellular fluid volume (about 200 ml/kg). Accordingly, nondepolarizing muscle relaxants cannot easily cross lipid membrane such as the blood-brain barrier or gastrointestinal epithelium. Therefore, they do not produce central nervous system (CNS) effects and are ineffective after oral administration. (Stoelting and Hillier 2006)

Many nondepolarizing relaxants are mostly eliminated unchanged by the kidney or the liver, such as vecuronium and rocuronium, doxacurium, pancuronium, and D-tubocurarine. Atracurium and cisatracurium were synthesized specifically to undergo Hofmann elimination (spontaneous hydrolysis at physiological pH and temperature); they also undergo ester hydrolysis and to a lesser degree, hepatic and renal eliminations. Given that elimination of these two drugs does not depend exclusively on organ function, they are indicated for patients with renal and hepatic failures. (Stoelting and Hillier 2006)

Mivacurium differs from the other nondepolarizing relaxants in that its major elimination pathway is the hydrolysis by pseudocholinesterases, the same enzymes

responsible for the elimination of succinylcholine. Although the clearance of mivacurium varies as a function of plasma cholinesterases activity, the range of enzymes activities in normal patients is sufficiently small and the rate of recovery sufficiently rapid that infusion requirements do not need to be adjusted for most patients. (Longnecker 1997)

Table 1. Nondepolarizing muscle relaxants pharmacokinetic parameters

NMBAs	Pharmacokinetic Parameters						
	Vd _s (L/kg)	CL (mL/min/kg)	T _{1/2} (min)			Metabolism	Elimination
			Normal	Kidney failure	Hepatic failure		
Short Acting							
Mivacurium							
<i>trans</i>	0.05	29	2	NA	NA	95-99%(Plasma cholinesterases)	< 5%
<i>trans</i>	0.05	46	2				Renal
<i>cis</i>	0.2	7	30				
Intermediate Acting							
Cisatracurium	0.2	3-4	22-30	25-34	21	70-90% Hofmann	10-30% Renal and/or Biliary
Atracurium	0.2	5.5	21	18-25	20-25	60-90% Hofmann et Esterases	10-30 % Renal
Vecuronium	0.27	5.2	50-110	80-150	49-198	NA	40-50%:50-60% Renal:Biliary
Rocuronium	0.3	4.0	87	97	97	NA	30-40%:60% Renal:Biliary
Long Acting							
Pancuronium	0.35	1.8	132	240-1050	208-270	NA	60-80%:10% Renal:Biliary
Doxacurium	0.22	2.7	95	NA	NA	NA	(90%:10%) Renal:Biliary

(Evers and Mervyn 2004)

1.3.2.3 Pharmacodynamics

Equipotent doses (ED_{95}) for nondepolarizing NMBAs are shown in Table 2. Unless stated otherwise, the ED_{95} is assumed to represent the potency of the NMBAs under nitrous oxide-barbiturate-opioid anesthesia. In the presence of a volatile anesthetic, the ED_{95} is greatly decreased compared with the value in the absence of these anesthetic drugs. (Stoelting and Hillier 2006)

Ideally, the onset of neuromuscular blockade in the non fasted anesthetized patients should occur within 1 minute after the injection of a muscle relaxant to minimize the risk of aspiration of gastric contents. (Wierda 1993) Although significant improvements have been made with the introduction of recent nondepolarizing NMBAs such as rocuronium, for most of them, there is a delay in onset of action, and complete muscle relaxation is observed only after 5 to 7 minutes. Therefore, it is important to determine the factors which modify the onset of action of neuromuscular blocking drugs in order to achieve the shortest time possible in clinical practice.

Table 2. Neuromuscular blocking agents pharmacodynamic parameters

NMBA	PHARMACODYNAMIC PARAMETERS			
	ED ₉₅ (mg/kg)	Onset to Maximum Twitch Depression (min)	Recovery index 25- 75% (min)	Clinical Duration (2 X ED ₉₅) (min)
Short Acting (12 - 20 min)				
Mivacurium	0.08	2-3	7	12-20
Intermediate Acting (30 - 60 min)				
Atracurium	0.25	3-5	10-15	30-45
<i>Cis</i> -atracurium	0.05	3-5	10-15	40-75
Vecuronium	0.05-0.06	3-5	10-15	45-90
Rocuronium	0.3	1-2	10-15	45-75
Long Acting (80 -120 min)				
Pancuronium	0.06-0.07	3-5	25	60-120
Doxacurium	0.03	4-6	30-50	90-120

(Evers and Mervyn 2004)

1.3.2.2.1 Factors affecting the onset of neuromuscular blockade

Speed of onset is affected mainly by: dose (initial plasma concentrations), distribution/redistribution kinetics (intercompartmental clearances), equilibration rate constant between plasma and effect compartment concentrations (k_{e0}), and pharmacodynamic factors such as potency (EC_{50}). (Hennis 1985; Swerdlow and Holley 1987)

In the clinically setting, the dose of NMBAs administered is about two to three times the ED_{95} . Larger doses cause higher peak blood concentrations which result in more drug being delivered to the neuromuscular junction in the first few circulation times. (Healy et al 1986) Increasing the dose also shortens the delay between injection and the time at which the concentration of drug at the neuromuscular junction exceeds that necessary to produce 100% blockade. Therefore, time to maximum blockade (T_{max}) decreases markedly with dose in the one to three times ED_{95} range. However, at doses greater than three times the ED_{95} , the time to 100% blockade does not decrease markedly with increasing dose. Thus, at high doses, the limiting factor appears to be the time required for the drug to reach the neuromuscular junction, which in turn, depends on circulatory factors, such as cardiac output, distance of the muscle from central circulation, and muscle blood flow. The onset of NMBAs was found to be shorter in infants, who have a relatively large cardiac output, compared to older children. (Bevan et al 1985; Smith et al 1987) By contrast, a longer onset time for doxacurium in the elderly was attributed to an age-related reduction in muscle blood flow. (Garipey et al 1993)

Onset of action does not occur immediately after administration of NMBAs. This discrepancy between drug plasma concentration and effect has been accounted for by a hypothesized effect compartment representing the biophase.(Sheiner et al. 1979) An index of drug equilibrium time delay to its effect site is expressed and indicated as a transfer rate from central compartment (blood) to effect compartment. Therefore, a fast equilibrium is expected to be associated with a rapid onset. Alternatively, k_{e0} is thought to be governed by several factors such as: perfusion or drug delivery to the biophase (blood flow), diffusion of drug from the capillary lumen to the biophase and blood/biophase drug partition coefficient (molecular weight, pKa, lipid solubility), protein binding (in plasma and tissues) and time required to occupy receptors and elicit drug effect (potency). (Hennis P 1985; Stanski et al. 1979) Thus, k_{e0} and onset time of action of NMBAs are intrinsically related. It is noteworthy that a shorter onset is not always associated with a faster k_{e0} as this proved to be the case for succinylcholine. (Roy et al. 2002) Since the rate limiting factors for k_{e0} and onset times are different, the net effect may differ.

An inverse relationship between onset and potency has been demonstrated for various aminosteroidal compounds.(Bowman et al. 1988) On theoretical ground, Donati and Meistelman(Donati and Meistelman 1991) presented a PK/PD model characterized by a finite concentration of receptors in the effect compartment to explain the relationship between a high potency and a slow onset of action for NMBAs. The principle of this model is that neuromuscular junction can be regarded as a dense cluster of receptors and no matter the potency of the neuromuscular blocking drug, a large proportional of receptors (more than 90%) must be occupied before neuromuscular blockade is

manifested.(Paton and Waud 1967) Since effect depends on the presence of a critical number of drug molecules at the site of action, no effect can be observed until a certain number of molecules have reached the receptors area. It follows that if the drug is potent, i.e., if a small dose has been given, fewer molecules are delivered to the neuromuscular junction per unit of time. Thus, this critical number will be reached after a longer period.

In contrast to dose-related onset time (TE_{max}), (Minto et al. 2003) time to peak effect compartment concentration (TEC_{max}) coincides with onset time only when the pharmacologic effect is submaximal and has to be derived mathematically for higher doses. While TEC_{max} is generally assumed to be dose-independent (Schnider and Minto 2001), this may not be the case when supramaximal dose is given. Thus, it cannot be excluded that, after a very high bolus dose of NMBA, anatomical constraints may limit the diffusion of NMBAs in the biophase and result in a nonlinear concentration-effect relationship.

1.3.2.2.2 Factors affecting the duration of neuromuscular blockade

The duration of action of NMBAs is also affected by several factors. Nondepolarizing agents which depend on organ metabolism and excretion may be expected to have a prolonged effect in old age, as organ function deteriorates. Because of the altered pharmacokinetics of NMBAs in hepatic and renal diseases, prolongation of action may be found in these conditions too.

Prior administration of succinylcholine also potentiates the effect and prolongs the duration of action of these NMBA's. Concomitant administration of a potent inhalational agent increases the duration of block. This is most marked with ester anesthetic agents such as isoflurane, enflurane and sevoflurane, but occurs to a lesser extent with halothane. (Aitkenhead 2007)

Metabolic and, to a lesser extent, respiratory acidosis extend the duration of block. With monoquaternary amines such as D-tubocurarine and vecuronium, this effect is produced probably by the ionization, under acidic conditions, of a second nitrogen atom in the molecule, making the drug more potent. (Aitkenhead 2007)

Hypothermia potentiates block as impairment of organ function delays metabolism and excretion of these drugs. Enzymes activity is also reduced. This may occur in patients undergoing cardiac surgery; reduced doses of muscle relaxants are required during cardiopulmonary bypass. (Aitkenhead 2007)

A low serum potassium concentration potentiates neuromuscular block by changing the value of the resting membrane potential of the postsynaptic membrane. A reduced ionized calcium concentration also potentiates block by impairing presynaptic ACh release. (Aitkenhead 2007)

2. Design NMBA pharmacokinetic/pharmacodynamic study

Proper design of PK/PD studies is essential for optimal extraction of information from the data. NMBA have often served for the development of PK/PD models because their effect can be measured repetitively and quantitatively. Methodological factors such as sampling site,(Donati et al. 1991) sampling schedule(Ducharme et al. 1993) and anesthetic procedure(Swen et al. 1989) are important sources of variation and often impede generalization of PK data shortly after a bolus dose of NMBA, a period which also corresponds to the induction of neuromuscular blockade.

Depending on blood sampling site, drug concentrations can be markedly different because of the high efficiency of drug uptake by sampling tissue (e.g. arm) during the very short transit through capillaries (1-3 sec).(Chiou 1989) In the first two minutes following the intravenous injection of a bolus in humans, the arterio-venous (A-V) gradient of some anesthetic agents such as D-tubocurarine(Cohen et al. 1957), atracurium(Donati et al. 1991), and midazolam(Mastey et al. 1995) may reach values as high as 50%. Drug concentration in arterial blood, and not in venous blood, is the driving force for drug distribution,(Chiou 1989) and will provide a more accurate representation of the amount of drug actually delivered to the neuromuscular junction. In the case of atracurium, k_{e0} and EC_{50} were decreased by almost 50% when using arterial data compared to venous data.(Donati et al. 1991) In addition, for drugs undergoing pulmonary or muscle tissue extraction, venous blood sampling may lead to a proportional overestimation of systemic clearance, the resultant error being more significant for highly extracted drugs.(Weiss 1997) A 34 and 42% A-V gradient of trans and cis trans isomers of mivacurium was observed in patients,

respectively.(Beaufort et al. 1999) Accordingly, the choice of the sampling site (arterial vs venous) has an important influence on the determination of pharmacokinetic parameters.

It is well recognized that the blood sampling schedule during the first minute after a bolus of a NMBA may have a significant impact on the estimation of its PK and, in turn, PK/PD parameters. Processes such as mixing, flow (circulatory factors) and diffusion (physico-chemical properties) will govern initial drug distribution.(Chiou 1989) In our laboratory, most of clinical PK/PD studies were designed to characterize the IVM (i.e. the first two minutes after injection) after bolus administration. These studies required intensive blood sampling and were meant to verify if the kinetics during the IVM phase (now sometimes referred to “front-end kinetics”) were the same for a series of NMBAs which, being hydrosoluble drugs, are expected to be distributed to a similar extent in the extracellular fluid. Vecuronium, atracurium, doxacurium, and succinylcholine peak arterial concentrations were not reached until approximately 30 sec after bolus injection. (Ducharme et al. 1993; Ducharme. et al. 1995; Roy et al. 2002; Zhu et al. 1997) For a drug having a very rapid elimination, such as mivacurium, intensive arterial sampling is crucial.(Lacroix et al. 1997) Indeed, for the trans trans and cis trans isomers the area under the curves (AUCs) obtained in the first 2 min represent 75 and 86% of total AUC, respectively; while that of the cis-cis isomer, which is more slowly eliminated, represents only 22% of total AUC. Using limited blood sampling (first samples drawn at 1 and 2 min only), the total AUC will be underestimated and will lead to an important overestimation of the $V_{d_{ss}}$. The sampling schedule during the first 2 min after bolus injection is also critical for adequate PK/PD modeling. For the same patient, vecuronium

$t_{1/2 k_{e0}}$ was prolonged by 50% (12 vs 8 min) when using intensive blood sampling during the first 2 min compared to limited blood sampling.(Donati et al. 1991) This proved also to be the case for atracurium, using retrospective comparisons (Ducharme. et al. 1995) This pattern was further accentuated when studying the PK/PD relationship of succinylcholine (Roy et al. 2002) and rocuronium (Dragne et al. 2002). Because of the rapid onset of action of these two drugs, frequent arterial sampling immediately after injection is essential.

Finally, the type of anesthetics used during the PK/PD study of a NMBA has to be considered. Our previous clinical studies were carried out under isoflurane anesthesia, but with the introduction of propofol as an intravenous anesthetic, changes needed to be made to the anesthetic procedure. This was verified in a PK/PD study where the PK of rocuronium was compared in patients anesthetized with either propofol or isoflurane. (Dragne et al. 2002) Our clinical PK/PD studies are now conducted under propofol anesthesia.

In most of the clinical studies conducted in our laboratory, NMBAs were given as a rapid bolus in order to mimic the input rate mostly used in clinical practice. The effect compartment proposed by Sheiner et al (Sheiner et al. 1979) for D-tubocurarine that became a standard in compartmental PK/PD studies uses a short infusion instead of a bolus administration because the onset of action is more gradual, allowing more data points during onset. Hence, a basic principle in PK/PD modeling is that parameters are unchanged by input rate. This assumption was tested in patients with doxacurium(Zhu et al. 1997) and PK/PD parameters derived after administration of a 1.5 ED₉₅ dose either

as a bolus (followed by extensive arterial sampling) or an infusion regimen were found to be similar and equally reliable.

3. Pharmacokinetic and pharmacodynamic modeling of NMBAs

3.1 Individually based pharmacokinetic/pharmacodynamic analysis

3.1.1 Individually based pharmacokinetic models

3.1.1.1 Noncompartmental pharmacokinetic models

The noncompartmental approach depends upon the following assumptions: 1) all dispositional procedure may be described by first order kinetics; 2) all drug molecules will be completely eliminated from the organism; and 3) the elimination process occurs from the sampling compartment, usually the circulatory system. This approach is based largely on the AUC of the observed drug concentrations versus time. The most significant advantage of noncompartmental models is that they do not assume specific compartments for chemicals or metabolites. Because noncompartmental model does not involve fitting a particular model to data, the model assumptions are minimized, and the moments are completely model-independent measures.

3.1.1.2 Classic compartmental pharmacokinetic models

Classic compartmental modeling is based on the assumption that organisms are composed of a system of interconnected “well-stirred” compartments from which a finite number can be kinetically described in a model. Often one assumes that each drug molecule has the same probability of transferring to or from a compartment, and that this

transfer is governed by first-order conditions where the transfer rate of a drug molecule from one compartment to another is proportional to its concentration within the original compartment. As an example, a typical two-compartment model is depicted in Fig. 5.

The advantage of this modeling approach is that there is no limitation for fitting the model to the experimental data. If a particular model is unable to describe the behavior of a particular data set, additional compartments can be added until a successful fit is obtained. Since the model parameters do not possess any intrinsic meaning, they can be freely varied to obtain the best possible fit, and different parameters values can be used for each data set in a related series of experiments. Once developed, these models are useful for interpolation and limited extrapolation of the concentration-time profiles which can be expected as experimental conditions are varied. They are also useful for statistical evaluation of a chemical's apparent kinetic complexity. However, since the compartmental model does not possess a physiological structure, it is often not possible to incorporate a description of these nonlinear biochemical processes in a biologically appropriate context. Without a physiological structure it is not possible to correctly describe the interaction between blood-transport of the chemical to the metabolizing organ and the intrinsic clearance of the chemical by the organ.

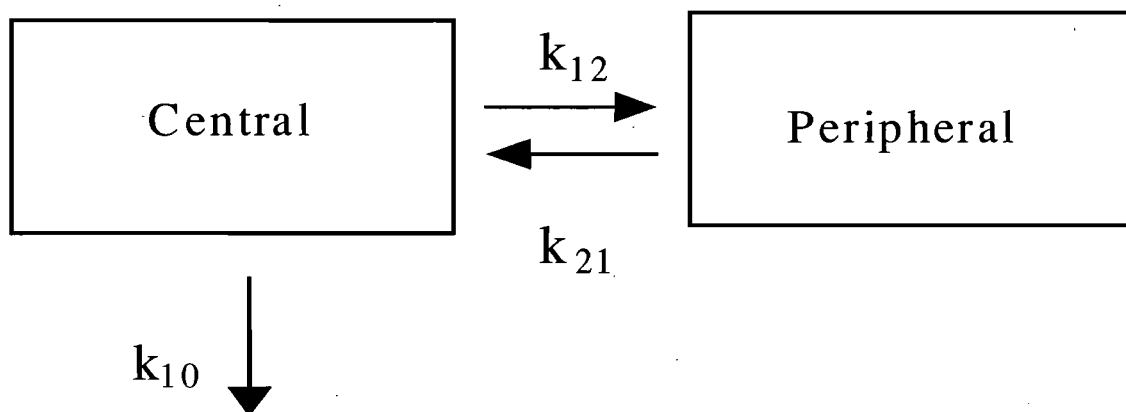


Figure 5. Example of an empirical 2-compartment pharmacokinetic model

Both traditional compartmental and noncompartmental modeling assume that elimination occurs solely from the central compartment. For some NMBA (e.g., cisatracurium and atracurium), elimination occurs from both the central (k_{10}) and the peripheral compartments (k_{20}). Two specific applications will be discussed here. In the first one, k_{20} is fixed to a predetermined $k_{in\ vitro}$ value obtained from the in vitro rate of degradation of the drug in plasma. In the second one, the primary assumption is that $k_{20} = \beta$ when empirical evidence has confirmed that the in vivo rate of elimination (β) is similar to the $k_{in\ vitro}$ measured in the same subject. Nakashima and Benet (Nakashima and Benet 1988) and Laurin et al (Laurin et al. 1999) described the consequences of these assumptions on PK parameter estimation and how to derive exit-site dependent and exit-site independent parameters for various PK models. Total body clearance is an exit-site independent parameter; therefore, values of clearance obtained from either model (e.g., traditional, with elimination from the central compartment only or non traditional models) must be equivalent. However, the steady-state volume of distribution depends on the exit-site(s) defined within the model. Therefore, the consequences of non-central elimination should be recognized and stated.

Table 3. Changes in estimated apparent volume of distribution of model drugs according to basic assumptions made during PK modeling.

Studies	Basic assumptions	Model		Reference
		Central elimination	Central + peripheral	
Human		V _{d_{ss}} (l/kg)	V _{d_{ss}} (l/kg)	
Atracurium	K ₂₀ = K _{invitro} plasma K ₂₀ = β	0.146	0.195 0.202	Unpublished
Cisatracurium	K ₂₀ = K _{invitro} plasma(Welch et al. 1995)	0.089	0.118	(Bergeron et al. 2001)
	K ₂₀ = K _{invitro} plasma(Welch et al. 1995)	0.075	0.098	(TV Tran 1998)
	K ₂₀ = K _{invitro} plasma(Welch et al. 1995)	0.171	0.207	(Imbeault et al. 2006)
Mivacurium				
Cis trans ^a	K ₁₀ = K _{invitro} plasma	0.032	0.064	(Laurin et al. 1999)
Trans trans ^a		0.043	0.058	
Succinylcholine	K ₂₀ = K _{invitro} plasma= β	0.019	0.039	(Roy et al. 2002)

^aA-V gradient of approximately 40% demonstrated in anesthetized patients (Laurin et al. 1999)

In pharmacokinetic studies where the first plasma sample (arterial or venous) is obtained one minute after intravenous bolus administration of a drug, the traditional mammillary compartment model is well accepted and sufficient for fitting the concentration-time data. However, it is well recognized that a poor characterization of the IVM phase will ensue if an instantaneous input in the central compartment is assumed in the model. (Ducharme et al. 1993; Ducharme. et al. 1995) Indeed, plasma samples obtained frequently during the first minute would reveal that, after a brief delay, drug levels rapidly rise to a peak, followed by oscillations that will eventually be followed by the expected monotonic decrease.(Bissinger and Nigrovic 1997) Depending on the terminal half-life of the drug, assuming an instantaneous input may result in subtle (Ducharme et al. 1993; Zhu et al. 1997) or large (Lacroix et al. 1997; Roy et al. 2002) errors in the estimation of major PK parameters. This limitation of the compartmental approach is almost impossible to overcome when one attempts to fit the concentration-effect data of anesthetic drugs having an onset of action within the very first two minutes.(Bergeron et al. 2001) One can overcome the structural limitations of conventional pharmacokinetics by using recirculatory (Krejcie et al. 1997) or other types of models. (Lafrance et al. 2002)

3.1.1.3 Recirculatory pharmacokinetic models

Recirculatory pharmacokinetic models were developed over 20 years ago.(Cutler 1979) They retain the relative simplicity of mammillary models, but incorporate descriptions of key physiological processes that have emerged as important determinants of intravenous anesthetic disposition. These include the role that cardiac output, lung

kinetics, and injection rate play in dictating initial drug concentrations after i.v. bolus administration.(Upton 2004) In contrast with physiologically-based pharmacokinetic models, all of the parameters are, in principle, estimable by administering not only the drug under study but also physiological markers of the intravascular compartment such as the indocyanine green (ICG) dye.(Avram et al. 1997; Henthorn et al. 1992; Krejcie et al. 1996)

3.1.2 Individually-based pharmacokinetic/pharmacodynamic models

3.1.2.1 Parametric PK/PD models

This approach of PK/PD modeling was first successfully applied to D-tubocurarine, (Sheiner et al. 1979) and is now often referred to as a full parametric model. This type of modeling requires prior knowledge of the pharmacokinetic model to describe the concentration-effect relationship, and the link model that characterizes the equilibrium kinetics between blood and the hypothetical effect compartment. The procedure for the parametric PK/PD modeling is as follows: PK parameters are estimated first by fitting an appropriate PK model to the plasma drug concentration (C_p) vs time data. If the PK model is, in fact correctly specified, then, PK parameters are fixed to these estimates. The second stage is the link model that derives the temporal profile of drug concentration in the effect compartment (C_e); then an appropriate PD model is fitted to the observed effect vs effect compartment concentration data.

Using the PK/PD model proposed by Sheiner et al, an increased sensitivity to and a longer recovery time of NMBAs was predicted in myasthenic patients (Buzello et al.

1986) on the basis of a smaller effect compartment concentration of drug at 50% effect (EC_{50}) and the steepness of the concentration-effect relationship (γ). Sheiner's model gives, however, no insight as to why these variables are changed in this group of patients. Therefore, Haes et al developed a novel PK/PD model, the unbound receptor model (URM), which takes into account the number of unbound AChRs and which may thus explain the altered EC_{50} and time course of NMBAs in myasthenic patients. (De Haes et al. 2002)

Parametric models are in common use for several reasons: the data are described with brevity by quoting the parameter estimates. The influence of different factors on the data can easily be compared in terms of parameter estimates; then the estimates can be used for interpolation/extrapolation or simulation. In the absence of model misspecification, the parametric method usually gives a better estimation of the PD model than the non parametric method. Indeed, the parametric method has valid assumptions about the true PK model, the true PD model and the true link model while the nonparametric method "knows" only the link model. However, in the presence of PK model misspecification, the nonparametric method can be of considerable benefit.

3.1.2.2 Nonparametric PK/PD models

Similarly to full parametric methods, nonparametric approaches have been proposed to link PK and PD data. These approaches differ mainly with respect to the prior knowledge required. The semi-parametric approach involves a nonparametric link submodel, but retains the parametric approach for PK data. (Fuseau and Sheiner 1984)

The value of k_{e0} is estimated as the value that causes the hysteresis curve (effect intensity vs concentration connected in time order) to collapse to a single curve that represents the steady-state concentration-effect relationship. Thus the value of k_{e0} is estimated without postulation of a particular parametric model for the concentration-effect relationship. The method has the important advantage that it allows inspection of the concentration-effect relationship, before selecting a particular pharmacodynamic model. In this way the risk of model misspecification is minimized.

On the basis of Fuseau's model, Unadkat et al (Unadkat et al. 1986) took one step further: the PK model is also approximated nonparametrically. This approach may be of value in exploratory data analysis and in situations where the pharmacokinetics can not be easily characterized on basis of a compartment PK model (e.g., sustained release preparations).

When the underlying PK and presumably PD models can be validated a priori, the parametric method is preferred because it produces precise estimation of the PD model. In reality, however, the true model is never known, and one can rarely be certain that model misspecification is absent. Therefore, the non-parametric approach may offer a distinct advantage for routine analysis of PK/PD data.

Based on a nonparametric PK/PD model with a modified effect compartment, the Rtot PK/PD model,(Donati and Meistelman, 1991) which included a finite concentration of receptors, was developed. Since neuromuscular blockade occurs only when a large proportion of receptors are occupied,(Paton and Waud 1967) it is assumed that the effect

compartment contains a finite concentration of receptors. The NMBA is either free or bound in a 1:1 molar ratio to the receptor. The transfer of drug from the central to the effect compartment is assumed to be proportional to the concentration gradient of the free drug. Total concentration of drug in the effect compartment is equal to free plus bound drug concentration. In this approach, k_{e0} and R_{tot} were estimated according to nonparametric PK/PD model. (Unadkat et al. 1986) Based on the optimal k_{e0} and R_{tot} , effect compartment concentrations, which correspond to free drug levels, were then derived. The validity of this approach has been proven with vecuronium (high potency drug) and showed that inclusion of a finite concentration of receptors in the effect compartment improves the goodness of fit between predicted and experimental data. (Ducharme. et al. 1994)

3.2 Population-based pharmacokinetic/pharmacodynamic analysis

Population PK/PD model describes the typical relationships between physiology and PK/PD parameters, the interindividual variability in these relationships, and their residual intraindividual variability.(Sheiner and Wakefield 1999) To construct a model, the data are pooled from more than one individual and then used to predict the mean PK/PD parameters and measurement errors in other individuals. Thus, the model can be carried out with data gathered from different subjects such as different groups of age, weight, gender etc. Again, there are basically two approaches: parametric and nonparametric. In the parametric approach, the shape of the population distribution is assumed to be known except for the unknown population parameter values (e.g., normal distribution with unknown means and covariances). In the nonparametric approach, no

such parametric assumptions about the form of the population parameter distributions are made. The entire distribution is estimated from the population data. It allows for nonnormal and multimodal distributions.(Mallet 1986) In the section below, we are focusing on the standard two-stage approach and parametric mixed effect modeling (MEM) approach.

3.2.1 Standard two-stage approach

In the first stage, the individual PK/PD parameters are calculated separately from a dense data set, using standard fitting procedures (e.g., Weighted Least Squares) as shown below:

$$\text{OBJ}(P_i) = (C_{\text{obs}j} - C_{\text{pred}j})^2 \times W_{ij} \quad \text{Equation 1}$$

Where P_i is the PK-PD parameters for i^{th} individual, W_{ij} is the weight of j^{th} observation in i^{th} individual. The weighted least squares assume a heteroscedastic error structure, where the random error is assumed to be some function of the observed concentrations, such as $W_{ij}=1/C_{\text{obs}j}$ which assumes that variance is inversely proportional to concentrations.

In the second stage, the population mean and variability of the PK/PD parameters are calculated for the study population. The relationship between the covariates and the PK parameters across subjects can be evaluated using a regression method. The population parameters (mean and variance) across the subjects can be calculated as below: (Sheiner and Wakefield 1999)

Arithmetic mean and variance:

$$Mean = \sum_{i=1}^N p_i / N \quad \text{Equation 2}$$

$$Variance = \sum_{i=1}^N (p_i - mean)^2 / N \quad \text{Equation 3}$$

When the number of subjects is large, estimated individual parameters and mean values of the parameter have little or no bias. Covariates can be included in the model. However, the random inter-individual variability from two-stage approach can be overestimated, which is associated with both true biological variability and the uncertainty of the individual parameter estimate. The traditional two-stage method requires intensive sampling measurements at appropriate times to obtain an accurate parameter estimate in stage 1. It is generally not applicable in the highly sparse data sampling situation (e.g., 1-2 samples per subject), since estimating the individual parameters is out of the question. (Sheiner and Wakefield 1999)

3.2.2 The mixed effect modeling approach

The MEM approach is a one-stage analysis approach, which considers the population study sample, rather than the individual, as a unit of analysis for the estimation of the distribution of parameters and their relationship with covariates within the population. The term “mixed” denotes the combination of fixed and random effects.

In the population analysis, it is natural to fit the data into a hierarchical modeling structure, which allows the variability to be separated into inter- and intra- individual

variability. The hierarchical structure in the two stages has been developed by Beal (Beal 1992) as described below:

1st Hierarchy:

Each subject has a set of drug concentrations and the predicted concentration is defined as below:

$$Y_{ij} = H_1(\theta_i, t_{ij}, d_i) + \varepsilon_{ij} \quad \text{Equation 4}$$

Where ε_{ij} is independent and identically distributed as $\varepsilon \sim N(0, \sigma^2)$; Y_{ij} is the j^{th} observed concentration in the i^{th} individual; H_1 , the functional form of PK model, $H_1(\theta_i, t_{ij}, d_i)$, is the j^{th} predicted concentration in i^{th} individual; d_i is the dosing history, including amount of dose and the time of administration for i^{th} individual; θ_i is the value of the i^{th} individual's PK parameter.

2nd Hierarchy:

The model used in the second stage is defined as below:

$$\theta_i = H_2(\mu, \text{Cov}_i) + \eta_i \quad \text{Equation 5}$$

With η_i independent and identically distributed as $\eta \sim N(0, \omega^2)$; Cov_i represents contribution of the covariates for the i^{th} individual and μ is the population parameter.

The predicted values of PK parameters for the i^{th} individual at time t_{ij} are defined by H_1 in equation 4. H_2 is a function which describes the relationship between i^{th} individual's covariates and i^{th} individuals' PK parameters. (Beal 1992)

Stage 1 and 2 of the hierarchy explicitly partition the variability in the observed data into two variance components. These are called intra- (sometimes also called residual

unknown variability) and inter-individual variability.

3.2.2.1 Model definition

Thus, the population PK/PD model is a combination of three basic components:

(1) The structural model component, which defines the PK-PD process behind the data much in the same way as do the traditional models for the individual approach. The structural (PK/PD) sub-model describes the overall trend in the data (e.g., one-compartment model or Emax model), using fixed effects parameters (e.g., clearance or Emax).

(2) The statistical model component, which comprises both intra- and inter-individual variability. The residual error model component describes the underlying distribution of the error in the measured PK/PD variable and the inter-individual error model component describes the inter-individual variation (IIV) in PK/PD parameters after correction for fixed effects.

(3) The covariate model component, which expresses relationships between covariates and model parameters.

3.2.2.1.1 Base model development

3.2.2.1.1.1. Structure of the PK/PD model

The structural part of a mixed-effects model in pharmacometric data analysis describes the pharmacokinetic and/or pharmacodynamic properties of a drug, which are shared among all individuals in a population. This could for example be a one-compartment model (PK) and an E-max model (PK/PD). The structure of the PK model represents the best description of the data without considering the effect of subject's specific covariates. It is usually expressed in terms of 'primary pharmacokinetic parameters', i.e. clearances and volumes, rather than rate constants because it is then easier to set up hypotheses about the influence of covariates like weight, sex, age or concomitant diseases which, for example, alter hepatic or renal function, or plasma protein concentration. (Rowland N 1995)

3.2.2.1.1.2. Inter-individual variability

In this model component, the individual parameter estimates are modeled as functions of a typical value for the population and individual random deviations. The inter-individual variability (IIV) of the PK parameters can be described as below:

Homoscedastic (additive or constant variance)

$$P_i = TV_{P_i} + \eta_{pi} \quad \text{Equation 6}$$

Heteroscedastic (proportional or constant coefficient of variation (CV))

$$P_i = TV_{P_i} \times (1 + \eta_{pi}) \quad \text{Equation 7}$$

Exponential (approximates constant CV)

$$P_i = TV_{P_i} \exp^{\eta_{pi}} \quad \text{Equation 8}$$

Where the fixed effects parameter TV_{P_i} represents the mean (typical) value in the population and η_{pi} is a random effect accounting for the individual difference from the

typical value. These η_i values are assumed to be normally distributed in the population, with a mean of zero and standard deviation ω_p .

3.2.2.1.1.3. Intra-individual variability

The difference between the predicted concentration/effect and the observed concentration/effect is defined as residual variability, which represents assay measurement errors, errors in the recorded time and dose, as well as model misspecification. It can be modeled using additive, proportional or combined error structure as described below:

$$\text{Additive error: } y_{ij} = \hat{y}_{ij} + \varepsilon_{ij} \quad \text{Equation 9}$$

$$\text{Proportional error } y_{ij} = \hat{y}_{ij} \times (1 + \varepsilon_{ij}) \quad \text{Equation 10}$$

$$\text{Combined additive and proportional error: } y_{ij} = \hat{y}_{ij} \times (1 + \varepsilon_{ij}) + \varepsilon_{ij}' \quad \text{Equation 11}$$

Where y_{ij} is the j^{th} observation in the i^{th} individual, \hat{y}_{ij} is the corresponding model prediction, and ε_{ij} (or ε_{ij}') is the individually weighted residual error that has a normal distribution centered around zero and a standard deviation, σ .

Correlation between individual parameters or between residual errors can be included in the model. Individual parameter correlations not associated with covariates in the model are included as covariance between different random effects (η). Correlations between the intra-individual errors (ε) may either be included as a function of time within the

same dependent variable and individual (auto-correlation), or as a covariance of ε between different dependent variables measured at the same time (e.g., observations of drug and metabolite or repeated assays of the same sample).(Karlsson et al. 1995) Unless otherwise noted, the random effects are assumed to be independently and identically distributed, i.e. without any correlation.

3.2.2.1.1.4. Inter-occasion variability

The pharmacokinetics of a drug may change over time within an individual. Concomitant medication of inducers/inhibitors of metabolic enzymes, progression of liver/kidney disease and the development of organ function in neonates are some possible causes for time-varying pharmacokinetics. The underlying processes that control the variation are often poorly understood and difficult to measure. Consequently, a large magnitude of this variability is usually not possible to explain. If the pharmacokinetics changes relatively fast, a time-dependence on the magnitude of the variability may be needed in the model. If the changes occur over a longer period of time, for example between different treatment periods or occasions, the variability between these periods (IOV) may also have to be quantified in the population PK-PD model. (Karlsson and Sheiner 1993) The model for IOV is described as follows:

$$P_{ik} = P_{TV} + \eta_i + k_{ik} \quad \text{Equation 12}$$

Where the parameter of the drug in individual i at occasion k (P_{ik}) differs from the mean P_{TV} by an additional (zero mean, variance π^2) random effect, k_{ik} , which accounts for the intraindividual, between-occasion variability.

The three sub-models are interrelated and the choice of structural (and statistical) model may affect the choice of covariate model and vice versa.(Wade et al. 1994)

3.2.2.1.2 Covariate model development

An important objective of a population PK analysis is to identify the sources of variability from observable covariates and their correlation with the individual PK/PD parameters, which can explain part of the inter-individual variability besides the part which has been explained by random effect in the base model. Covariates may also influence the random effects distribution, e.g., the magnitude of the IIV or residual error (Karlsson et al. 1995) or the probability of belonging to a certain mixture.(Davidian and Gallant 1992; Park et al. 1998) A mixture could, for example, consist of poor and extensive drug metabolizers. Many factors in the biological system can potentially contribute to variability such as age, sex, weight, renal function, polymorphic enzymes and concomitant medication. Quantitative assessment of the relationship between covariates and PK/PD parameters is important for drug development because it provides information on whether the special dosage is necessary for a subgroup of patients.

Covariates can be incorporated into a model in various ways depending on their type, shape and range. Usually covariates can be classified as: continuous covariate (e.g., age, weight, height), or discrete covariates (e.g.: sex, race, and enzyme genotypes). These two types of covariates can be incorporated into the model as described below:

For continuous covariate

Linear function

$$p_i = TV_{pi} + \theta_{pcov} \times cov_{ij} \quad \text{Equation 13}$$

Where p_i is the individual estimate incorporating the covariate; TV_{pi} is the typical value at $cov_{ij} = 0$; θ_{pcov} is the covariate coefficient.

Eq 13 can be reparameterized so that the relationship is centered on a value in the covariate distribution, e.g., the (baseline or overall) median covariate value, denoted as \bar{cov} :

$$p_i = TV_{pi} \times \left[1 + \theta_{pcov} \times (cov_{ij} - \bar{cov}) \right] \quad \text{Equation 14}$$

In many cases, and especially if the covariates cover a large range of values, the data may not be satisfactorily described by linear models. Nonlinear relationships are obtained using a power model:

$$p_i = TV_{pi} \times \left[cov_{ij} / \bar{cov} \right]^{\theta_{pcov}} \quad \text{Equation 15}$$

Where p_i is the individual estimate incorporating the covariate; TV_{pi} is the typical value at $cov_{ij} = \bar{cov}$; \bar{cov} is the median value of Cov_{ij} .

For a discrete covariate

The incorporation of a discrete covariate involves assigning a numeric value to the covariate (e.g., sex, male = 0, female = 1). The equations below show multiple categorical covariates.

$$P_i = \begin{cases} 0 & \text{if cov at 0} \\ \theta_{pcov1} & \text{if cov at 1} \\ \theta_{pcov1} \times (1 + \theta_{pcov1}) & \text{if cov at 2} \\ \theta_{pcov1} \times (1 + \theta_{pcov2}) \times (1 + \theta_{pcov3}) & \text{if cov at 3} \\ \dots & \dots \end{cases} \quad \text{Equation 16}$$

Where θ_{pcov1} is a coefficient describing the effect relative to the previous level. Restricting θ_{pcov2} , θ_{pcov3} , etc. to positive values confines the effects to be either increasing or decreasing as the level of the covariates increases. (Bonate 2005) Missing covariate values cannot be ignored in an analysis. One way to handle missing covariate information is to delete the observation from the analysis, the so-called “complete case” approach. This approach tends to be most useful when the sample size is large and a small fraction of the covariate is missing. (Bonate 2005) Complete case analysis does not result in biased parameter estimates but simply acts to decrease the precision of the estimates by decreasing the sample size. More often, it is better to impute the missing covariate values for these subjects than to exclude them from analysis which will decrease the sample size and lose information. The “simple imputation” approach includes mean estimation and predicting missing values from regression. (Bonate 2005) The mean estimation method replaces missing data with the median or mean covariate value calculated from non-missing subjects in the population dataset. To predict missing values from regression one has to impute each independent variable on the basis of other independent variables in model using regression analysis. Simple imputation does not take into account the estimate of the imputed value, a criticism which may be alleviated by using the “multiple imputation” technique of Rubin. (Rubin, 1996) Multiple

imputation requires the assumption of independency and missing at random. The first assumption means the probability that some data are missing does not depend on the actual values of the missing data, while the second one means the probability of an observation being missing does not depend on observed or unobserved measurements. The advantage of multiple imputation is that they introduce random error into the imputation process which reduces the probability of introducing biased estimate of all parameters.. It also allows one to obtain good estimates of the standard errors. However, there are often strong reasons to suspect that the data are not missing at random; where even accounting for all the available observed information, the reason for observations being missing still depends on the unseen observations themselves.

Covariates are often selected in a stepwise manner, e.g. a forward inclusion / backward elimination using the likelihood ratio test.(Jonsson and Karlsson 1998) In general, covariates that are significant at the 0.05 level are retained in the model (χ^2 , $\Delta\text{OFV} = -3.84$, $\text{df} = 1$). Once all the covariates that are significant at the 0.05 level have been included in the model, a backward elimination process is conducted. A significant level of 0.01 is used for the backward elimination (ΔOFV (objective function value) = -6.63, $\text{df} = 1$). The backward elimination process is repeated until all remaining covariates are significant ($p < 0.01$). Covariate factors should also have clinical or physiological relevance. Thus, if the magnitude of covariate effects is less than 20% of the parameter estimates for the typical subjects, the covariates may not be considered clinically relevant and may not be included into final model despite reductions in the OFV. Several covariates are investigated, possibly on a number of structural model parameters and in several different functional forms. Therefore, the overall type-I error rate (i.e. the

probability of including one or more false covariate coefficients into the model) is higher than indicated by the required p-value. This is a problem arising from multiple comparisons.(O'Neill R 1971) To correct for this, a stricter p-value is often used in the selection; although this can in turn result in omitting relations that are actually important. Further, correction of the p-value is only approximate or even arbitrary. Because of correlations, finding the value that corresponds to the overall type-I error rate is very computer intensive. Thus, although the p-value is used as a criterion for selection based on the ideas of hypothesis testing, the actual strength by which the null hypothesis has been rejected is remains unknown in the case of multiple comparisons. (Jonsson and Karlsson 1998)

3.2.2.1.3 Estimation method

Fitting the model means estimating the model parameter values resulting in the best fit to the available information (e.g. data). These 'best' parameter estimates in the model are typically obtained by minimizing or maximizing objective function (OBJ), such as ordinary least squares, weighted least squares and extended least squares. (Bonate, 2005) The objective function quantifies the difference between observed and predicted data for a given parameter set. The objective functions are shown below:

$$\text{Ordinary Least Squares (OLS): } OBJ = \sum_{i=1}^n (Y_{Obj_i} - Y_{Pred_i})^2 \quad \text{Equation 17}$$

$$\text{Weighted Least Squares (WLS): } OBJ = \sum_{i=1}^n [(Y_{Obj_i} - Y_{Pred_i})^2 XW_i] \quad \text{Equation 18}$$

$$\text{Extended Least Squares (ELS): } OBJ = \sum_{i=1}^n \left[\frac{(Y_{Obj_i} - Y_{Pred_i})^2}{\text{var}_i} + Ln \text{ var}_i \right] \quad \text{Equation 19}$$

Where var_i models the variance of the observation; Y_{Obj} is the observed concentrations and Y_{Pred_i} represents the predicted concentrations. W_i is the weight which reflects the relative uncertainty attached to the individual estimate. The extended least square is designated as a maximum likelihood (ML) if the random effects are assumed to be normally distributed.

The estimation method commonly used in nonlinear mixed effect modeling is the ML approach, which is an alternative of the ELS. The likelihood for the population parameters are shown below:

$$L = \prod_{i=1}^n \frac{1}{2\pi \text{var}_i} e^{-\frac{1}{2\text{var}_i} (Y_{Obj_i} - Y_{Pred_i})^2} \quad \text{Equation 20}$$

$$-2 \log(L) = n \log(2\pi) + \sum_{i=1}^n \left[Ln(\text{var}_i) + \frac{(Y_{Obj_i} - Y_{Pred_i})^2}{\text{var}_i} \right] \quad \text{Equation 21}$$

Where L is likelihood, var_i models the variance of the observation, Y_{Obj} are the observed concentrations and Y_{pred_i} represent the predicted concentrations.

The likelihood is the product of probabilities for each individual observation (i) to occur, given the respective model and parameters. Since the parameters are selected to maximize the probability, the greater the likelihood of the model means the larger the probability of the dependent variable to occur, therefore, the better the model describes the data.

3.2.2.1.4 Model building criteria

The adequacy of the developed structural models is evaluated using both statistical and graphical methods. The likelihood ratio test is used to discriminate between alternative (nested) models. The likelihood ratio test is based on the property that the ratio of the NONMEM objective function values (approximately $-2 \log$ likelihood) is asymptotically χ^2 distributed.

As already mentioned, a reduction of the objective function by 3.84 units is considered significant (χ^2 , $P < 0.05$ $df = 1$). For comparison between non-nested models, the Akaike Information Criterion (AIC) can be applied, (Yamaoka K 1978) where AIC is equal to the OFV plus 2 times the number of parameters.

3.2.2.1.5 Model Validation

Model validation aims to determine whether the model is a good description of the validation data set. Depending on the objective of the analysis, the need for model validation may vary. Model validation can be classified as: internal (e.g., bootstrap, posterior predictive check, data splitting and cross validation); or external (e.g., data from new studies) based on the sources of the data. External validation is the most

stringent type of validation. However, it needs external data from a new study, which is usually not available in most situations. Internal validation methods are commonly used, which rely on the analysis of the subsets from the total data with the majority of data used in model building.

Data splitting method (Bonate, 2005) involves randomly dividing data into an 'index' part and a 'test' part, where the index part (e.g. 2/3 of the original data set) is used to develop the model and the test part (e.g. 1/3 of the original data set) is used to evaluate the model performance.

Cross validation (Bonate, 2005) is a repeated data splitting method. Data are divided into n subsets. Fit the models from $n-1$ data set and each of the $n-1$ estimation subsets is used to predict the unused subset. The mean predictive error ($Y_{pred} - Y_{obs}$) calculated for each of these n models is used as measure of accuracy and mean absolute predictive error is used for precision measurement.

Bootstrap analysis (Parke et al. 1999) is a widely used internal validation approach. The nonparametric bootstrap is used to generate a series of data sets of size equal to the original data set by resampling with replacement from the observed data set, and the final model is fitted to each data set. The results provide a good measure of model stability, confidence intervals, variances and parameter distributions.

Another model evaluation method is the predictive performance check.(Yano et al. 2001) It is based on comparing meaningful statistics from observed data with

corresponding statistics calculated from data simulated under a model. Briefly, fixing the values of the model parameters to the final values obtained using maximum likelihood, data are then simulated. Some statistics of calculated data (e.g., half-life or AUC) are then compared to the observed statistic obtained with real data. More typically a histogram of the simulated statistics of interest is plotted and the location of the observed statistic is noted. Unusually small or large values are indicative of poor model validity.

4. Interspecies extrapolation

Despite exist a wide variety of body mass in animals, there is a regular pattern in physiological processes. Interspecies allometric scaling is based on the assumption (a correct assumption) that there are anatomical, physiological, and biochemical similarities among animals, which can be described by mathematical models. (Mahmood 2005) It is now a well-established fact that many physiological processes and organ sizes exhibit a power-law relationship with the body weight of the species. There are two approaches for interspecies kinetic modeling: physiological models and allometry.

4.1 Physiological models

The physiological models offer a mechanistic approach which accounts for transport mechanisms and metabolism within the body. For conducting interspecies extrapolation using physiologically-based pharmacokinetic models (PBPK), quantitative estimates of test and scaled species differences in the models' parameters (i.e., partition coefficients, physiological parameters, and metabolic rate constants) should be obtained. For

example, the tissue:air partition coefficients of chemicals appear to be relatively constant across species, whereas blood:air partition coefficients show some species-dependent variability. (Hayes 2001) Therefore, the tissue:blood partition coefficients for human PBPK/PD models have been calculated by dividing the rodent tissue:air partition coefficients by the human blood:air partition values. The tissue:air and blood:air partition coefficients for volatile organic chemicals may also be predicted using appropriate data on the content of lipids and water in human tissues and blood. Whereas the physiological parameters vary across species, the kinetic constants for metabolizing enzymes do not necessarily follow any type of readily predictable pattern, making the interspecies extrapolation of xenobiotic metabolism difficult. Therefore, the metabolic rate constants for xenobiotics should be obtained in the species of interest. (Hayes 2001) Once the PBPK model has been scaled to the target species after assuming that both the whole body and tissue models have an identical structure in the test and scaled species, blood and tissue concentration-time profiles or response can be predicted.

The PBPK approach should be used when a detailed distribution of the chemical is the major focus, when the central compartment is not the site of action, when protein binding is strong or nonlinear (Mordenti 1986) Using this approach, the models would be anatomically, physiologically, thermodynamically, and biochemically realistic.

4.2 Allometry

In contrast to the mechanistic approach of physiological models, allometry is purely empirical, examining relationships between size, time and its consequences

(pharmacokinetic/pharmacodynamic in our case) without necessarily understanding the underlying mechanisms.(Ings 1990) A linear regression of a log-log plot of the kinetic parameters vs the body weight of the animal species produces an allometric relationship from which a particular kinetic/dynamic parameter in human can be calculated.

$$Y = AW^b \qquad \text{Equation 22}$$

Where, Y is the biological parameter, and A and b are constants relating Y to body weight (W)

4.1.1 Interspecies scaling of clearance

Clearance (CL) is the most important pharmacokinetic parameter, therefore a lot of emphasis has been given to prediction of clearance from animals to man. Allometric scaling has been one of the most widely used approaches for predicting human drug clearance (CL) based upon measured values of CL in animal species.(Boxenbaum 1982) Because of its empirical nature and the numerous observed failures in predicting human CL, various modified allometrically based scaling methods have been proposed with the intent of improving predictability in humans. These methods primarily include corrections for maximum life-span potential (MLP),(Boxenbaum 1982) corrections for brain weight (BrW),(I., 1996b #107) corrections for unbound fraction of drug in plasma (f_u), (Feng 2000) the "rule of exponents" (ROE),(Mahmood and Balian 1996) liver blood flow (LBF) methods, (Rakesh. and Keith. 2004) corrections for in vitro metabolic CL,(Lave 1996) and empirical models correcting for plasma binding differences between animals and humans.(Tang and Mayersohn 2005)

To predict clearance in humans, allometric scaling is generally performed on data obtained from at least three animal species. In a recent paper, a general allometric equation (GAE) has been derived to illustrate the role of species selection in allometric scaling. Most interestingly, the GAE revealed that some species made little or no contribution to the predicted value in humans when a combination of animal species was used in allometric scaling. (Tang. and Mayersohn. 2005a) Using the published intravenous CL data sets (n = 102) in rats, dogs, monkeys, and humans, a data-driven approach (Rakesh. and Keith. 2005) was adopted to derive new one- and two-species-based methods for predicting human drug clearance (CL). The new one-species methods were developed as $CL_{\text{human}}/\text{kg} = 0.152 \cdot CL_{\text{rat}}/\text{kg}$, $CL_{\text{human}}/\text{kg} = 0.410 \cdot CL_{\text{dog}}/\text{kg}$, and $CL_{\text{human}}/\text{kg} = 0.407 \cdot CL_{\text{monkey}}/\text{kg}$, referred to as the rat, dog, and monkey methods, respectively. (Tang. et al. 2007)

Drugs and their metabolites are usually eliminated from the body via urine or bile or, sometimes, both. The relative contribution of biliary and urinary excretion to the overall elimination of drugs depends on the nature of the drugs and the animal species. (Smith 1971)

4.1.1.1 Prediction of human renal clearance based on GFR values

Many drugs are excreted mainly as unchanged drugs by the kidneys. The rate of renal excretion (renal clearance) is dependent on renal blood flow, glomerular filtration rate (GFR), and tubular secretion and reabsorption. The GFR values vary considerably among species ranging from 1.8 ml/min/kg for humans to 10 ml/min/kg for mice

because of species differences in the number of nephrons.(Renkin 1973.; Lin 1995)

Both the GFR and number of nephrons show a good allometric relationship.

Although the renal clearance of a drug in humans can be predicted reasonably well by use of the allometric approach, this approach requires at least three animal species in order to obtain a proper allometric relationship, thus limiting its practical value in drug development. A more simplistic yet useful alternative to predict human renal clearance is to use the ratio of GFR between animals (rats or dogs) and humans, because it is generally believed that the GFR accurately reflects the renal function. (Lin 1995)

Renal clearances can also be predicted by incorporating a 'correction factor' as shown in equation :(Mahmood 2005)

$$\text{(Glomerular filtration rate*Kidney blood flow)/(Body weight*Kidney weight)}$$

Equation 23

The concept of a 'correction factor' is based on the fact that renal secretion of drugs is influenced by blood flow. It has been advocated in the literature that drugs which are mainly eliminated by the renal route, can generally be scaled across species reasonably well. (Mahmood 2005) This is not necessary true. There are many drugs renally secreted and, for a given drug, the nature of renal excretion may vary from species to species. The renal excretion of drugs may follow filtration, reabsorption, or secretion or different combinations of these processes. Is is also possible that a particular drug may exhibit secretory mechanism in animals, whereas in humans this drug may be only filtered or reabsorbed.(Mahmood 2005)

4.1.1.2 Prediction of human clearance for biliary excretion of drugs

Besides being eliminated from the body by metabolism, by the renal route or by both mechanisms, drug eliminated into bile may undergo enterohepatic recycling. The amount of an organic chemical that is excreted in bile varies widely among species. In general, mice, rats and dogs are good biliary excreters, while rabbits, guinea pigs, monkeys and humans are relatively poor biliary excreters. Species differences in hepatic blood flow and bile flow do not seem to correlate with the biliary excretion of compounds.(Smith 1971; Smith 1973.) Thus, it is difficult to predict the biliary excretion of drugs in humans from animal data. Mahmood et al.(Mahmood 2005) compared ten approaches such as the simple allometric approach; the rule of exponents; the rule of exponents with a correction factor; the ratio of human and monkey liver blood flow (MLBF) clearance; product of clearance and bile flow; product of clearance and uridine diphosphate glucuronyltransferase (UDGPT); product of clearance, bile flow, and UDGPT; and a modified version of the last three approaches in association with the rule of exponents. The results indicate the rule of exponents with the correction factor is the best approach for the prediction of human clearance for drugs which are excreted in the bile. The worst approach is the product of clearance, bile flow, and UDGPT. The simple allometry and the monkey liver blood flow (MLBF) approaches gave almost similar results. For some drugs the simple allometry predicted clearance was better than the MLBF approach and vice versa.(Mahmood 2005) Again, it is very difficult to generalize and empirical data are always needed to confirm the approach.

5. Cisatracurium

Cisatracurium was chosen as the model drug for two of our studies and its physicochemical, PK and PD characteristics will be detailed below.

5.1 Chemical Structure

Cisatracurium besylate, one of the 10 stereoisomers that constitute atracurium besylate, is a NMBA with an intermediate duration of action (fig. 6). This R-R' optical isomer in the cis-cis configuration, accounts for 14% of the atracurium besylate mixture. (Welch et al. 1995)

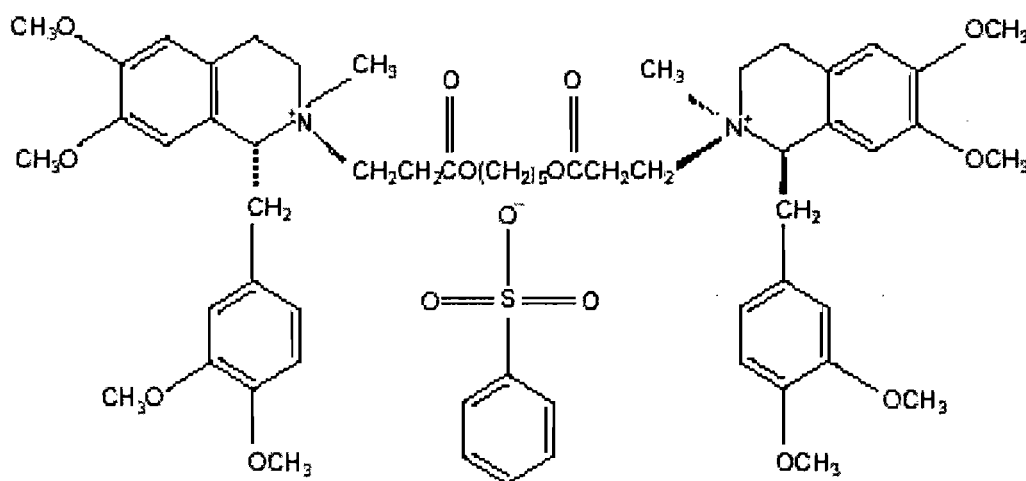


Figure 6. Structural formula of cisatracurium besylate

5.2 Pharmacokinetics

Organ-independent Hofmann elimination is the predominant pathway for the elimination of cisatracurium. In vitro work in Sørensen buffer (pH 7.4, 37°C) and plasma (pH 7.39 to 7.42, 37°C) from nine healthy volunteers suggests that cisatracurium besylate undergoes temperature and pH-dependent Hofmann elimination to form laudanosine and a monoquaternary acrylate metabolite (fig.7). (Welch et al. 1995) The monoquaternary

acrylate then undergoes ester hydrolysis, via nonspecific plasma esterases, to form the monoquaternary alcohol metabolite and acrylic acid. In turn, the monoquaternary alcohol undergoes Hofmann elimination, at a much slower rate than cisatracurium besylate, to form a second molecule of laudanosine. The degradation rate of cisatracurium besylate in Sørensen buffer and plasma was similar in the presence or absence of a nonspecific plasma esterase.(Welch et al. 1995) However, the formation rate of the monoquaternary alcohol from the monoquaternary acrylate was significantly reduced by the addition of the nonspecific esterase,(Welch et al. 1995) suggesting that ester hydrolysis was not a metabolic pathway for the direct metabolism of cisatracurium besylate.

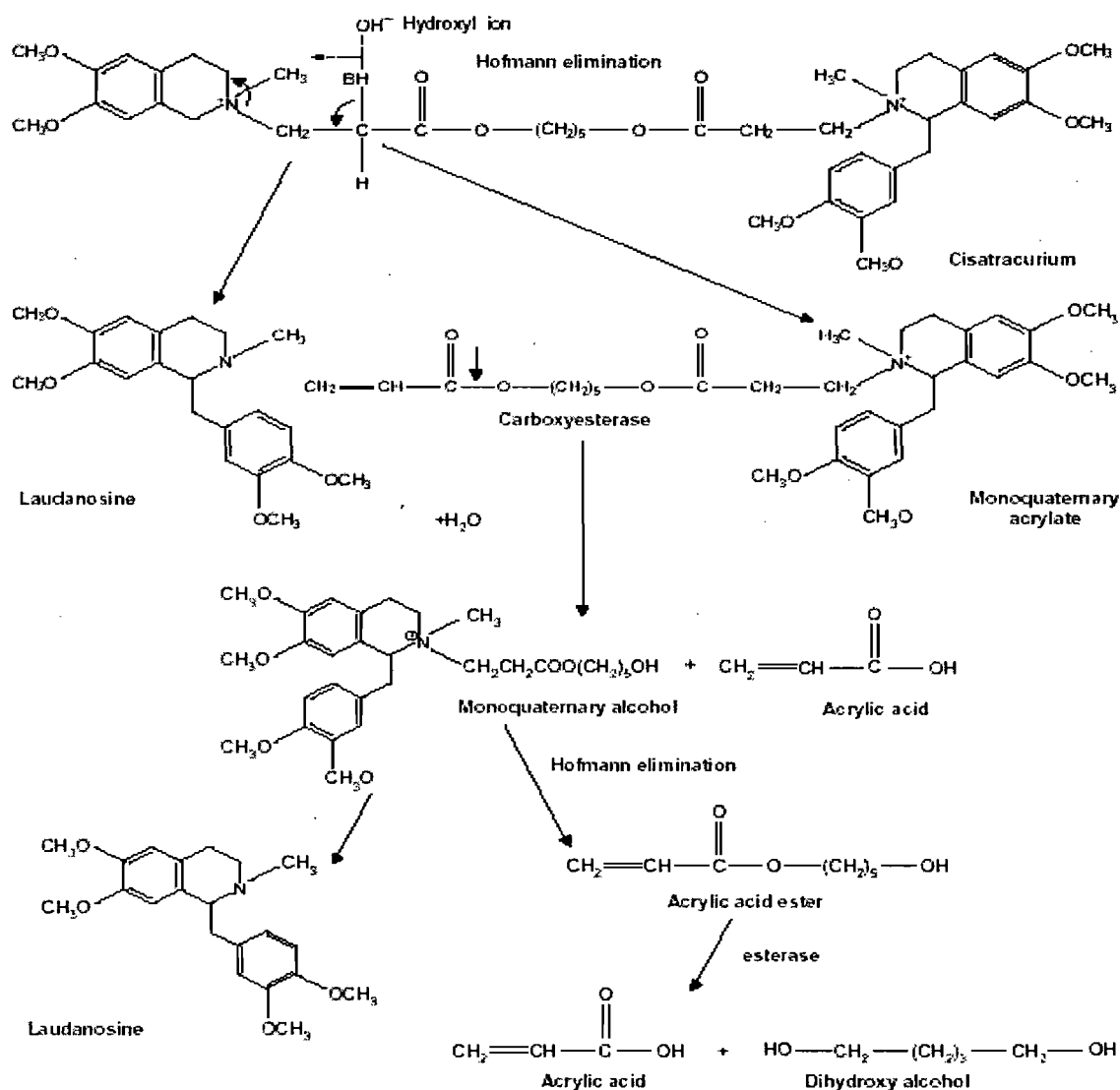


Figure 7. Proposed metabolic elimination pathways for cisatracurium besylate in human plasma.

Using pharmacokinetic models that assume drug elimination from the central compartment only, the $V_{d_{ss}}$ of cisatracurium in healthy adults ranges from 0.11 to 0.16 l/kg Table 3. However, as Hofmann elimination is the predominant elimination pathway of cisatracurium, the values obtained from these studies may therefore underestimate $V_{d_{ss}}$. (Bergeron et al. 2001; Kisor et al. 1996; Lien et al. 1996) Recently, we have shown in our laboratory, that when peripheral elimination of a drug is suspected, k_{20} can either

be assumed to be equal to $k_{in\ vitro}$ ideally obtained from each patient's or animal's plasma or equal to the terminal elimination rate constant, β . If it has already been demonstrated that if $\beta = k_{in\ vitro}$ for a given patient or animal, then k_{20} could be fixed to β without the necessity of performing further in vitro studies.

Table 4. Cisatracurium pharmacokinetic parameters

Reference	Population	Sampling	Dose (mg/kg)	N	$T_{1/2\beta}$ (min)	Vd_{ss} (l/kg)	CL (ml/min/kg)
(Boyd et al. 1996)	Intensive care unit patients	NA	0.18 infusion (1 hr)	6	27.6 ± 3.6	0.317 ± 0.006	8.0 ± 1.1
(Sorooshian et al. 1996)	Adults	Venous	0.1 IV bolus	31	28.4	0.133 ± 0.045	4.5 ± 0.8
	Elderly	Venous	0.1 IV bolus	33	36.3	0.190 ± 0.065	4.5 ± 1.8
(De Wolf et al. 1996)	Adults End-stage liver disease	Arterial	0.1 IV bolus	11	23.5 ± 3.5	0.136 ± 0.007	5.7 ± 0.8
		Arterial	0.1 IV bolus	14	24.4 ± 2.9	0.136 ± 0.007	6.6 ± 1.8
(Eastwood et al. 1995)	Adults	Venous	0.1 IV bolus	15	30.0 ± 1.2	0.161 ± 0.023	4.2 ± 0.14
	Renal disease	Venous	0.1 IV bolus	17	34.2 ± 1.2	0.195 ± 0.038	3.85 ± 0.18
(Schmith et al. 1997)	Adults	Venous Arterial	0.015-0.8 IV bolus	241	NA	0.145 ± 0.016	4.57 ± 2.8

(Ornstein et al. 1996)	Eldly	Arterial	0.1 IV bolus	12	25.5 ± 3.7	0.126 ± 0.016	5.0 ± 0.9
	Young		0.1 IV bolus	12	21.5 ± 2.4	0.108 ± 0.013	4.6 ± 0.8
(Bergeron et al. 2001)	Adults	Arterial	0.075 IV bolus	15	NA	0.192 ± 0.033	5.77 ± 0.96
			0.15 IV bolus	16	NA	0.173 ± 0.031	5.24 ± 1.05
			0.3 IV bolus	17	NA	0.189 ± 0.039	5.27 ± 1.08
(Tran et al. 1998)	Adults	Arterial	0.1 infusion (5 min)	14	23.9 ± 3.3	0.118 ± 0.027	3.7 ± 0.8
(Imbeault et al. 2006)	Children	Venous	0.1 IV bolus	9	22.9 ± 4.5	0.207 ± 0.031	6.7 ± 0.7

Total body clearance of cisatracurium is 0.27 l/h/kg and is independent of dose (Bergeron et al. 2001; Lien et al. 1996) It correlates positively with V_{ss} , which is not surprising, since Hofmann degradation occurring within whole body is organ independent and responsible for 77% of the elimination of cisatracurium. The $t_{1/2\beta}$ of cisatracurium in healthy adults ranges from 22 to 35 minutes, which is longer than that of atracurium (21 minutes).(Fahey et al. 1984; Parker and Hunter 1989) Population pharmacokinetic analyses performed on data from healthy adult patients undergoing surgery showed that certain covariate such as age, anesthesia type, obesity were associated with statistically significant effects on clearance or volume of the central compartment of cisatracurium besylate. These covariates were not associated with clinically significant changes in the predicted recovery profile of cisatracurium besylate.(Schmith et al. 1997)

Compared with children, steady-state volume of distribution and total body clearance were significant larger than those published for adults.(Imbeault et al. 2006) Compared with young adults, the $V_{d_{ss}}$ of cisatracurium was increased by 17 to 38 % and the $t_{1/2\beta}$ by 19 to 28% in the elderly.(Ornstein et al. 1996; Sorooshian et al. 1996) No difference between elderly and young adult patients in CL was shown. However, the values for $V_{d_{ss}}$ reported for these patients were most likely underestimated, as the models applied did not account for elimination from the peripheral compartment. Also interestingly, the relationships between the pharmacokinetic variables (e.g., CL and $V_{d_{ss}}$), were not seen in these studies. The reason for this is not clear.

Renal dysfunction has no effect on the Vd_{ss} of cisatracurium. Clearance was reduced by 13% and $t_{1/2\beta}$ increased by 14% in renal dysfunctional patient group. These changes are probably explained by a reduction in renal elimination.(Eastwood et al. 1995) In patients with liver disease given cisatracurium, the Vd_{ss} was increased by 21% and CL by 16%; this resulted in no change in $t_{1/2\beta}$.(De Wolf et al. 1996)

Following a 38-hour infusion of cisatracurium in critically ill patients, the CL, Vd_{ss} and $t_{1/2\beta}$ were 33 L/h, 22 L and 28 minutes, respectively. These results suggest that cisatracurium is noncumulative in this patient group. CL and Vd_{ss} are both increased in these patients with oedema. (Boyd et al. 1996)

The binding of cisatracurium to plasma proteins has not been successfully studied due to its rapid degradation at physiologic pH. Inhibition of degradation requires nonphysiological conditions of temperature and pH which are associated with changes in protein binding.

5.3 Pharmacodynamics

In healthy adults receiving nitrous oxide/opioid/ barbiturate anesthesia, on a molar basis, cisatracurium besylate is 3.5 times more potent than atracurium besylate, with an ED_{95} of 0.05 mg/kg.(Belmont et al. 1995; Lepage 1994) With bolus doses of 3 and 4 times the ED_{95} (0.15 and 0.2 mg/kg, respectively), the mean time to 90% suppression (90% neuromuscular block) was 3.4 and 2.8 minutes, respectively.(Bluestein et al. 1996) As expected, the time of onset of neuromuscular block decreased as the dose of

cisatracurium besylate increased.(Belmont et al. 1995; Bluestein et al. 1996; Lepage 1994) Also as it would be expected, the clinically effective duration of neuromuscular block (the time from injection to 25% recovery of neuromuscular function) increased with increasing cisatracurium besylate dose in a predictable fashion. (Belmont et al. 1995; Lepage 1994)

The onset of block was delayed by 1 minute in the elderly, which could be explained by a reduction in cardiac output. There was no difference in the recovery profile between the young and elderly groups.(Ornstein et al. 1996; Sorooshian et al. 1996)

In the healthy and renal failure patients who received cisatracurium, there were no significant differences in any of the onset or recovery variables. In patients with liver diseases given cisatracurium, onset of block was delayed by 1 minute but there was no alteration in the recovery profile.(De Wolf et al. 1996)

Table 5. Cisatracurium pharmacodynamic parameters

Reference	Population	Anesthesia	Dose (mg/kg)	N	Monitoring	Maximum Block (%)	Onset (min)	25% Recovery (min)
(De Wolf et al. 1996)	Adults End-stage liver disease	Nitrous oxide-oxygen, thiopentone, fentanyl, midazolam, isoflurane	0.1 IV bolus	11	TOF	99.8 ± 0.6	3.3 ± 1.0	46.9 ± 6.9
			0.1 IV bolus	12	TOF	99.5 ± 1.4	2.4 ± 0.8	53.5 ± 11.9
(Ornstein et al. 1996)	Elderly Young	nitrous oxide-oxygen, isoflurane, fentanyl	0.1 IV bolus	12	TOF	99.0 ± 1.8	3.4 ± 1.0	61.1 ± 13.8
			0.1 IV bolus	12	TOF	99.5 ± 1.0	2.5 ± 0.6	55.6 ± 9.3
(Bergeron et al. 2001)	Adults	nitrous oxide-oxygen, propofol, fentanyl	0.075 IV bolus	15	TOF	99.2 ± 2.4	4.8 ± 2.3	35.3 ± 5.8
			0.15 IV bolus	16	TOF	99.3 ± 2.6	2.4 ± 0.6	58.9 ± 10.4
			0.3 IV bolus	17	TOF	100.0 ± 0.0	1.8 ± 0.5	81.5 ± 15.4
(Tran et al. 1998)	Adults	Nitrous oxide Sufentanil, propofol	0.1 infusion (5 min)	14	TOF	99.0 ± 2.0	6.7 ± 2.2	53 ± 9
(Imbeault et al. 2006)	Children	Nitrous oxide Fentanil, propofol	0.1 IV bolus	9	TOF	99.0 ± 0.0	2.5 ± 0.8	37.6 ± 10.2

5.4 Pharmacokinetic-Pharmacodynamic Relationship

The k_{e0} value ranged from 0.1 to 0.179 min^{-1} and the EC_{50} for cisatracurium besylate ranged from 89 to 168 mg/L in healthy adult surgical patients receiving a single bolus dose of cisatracurium besylate during opioid or inhalation anesthesia respectively. (De Wolf et al. 1996; Schmith 1996)

Slower equilibration delays between the plasma and effect compartment (decreased k_{e0}), corresponding to longer onset times, were observed in elderly vs young patients for cisatracurium (Sorooshian et al. 1996) whereas the effect compartment concentration at 50% block was similar in both patient groups.

PK/PD analysis revealed faster k_{e0} in pediatric patients for cisatracurium. This observation is compatible with the shorter onset observed in children when compared with adults. EC_{50} of cisatracurium besylate in healthy children undergoing surgery were similar to the values reported for healthy adults undergoing surgery. (Imbeault et al. 2006)

Using population pharmacokinetic approach in healthy adult patients revealed that patients with mild to moderate renal dysfunction [creatinine clearance 1.68 to 4.2 L/h (28 to 70 ml/min)] had a 16% slower k_{e0} than patients with normal renal function. (Schmith et al. 1997) In the presence of inhalational anesthesia, an increased k_{e0} is physiological based (i.e. altered distribution due to changes in regional blood flow associated with the use of inhalation anesthesia). Gender and the presence of obesity produced small changes in k_{e0} . Adult female patients undergoing surgery had a 14%

increase in k_{e0} compared with nonobese patients. However, these effects were not associated with any clinically significant alterations in the predicted onset or recovery profile for cisatracurium besylate. (Schmith et al. 1997)

In a recent dose-ranging study comparing the pharmacokinetic and pharmacodynamic (PK/PD) parameters of three different doses of cisatracurium besylate in patients, a dose-dependent effect on PK/PD parameters was observed.(Bergeron et al. 2001) These findings have important clinical implication as the EC_{50} is the index of potency for NMBAs drugs and potency has a direct impact on the onset of action of these drugs. However, collection of data did not allow characterization of the initial mixing phase of cisatracurium (front-end kinetics). Hence, it was postulated that the dose-dependency observed resulted from methodological factors. The mean estimates for k_{e0} and EC_{50} values in Bergeron et al study are almost identical to those reported in Schmith et al's study using a parametric population approach.(Schmith et al. 1997) However, the interpatient coefficients of variability in the population analysis were quite higher (61 and 52%, respectively) than those reported by Bergeron et al (Bergeron et al. 2001) for each dose group (both less than 20%). As dose impact was not tested (considered as a covariate) in NONMEM population analysis, the possibility of a dose-related change in the PK/PD parameters was not examined.

Table 6. Cisatracurium pharmacokinetic/pharmacodynamic parameters

Reference	Population	N	METHODOLOGY				PK-PD PARAMETERS		
			Dose (mg/kg)	Anesthesia	Sampling		k_{e0} (min ⁻¹)	EC ₅₀ (ng/ml)	γ
					Site	Type			
(Sorooshian et al. 1996)	Adults	31	0.075	nitrous oxide, isoflurane, fentanyl	Venous	Limit	0.071	98	4.1
	Elderly	33	IV bolus		Venous	Limit	0.060	90	3.7
(De Wolf et al. 1996)	Adults End-stage liver disease	11	0.1 IV bolus	nitrous oxide-oxygen, thiopentone, fentanyl, midazolam, isoflurane	Arterial	Limit	0.179 ± 0.079	98 ± 34	4.0 ± 1.6
		12	0.1 IV bolus				0.145 ± 0.029	79 ± 33	4.7 ± 1.9
(Schmith et al. 1997)	Adults	241	0.015-0.8 IV bolus	Inhalation opioid	Venous Arterial	Limit	0.058 ± 0.116	141.0 ± 5.9	4.01 ± 3.6
(Bergeron et al. 2001)	Adults	15	0.075 IV	nitrous oxide-oxygen, propofol, and fentanyl	Arterial	Limit	0.087 ± 0.024	126 ± 21	5.10 ± 1.30
		16	bolus				0.081 ± 0.024	131 ± 30	4.98 ± 1.24
		17	0.15 IV bolus 0.3 IV bolus				0.070 ± 0.016	158 ± 27	5.39 ± 0.94
(Tran et al. 1998)	Adults	14	0.1 infusion (5 min)	Nitrous oxide Fentanyl propofol	Arterial	Intensive	0.054 ± 0.013	153 ± 33	6.9 ± 1.3
(Imbeault et al. 2006)	Children	9	0.1 IV bolus	Nitrous oxide Fentanyl propofol	Venous	Limit	0.115 ± 0.025	127 ± 27	6.5 ± 1.3

6. Research objectives

During anesthesia induction, NMBAS are administered to provide good intubating conditions and thus, their maximum effect should be induced rapidly. For agents with an ultra-rapid onset of action (succinylcholine) or when administered at high doses (cisatracurium), the relaxant effect occurs during the intravascular mixing phase, which complicates the analysis and interpretation of data.

The general aim of this thesis was to enhance knowledge and understanding of the impact of dose in the early concentration-effect relationship of neuromuscular agents in anesthetized patients and animals.

In particular, the three major objectives were:

1. To verify whether the relation concentration-effect of cisatracurium is dose-dependent in an animal model.
2. To compare the *in vitro* - *in vivo* correlation of cisatracurium in the anesthetized dog to that reported in anesthetized patients.
3. To develop and validate a pharmacokinetic model taking into account the intravascular mixing phase.

**7. Manuscrit No. 1: Dose-dependency of PK/PD parameters after
Intravenous bolus doses of cisatracurium**

(British Journal of Anaesthesia 2008 101(6):788-797)

ChunLin Chen¹, Nobuharu Yamaguchi¹ and France Varin^{1,2}

1. Faculté de pharmacie
Université de Montréal

2. Author to whom correspondence should be addressed :
France Varin
Université de Montréal
Faculté de pharmacie
C.P. 6128, Succursale Centre-ville
Montréal (Québec)
H3C 3J7
Canada
Tel: (514) 343-7016



RUNNING TITLE

Dose-dependency of PK/PD parameters

BACKGROUND: Pharmacokinetic/pharmacodynamic (PK/PD) parameters of neuromuscular blocking agents (NMBA) are generally assumed to be dose-independent. To our knowledge, there are very few clinical reports where the PK/PD parameters of a NMBA were derived separately for each dose group during a formal dose-ranging study. The primary objective of this study was to challenge a potential dose-dependency of cisatracurium PK/PD parameters by conducting a well controlled experimental study.

METHODS: Eight dogs were anaesthetized with pentobarbital and mechanically ventilated. Two doses of cisatracurium ($1.5 \times ED_{95}$ and $6 \times ED_{95}$) were administered in a randomized cross-over design after an appropriate wash-out period. Neuromuscular function was monitored using train-of-four (TOF) stimulation. Arterial blood was sampled continuously for the first min after cisatracurium injection and at frequent intervals thereafter. Cisatracurium plasma concentrations were determined by HPLC analysis. Pharmacokinetic-pharmacodynamic (PK-PD) modeling of individual data sets was performed with NONMEM using a non parametric approach and a descriptive sigmoid E_{max} model.

RESULTS: Cisatracurium PKs were linear over the dose range studied. Using non parametric PK-PD analysis, mean values for plasma - effect compartment equilibration delay (k_{e0}) were 0.0600 vs 0.1278 min^{-1} ($p < 0.05$) and sensitivity (EC_{50}) were 323 vs 235 ng ml^{-1} ($p < 0.05$) for the high and low doses, respectively.

CONCLUSIONS: A dose-dependent effect on the PK/PD parameters of cisatracurium bears important clinical implication as an accurate estimate of the EC_{50} is desirable. PK/PD parameters derived after intubating bolus doses of cisatracurium would be more reliable.

Key words: pharmacokinetics, pharmacodynamics, cisatracurium, dose-dependency, early pharmacokinetics.

Introduction

Over the range of doses used in clinical practice, the equilibration rate constant between plasma and effect compartment concentrations (k_{e0}) is believed to be concentration independent for most drugs.¹ However, this may not be the case after high bolus doses of drugs that reach maximum effect within the first two minutes after intravenous administration. There are very few reports where the PK/PD parameters of neuromuscular blocking agents (NMBAs) were derived separately for each dose group during a formal dose-ranging study. In a study² comparing the PK parameters of three different i.v. bolus doses of cisatracurium besylate (0.075, 0.15 and 0.3 mg kg⁻¹ corresponding to 1.5, 3 and 6 x ED₉₅) in anaesthetized patients, we previously observed a dose-dependent effect on pharmacokinetic/pharmacodynamic (PK/PD) parameters. These changes were observed without affecting the dose proportionality of PK parameters. This dose-dependency may have resulted from methodological factors because the plasma concentration profile was not characterized properly during the first 2 minutes.³ Similar changes in the dose-effect relationships had previously been reported for vecuronium in patients when using pharmacodynamic modeling.⁴ Changes that were later confirmed using a traditional PK/PD approach.⁵ Finally, clinical evidence has also been provided that the dose-response relationship of a NMBA may depend on the administration rate when high bolus doses are given. Dose requirements of cisatracurium were found significantly greater when given by high bolus (8 x ED₉₅) than with continuous infusion during cardiac surgery.⁶ The question whether PK/PD data obtained after very high bolus doses of NMBA should be included in a classical Sigmoid E_{max} model remained to be investigated. The primary objective of this study was to challenge

a potential dose-dependency of cisatracurium PK/PD parameters by conducting a well controlled experimental study.

Materials and Methods

Study design. The study was conducted as a two-period, randomized cross-over design including a washout period. Purpose-bred dogs were naïve animals kindly donated by a pharmaceutical company. Dogs were randomly allocated to two groups. Group A first received the low dose (1.5 x ED₉₅) while Group B first received the high dose (6 x ED₉₅). To provide a maximum control on experimental conditions, four persons were responsible for drug administration, arterial blood sampling, pharmacodynamic monitoring or sample processing. Their respective role remained unchanged throughout the study.

Chemicals. A commercial preparation of cisatracurium besylate (Nimbex[®], Abbott Canada Ltd. Montréal, Québec, Canada) was used. The internal standard (n-methyl laudanosine) was provided by Glaxo-Wellcome (Stevenage, UK). All solvents were of HPLC grade and purchased from Anachemia (Montréal, Québec, Canada).

Experimental conditions. The experimental protocol was approved by our institutional Animal Care Committee and was in accordance with the Canadian Council on Animal Care. Veterinary care and housing facilities met Good Animal Practice standards. For the study, eight adult male beagles (7.5 – 10.5 kg) were singly housed and maintained under a 12-h light/dark cycle at 21 ± 0.9 °C and 50 ± 10 % relative humidity. Food was freely available up to 18 h before experiment. There was no restriction for water.

General Anaesthesia. Dogs were anaesthetized with an initial injection of 30 mg kg^{-1} i.v. sodium pentobarbital (Somnotol®; Abbott Laboratories, Montréal, QC, Canada) administered in the cephalic vein of the left leg. Monitoring of the level of anaesthesia was based on haemodynamic parameters as well as neurosensory reflexes (hind feet retraction to pinching and cornea response to light touch). Measures were taken every 15 min as well as at blood sampling times. An adequate level of anaesthesia was maintained with supplemental i.v. doses of pentobarbital ($3 - 5 \text{ mg kg}^{-1}$). Respiration was controlled mechanically (Model 607, Harvard Apparatus, South Natick, MA) with room air delivered through an endotracheal tube.

Animal preparation. After satisfactory level of anaesthesia and stability of physiological parameters were achieved, the left femoral vein was cannulated for cisatracurium and pentobarbital administration. The right femoral artery was cannulated for blood sampling. A three-way stopcock was installed on the arterial line for arterial blood pressure monitoring. Haematocrit was measured after administration of each dose and at the end of the experiment. Heart rate was monitored via the arterial pulse. An electromagnetic flow probe (3mm i.d., model FR-030T, Nihon Kohden, Tokyo, Japan) was installed on the left femoral artery and connected to a polygraph system (model RM-6000, Nihon Kohden) for muscle blood flow measurement. The animal was kept warm using a heated surgical table and an insulated sheet. Central body temperature was monitored by means of a rectal probe and kept constant throughout the experiment with a controller. At the end of the experiment, animals were euthanized using an overdose of pentobarbital and saturated KCL before incineration.

Neuromuscular monitoring. The medial antebrachial cutaneous nerve was stimulated supramaximally (40 to 70 mA) at the right forelimb through surface electrode with a train-of-four (TOF) stimulation. Impulses of 0.2 msec duration were delivered at a frequency of 2 Hz for 2 sec. TOF stimulation was repeated every 12 seconds. The resulting force of contraction was measured using a force transducer (Grass F-10). A stabilization period where the tension of the first twitch (T_1) in the TOF did not change (baseline value) was allowed before injection of cisatracurium. Time zero for PD measures corresponded to 6 sec before drug injection to ensure that PK samples (drawn every 6 sec during the first min) were synchronized with the beginning and middle of each 12 sec TOF interval. Muscle relaxation was monitored continuously until full recovery. During the washout period, neurostimulation was stopped. A new baseline value was obtained before the second dose.

Blood sampling. After stabilization of anaesthesia and TOF response, a blank sample was drawn before the first bolus dose of cisatracurium besylate was administered. Drug administration was similar for both doses. Intravenous tubing was prefilled with the injectable drug solution and flushed completely over 2 sec (approximately 1/4 volume per 0.5 second). For the first minute, arterial blood was let to flow freely from a cannula into 2 ml Eppendorf tubes that were changed every six seconds. The diameter of this cannula was selected during preliminaries so that approximately 1 ml of blood could be collected in a 6 sec interval, yielding approximately 0.5 ml plasma. Thereafter, arterial blood samples (2 ml) were drawn directly from the stopcock and transferred into heparinized tubes at 1.5, 3, 5, 7, 15, 30, 45, 60 and 80 min. Additional samples were taken for the higher dose when full recovery was not reached. After a washout period, a

blood sample was drawn immediately before the injection of the second bolus (to document the residual plasma concentration, if any) and thereafter, as described above. The volume of blood taken was replaced by saline. To minimize the in vitro degradation of cisatracurium, samples were kept on ice water bath and centrifuged within 2 minutes at 4°C. Plasma was then transferred into pre-acidified tubes (30µl of 2M H₂SO₄) to obtain a final pH between 3 and 4 and frozen immediately on dry ice. Samples were stored at -70°C until analysis.

HPLC analysis. Plasma concentrations of cisatracurium were determined using a high performance liquid chromatograph coupled to a fluorescence detector set at 280 nm (excitation) and 320 nm (emission). Bond-Elut® phenyl solid-phase extraction cartridges (Varian, Harbor City, CA) were used for extraction of cisatracurium from plasma. The method published by Bryant et al⁷ for urine samples was slightly modified and validated for plasma in our laboratory. Cisatracurium was separated from its major metabolites on a Spherisorb SCX column (150 X 4.6 mm i.d., 5 µm; Phenomenex®, Torrance, CA, USA), using a stepwise gradient (Thermo Separation Products, Riviera Beach, FL, USA). The mobile phase changed from a first phase (14 mM Na₂SO₄ in 0.5 mM H₂SO₄: ACN: H₂O 40:60:6) during 5 min to a second phase (70 mM Na₂SO₄ in 0.5 mM H₂SO₄: ACN 40:60) during 6 min. The solvent flow rate was 2 ml min⁻¹ and the column maintained at 50°C. This assay proved to be sensitive (lower limit of quantification, 6.5 ng ml⁻¹), precise (mean coefficient of variation, 11%), and linear up to 2500 ng ml⁻¹ (r^2 : 0.995). Samples obtained during the first minute were diluted with blank plasma prior to extraction. Dilution algorithms were established during

preliminaries. When samples still exceeded the upper limit (generally between 30 and 90 sec), samples were further diluted and re-assayed. This procedure had been previously validated. When running diluted samples, a diluted quality control sample (QC) was extracted at the same time. The mean coefficient of variation for precision was 3.3 % with an overall bias of 5.4 %.

Pharmacodynamic analysis. Only the first twitch response (T_1) to the TOF was considered. The degree of neuromuscular block was expressed as percentage of twitch height depression relative to the T_1 baseline value. The first times where recovery reached final T_1 value and full recovery ($T_1=T_4$) were recorded. Onset time was defined as the time required for reaching maximum block after drug injection. Clinical duration was the time comprised between injection and recovery of twitch height to 25% of its baseline value. Recovery index, or the time elapsed between 25% and 75% twitch height recovery, was also measured.

Dose linearity of pharmacokinetics. Linearity in pharmacokinetics of the complete data sets was first verified using standard noncompartmental methods (WinNonLin Pro, Pharsight Corp, version 5.2). During the first minute, the time assigned to each sample was the midpoint of the 6 sec sampling interval. The terminal elimination rate constant, k_{el} , was determined by log linear regression. Dose-normalized AUCs of the plasma concentration vs time curve for the first minute (AUC_{0-1}) and for time zero to infinity ($AUC_{0-\infty}$) were calculated using trapezoidal integration. The maximum plasma concentration (C_{max}) and time to reach C_{max} (T_{max}) occurring during the first minute were read directly from the experimental data.

Nonparametric PK/PD analysis. All individual PK/PD analyses were performed using NONMEM VI (GloboMax LLC, Hanover, MD). We used a nonparametric approach^{5,8} where concentrations between the preceding and subsequent measured values are interpolated as a straight line when the concentrations are increasing and as a simple log-linear function when the concentrations are decreasing. The convolution of this with $k_{e0} \cdot e^{-k_{e0} t}$ calculates the effect site concentration-time profile. The effect site was then assumed to be linked to the plasma by a compartment of trivial volume with a first-order equilibrium constant (k_{e0}). The sigmoid E_{max} model was used to correlate the effect with the effect compartment concentration, thus computing the effect compartment concentration at 50% of maximal effect (EC_{50}) and the slope factor (γ). E_{max} values fixed to 100% or estimated were tested. Values for dose-normalized EC_{max} (EC_{max}/D) and T_{ECmax} were also estimated.

For the initial analysis, we used a two-stage approach in which the PK/PD values for each animal and each dose are determined independently. To determine whether the PK/PD parameters of cisatracurium varied as a function of dose, data from both doses were analyzed simultaneously. Two types of analyses were performed for each individual: (1) values for k_{e0} , EC_{50} and γ were assumed to be identical for both doses; and (2) values for k_{e0} , EC_{50} and γ were permitted to vary between doses. Goodness of fit was indicated by an improvement in the NONMEM objective function and by visual inspection of the fit of predicted versus observed values.

Statistical analysis. Based on our previous study², a sample size of 8 was estimated to provide 80% power to detect a 25 % difference in the EC₅₀ for the low and high dose with the expected standard deviation of ± 27 ng/ml at an alpha significance level of 0.05 (SigmaStat, version 3.1; Systat Software, Inc., Point Richmond, CA).

Physiological values, pharmacodynamic, pharmacokinetic and PK/PD parameters obtained in each animal after the high and low doses were compared using Paired t test with resampling technique⁹ using Insightful software version 8 (Seattle, WA, USA). NONMEM objective function (approximately - 2 log likelihood values) from the analyses in which k_{e0} , EC₅₀, and gamma were permitted to vary between doses were also analyzed using a paired-sample t test with resampling technique to determine whether this dose-related effect was systematic.

An analysis of variance (ANOVA) test was also carried out to exclude the presence of sequence or period effect for pharmacodynamic and PK/PD parameters (R 2.6.2 Software, the R Foundation for Statistical Computing). The factors included in the ANOVA were sequence, period (first vs second administration), treatment (high or low dose) and subjects nested within sequence. Therefore, results are presented as individual data (n=8) and expressed as mean values \pm standard deviation (SD) in the summary tables. The threshold for statistical significance (α) was set at 0.05.

Results

Physiological parameters are reported in Table 1. Arterial blood pressure, heart rate and hind limb vascular resistance were stable throughout the experiment (baseline and onset time data presented only). Haematocrit was similar during the first and second period ($38\% \pm 4\%$ vs $38\% \pm 4\%$, respectively).

The experimental time flow for each randomization sequence is summarized in Table 2. For the baseline value, a stabilization period of approximately 5 min was allowed before injection of cisatracurium. Times to recovery to final T_1 value and $T_1=T_4$ did not differ markedly. Recovery was assumed complete after a stable period of $T_1=T_4$ of approximately 5 min.

Return to 100% of baseline value was observed in 4 (low dose) and 3 dogs (high dose). When the final T_1 response did not return to the baseline value, all recovery parameters based on the twitch height were adjusted to the final T_1 value (normalization). After the low dose, normalization ranged from 95 to 107 % ($n = 4$) while it ranged from 89 to 111 % ($n = 5$) for the high dose. A systematic bias was ruled out statistically.

All 8 dogs reached 100% neuromuscular block after both doses (Table 3). After the high dose, 100% block lasted for 44 to 59 min (mean: 52). Onset time after the higher dose was decreased by approximately twofold compared with the lower dose. After the high dose, 4 to 8 measures of muscle twitch (mean: 6.6) that were not the 0 and 100% values were observed during onset of block. Clinical duration and recovery times were

increased by more than twofold after the high dose. No statistical difference was observed for the recovery index.

For illustration purposes, mean dose-normalized cisatracurium plasma concentrations versus time observed for each dose group were adjusted to a 0.1 mg kg^{-1} dose and found to be superimposable (Figure 1). Individual dose-normalized plasma concentrations observed during the first minute after the low and high dose are presented in Figure 2A and 2B, respectively. Prior to dose administration, cisatracurium plasma concentrations were always below the lower limit of quantification, thus confirming an adequate washout period. Cisatracurium peak concentrations occurred between 12 and 30 sec dosing in dogs.

Non compartmental PK parameters are listed in Table 4. Mean terminal elimination half-lives ($T_{1/2\beta}$) for the 0.15 and 0.6 mg kg^{-1} dose were 17.6 min and 17.8 min, respectively. No dose-dependency in any PK parameters was observed.

Mean dose-normalized cisatracurium effect compartment concentrations at each dose level are shown in Figure 3. At the time of the second dose, predicted effect compartment concentrations of cisatracurium were negligible. The hysteresis curves observed between plasma concentration and effect after a high and low dose in a representative dog are presented in Figure 4A. Using nonparametric PK/PD analysis, the corresponding sigmoid E_{\max} curves derived from the observed effect and predicted effect compartment concentration are presented in Figure 4B.

Table 5 shows the stepwise decrease in NONMEM objective function values ($-2 \log$ likelihood) for the investigated models. The largest decrease was observed with k_{e0} (step 1). Then, addition of EC_{50} further decreased the objective function value (step 2). However, there was no significant benefit to adding distinct values of gamma for the two dose groups (step 3).

With the final model, k_{e0} values were typically twofold lower after the high dose compared to the low dose values. A typical example of the collapsed hysteresis curve is presented in Figure 5. Sigmoid E_{max} curves were shifted to the right resulting in a 38 % higher predicted EC_{50} for the high dose (Table 6 and Figure 4B). Predicted E_{max} was used because the objective function was slightly better than when E_{max} was fixed to 100% . Only minor differences (less than 1%) were observed for the PK/PD parameters between the two approaches. Individual data for k_{e0} and EC_{50} at each dose level are represented in Figure 6. The results of the ANOVA showed no evidence of a statistically significant sequence or period effects for PK/PD parameters k_{e0} , EC_{50} , T_{ECmax} and EC_{max}/D (power greater than 80%).

Discussion

Using a nonparametric PK/PD approach and a descriptive sigmoid E_{max} model, a dose-dependent effect on the PK/PD parameters of cisatracurium was observed in anaesthetized dogs. Mean EC_{50} values increased and mean k_{e0} values decreased by almost 50% after the high bolus dose. Several factors have to be considered in the interpretation of this dose-dependency.

When conducting the animal study, experimental conditions were rigorously controlled to avoid any systematic bias. As both low and high bolus doses were given in each dog, any period and/or sequence effect in the cross-over design was statistically ruled out before pooling data. At each dose level, there were no significant changes in muscle blood flow or hind limb vascular resistance during onset time when compared to baseline values, excluding changes in regional haemodynamics as a potential bias. Instead of giving a continuous infusion, small doses of pentobarbital were given when indicated by corneal reflex. This approach was preferred because, once catheters were installed, there were no manipulations of the animal. These small doses did not produce any noticeable effect on physiological parameters.

It is well recognized that the blood sampling schedule during the first minute after a bolus of a neuromuscular blocking agent may have a significant impact on the estimation of its PK and, in turn, PK/PD parameters.¹⁰⁻¹² Plasma concentrations were therefore measured frequently during the first minute after each administration of cisatracurium to our dogs. We have first confirmed that the pharmacokinetic parameters

of cisatracurium obtained for the complete and first minute data sets were both linear before proceeding to the PK/PD analysis. Therefore, the dose-dependent effects are not likely to result from differences in the central pharmacokinetics.

Given the fourfold difference in dose, a higher span of plasma concentrations were observed at a given degree of block during onset of action (ascending limb) while the concentrations associated to a given effect did not vary greatly during recovery (descending limb) of the hysteresis curves (Figure 4A). This difference did not have a major impact on the efficiency of the link model since plasma concentrations from both the onset and recovery limbs were adequately collapsed, and that, independently of the dose given (Figure 5). Many data points were either 0 or 100 % after the higher dose, rendering the collapsing of the hysteresis loop mostly dependent on the ascending and descending limbs. This potential modeling artifact cannot be excluded, however it is unclear to what extent it may contribute to the rightward shift of the effect vs effect compartment concentration curve after the higher bolus dose.

Onset time ($T_{E_{max}}$) is dose-related when neuromuscular blocking agents (NMBAs) are given at doses producing complete block.¹³ Conversely, time to peak effect compartment concentration ($T_{EC_{max}}$) coincides with onset time only when the pharmacologic effect is submaximal and had therefore to be derived mathematically for the present study. While $T_{EC_{max}}$ is generally assumed to be dose-independent¹, it was significantly delayed after the higher dose in our dogs. Thus, a shorter onset time was associated with a longer $T_{EC_{max}}$. This apparent discrepancy can be explained by the fact that, for a given drug, calculated $T_{EC_{max}}$ depends solely on the plasma-effect

compartment equilibration rate (k_{e0}). It is noteworthy that a shorter onset is not always associated with a faster k_{e0} as this proved to be the case for succinylcholine.¹⁴ Since the rate limiting factors for k_{e0} and onset times are different, the net effect may differ.

The equilibration rate k_{e0} lumps together access to the receptor and any other post-receptor event that might contribute to time delays in response. As previously mentioned, the equilibration rate k_{e0} is believed to be concentration independent for most drugs at doses generally used in clinical practice, and is thus presented as a constant value.¹ However, this appeared not to be the case in our study where a significant decrease in k_{e0} was observed in the higher bolus dose group. According to our stepwise exploration, there was a statistically significant improvement in the objective function when k_{e0} values were allowed to change in the two dose groups. The first determinant single parameter for adequate fitting of the PK/PD model was k_{e0} , while changes in both the EC_{50} and k_{e0} came second. At high input rates, plasma concentrations rise more rapidly than do effect-site concentrations. As a result, circulation delays and effect site/plasma equilibration times become determinant.¹⁵

In view of its high molecular weight, low lipid solubility and ionic nature, the transcapillary transfer of cisatracurium is expected to be mostly restricted to pores.¹⁴ In the human forearm, the intercellular pore radius is approximately 16 nm¹⁶. In addition, muscle capillaries present numerous membranous vesicles¹⁷ that, after transient fusion, would create transendothelial channels or “small pores”.¹⁸ It is unknown whether these pore sizes are different in canines but capillary permeability in the muscle tissue was found similar across mammalian species.¹⁹ In addition, microperoxidase (molecular

weight of 1, 900 and molecular span of 2 nm) was found to diffuse readily through the small pore of muscle capillary in rats.²⁰ Since the molecular span of many NMBAs is approximately 2 nm between both quaternary amines²¹, transcapillary exchange should not be a rate limiting step for cisatracurium. Muscle interstitial concentrations of rocuronium measured by microdialysis under steady-state conditions, were found equivalent to those predicted for the effect compartment²². Although cisatracurium is a larger molecule, it appears unlikely that restricted access to muscle interstitial space is responsible for the dose-dependency.

In our opinion, the mechanisms underlying the nonlinearity of the predicted effect compartment concentration of cisatracurium after a high bolus dose would most probably occur within the synaptic cleft itself. Although no anatomical barriers prevents diffusion of drugs from muscle interstitial space into the synaptic cleft,²³ there is a limited space (30-50 nm) available for diffusion of NMBAs within the synaptic cleft itself.²⁴ After a high bolus dose, a transient increase in the unbound concentration of cisatracurium may occur as nicotinic receptors and nonspecific sites become suddenly occupied, thus reducing the concentration gradient of unbound cisatracurium between the interstitial fluid and synaptic cleft. Due to the very high density of nicotinic receptors, a slower diffusion of NMBAs into this restricted space may ensue. The nerve terminal would also represent a physical barrier to the diffusion of NMBAs out of the cleft, thus enhancing the repetitive binding to acetylcholine receptors.²⁵ This concept of “buffered diffusion” was recently tested²⁶ and simulations predicted that time to peak effect would decrease when submaximal bolus doses of NMBAs are increased. However, our findings suggest that this may not apply for high bolus doses. All these

mechanisms related to “steric hindrance” may explain why the effect compartment concentration associated with a given effect is larger after the higher dose of cisatracurium (Figure 4B).

If steric hindrance is an issue, this effect should disappear during the recovery phase when the rapid changes in concentrations have stopped. Recovery is more akin to a steady-state situation. It would have been interesting to compare these results with post-tetanic count (PTC). It is a well established method of evaluating neuromuscular recovery during intense block²⁷ and constitutes an excellent mean to distinguish between intense and deep blocks, that may have allowed some better quantification.²⁸ Experimental confirmation of these hypotheses was beyond the scope of this study but deserve further studies.

Dose-dependent changes in the sensitivity of the neuromuscular junction were also observed in our dogs after the higher bolus dose of cisatracurium. Molecular size but also factors such as the flexibility of the molecule and its conformation in the biophase at the moment of interaction with the acetylcholine receptors would impact on the onset time and duration of action of NMBAs.²⁹ The size of the active cation has once been suggested as a limiting factor influencing the rate of onset of NMBAs.³⁰ Thus, physicochemical interactions as a potential mechanism should not be overlooked. Indeed, a good correlation was shown between EC_{50} values obtained in anaesthetized patients and molecular weight for a series of NMBAs.¹⁴ This finding is in agreement with the hypothesis that a restricted diffusion within the synaptic cleft may alter the potency of NMBAs.

As mentioned previously, there are very few reports where the PK/PD parameters of a NMBA were derived separately for each dose group during a formal dose-ranging study. A parametric population approach was applied to data gathered from 241 patients having received up to a 8 x ED₉₅ bolus dose of cisatracurium during eight prospectively designed Phase I-III studies.³¹ Their mean estimates for k_{e0} and EC₅₀ values are almost identical to those reported in Bergeron *et al*'s study² when compared to the mean value of the three doses. However, the interpatient coefficients of variability in the population analysis were quite higher (61 and 52%, respectively) than those reported by Bergeron *et al*² for each dose group (both less than 20%). As dose impact was not tested (considered as a covariate) in NONMEM population analysis, the possibility of a dose-related change in the PK-PD parameters was not examined.

Our findings clearly indicate that PK/PD data obtained after i.v. bolus doses that are beyond those used in clinical practice should be tested for linearity of PK/PD estimates before including them in the general model. For illustration purposes, using PK/PD parameters obtained after an intubating dose of cisatracurium to predict the effect after a high bolus dose would yield faster onset and recovery times than were actually observed (Figure 7). Alternately, if PK/PD parameters obtained for the high dose of cisatracurium were used to simulate the effect after an intubating dose, the predicted peak effect would be highly underestimated (Figure 8) and this would eventually lead to overdosing. These results bear important clinical implication as an accurate estimate of the EC₅₀ is desirable for target-controlled infusion systems. In our opinion, PK/PD parameters derived after an intubating dose of cisatracurium would be more reliable.

In conclusion, after 1.5 and 6 x ED₉₅ bolus doses of cisatracurium, the effect compartment concentration at 50% block (EC₅₀) increased and the effect compartment equilibration rate constant (k_{e0}) decreased at the higher dose when using a descriptive sigmoid E_{max} model. As this study was not meant to be mechanistic but descriptive, it is not possible to delineate whether the PK/PD dose dependency is a real phenomenon or a modeling artifact. Only hypotheses regarding the factors responsible of the dose-related changes in PK/PD parameters can be formulated and further confirmatory studies are required. In the meanwhile, these results indicate that dose impact should be tested when data gathered during dose-ranging studies are pooled to derive population PK/PD parameters. This is particularly the case after i.v. bolus doses of drugs having a rapid onset of action.

Acknowledgements

We would like to thank Johanne Couture and Sanae Yamaguchi for their technical support.

Funding

This research program was supported by the Canadian Institutes of Health Research (grant MA-10274).

References

1. Schnider TW, Minto CF. Predictors of onset and offset of drug effect. *Eur J Anaesthesiol Suppl* 2001; **23**: 26-31
2. Bergeron L, Bevan DR, Berrill A, Káhwaji R, Varin F. Concentration-effect relationship of cisatracurium at three different dose levels in the anesthetized patient. *Anesthesiology* 2001; **95**: 314-23
3. Paul M, Fisher DM. Pharmacodynamic modeling of muscle relaxants: effect of design issues on results. *Anesthesiology* 2002; **96**: 711-7
4. Bragg P, Fisher DM, Shi J, et al. Comparison of twitch depression of the adductor pollicis and the respiratory muscles. Pharmacodynamic modeling without plasma concentrations. *Anesthesiology* 1994; **80**: 310-9
5. Fisher DM, Szenohradszky J, Wright PM, Lau M, Brown R, Sharma M. Pharmacodynamic modeling of vecuronium-induced twitch depression. Rapid plasma-effect site equilibration explains faster onset at resistant laryngeal muscles than at the adductor pollicis. *Anesthesiology* 1997; **86**: 558-66
6. Cammu G, Boussemaere V, Foubert L, Hendrickx J, Coddens J, Deloof T. Large bolus dose vs. continuous infusion of cisatracurium during hypothermic cardiopulmonary bypass surgery. *Eur J Anaesthesiol* 2005; **22**: 25-9
7. Bryant BJ, James CD, Cook DR, Harrelson JC. High performance liquid chromatography assay for cisatracurium and its metabolites in human urine. *J Liquid Chromatogr Relative Technol* 1997; **20**: 2041-51
8. Struys MM, Coppens MJ, De Neve N, et al. Influence of administration rate on propofol plasma-effect site equilibration. *Anesthesiology* 2007; **107**: 386-96
9. Moore DS, McCabe GP. *Introduction to the Practice of Statistics*. New York: W.H. Freeman and Company, 2005
10. Ducharme J, Varin F, Bevan DR, Donati F. Importance of early blood sampling on vecuronium pharmacokinetic and pharmacodynamic parameters. *Clin Pharmacokinet* 1993; **24**: 507-18
11. Lacroix M, Donati F, Varin F. Pharmacokinetics of mivacurium isomers and their metabolites in healthy volunteers after intravenous bolus administration. *Anesthesiology* 1997; **86**: 322-30

12. Beaufort TM, Proost JH, Kuizenga K, Houwertjes MC, Kleef UW, Wierda JM. Do plasma concentrations obtained from early arterial blood sampling improve pharmacokinetic/pharmacodynamic modeling? *J Pharmacokinet Biopharm* 1999; **27**: 173-90
13. Minto CF, Schnider TW, Gregg KM, Henthorn TK, Shafer SL. Using the time of maximum effect site concentration to combine pharmacokinetics and pharmacodynamics. *Anesthesiology* 2003; **99**: 324-33
14. Roy JJ, Donati F, Boismenu D, Varin F. Concentration-effect relation of succinylcholine chloride during propofol anesthesia. *Anesthesiology* 2002; **97**: 1082-92
15. Gentry WB, Krejcie TC, Henthorn TK, et al. Effect of infusion rate on thiopental dose-response relationships. Assessment of a pharmacokinetic-pharmacodynamic model. *Anesthesiology* 1994; **81**: 316-24; discussion 25A
16. Driscoll DF. Lipid Emulsions in I.V. Therapy: Clinical and Pharmaceuticals Issues. *Anesthesiology News* 2000
17. Johansson BR. Size and distribution of endothelial plasmalemmal vesicles in consecutive segments of the microvasculature in cat skeletal muscle. *Microvasc Res* 1979; **17**: 107-17
18. Simionescu N, Simionescu M, Palade GE. Permeability of muscle capillaries to small heme-peptides. Evidence for the existence of patent transendothelial channels. *J Cell Biol* 1975; **64**: 586-607
19. Schmittmann G, Rohr UD. Comparison of the permeability surface product (PS) of the blood capillary wall in skeletal muscle tissue of various species and in vitro porous membranes using hydrophilic drugs. *Journal of Pharmaceutical Sciences* 2000; **89**: 115-27
20. Wissig SL. Identification of the small pore in muscle capillaries. *Acta Physiol Scand Suppl* 1979; **463**: 33-44
21. Bovet D, Bovet-Nitti F. *Structure et activité pharmacodynamique des médicaments du système nerveux végétatif*. Bâle: S.Karger, 1948

22. Ezzine S, Varin F. Interstitial muscle concentrations of rocuronium under steady-state conditions in anaesthetized dogs: actual versus predicted values. *Br J Anaesth* 2005; **94**: 49-56.
23. Nigrovic V, Proost JH, Amann A, Bhatt SB. Volume of the effect compartment in simulations of neuromuscular block. *Theor Biol Med Model* 2005; **2**: 41
24. Couteaux R. Structure and cytochemical characteristics of the neuromuscular junction. In: Cheymol J, ed. *Neuromuscular blocking and stimulating agents*. Oxford: Pergamon Press, Ltd, 1972: 7-56
25. Armstrong DL, Lester HA. The kinetics of tubocurarine action and restricted diffusion within the synaptic cleft. *J Physiol* 1979; **294**: 365-86
26. Proost JH, Houwertjes MC, Wierda JM. Is time to peak effect of neuromuscular blocking agents dependent on dose? Testing the concept of buffered diffusion. *Eur J Anaesthesiol* 2008; **25**: 572-80
27. Viby-Mogensen J, Howardy-Hansen P, Chraemmer-Jorgensen B, Ording H, Engback J, Nielsen A. Posttetanic count (PTC): a new method of evaluating an intense non-depolarizing neuromuscular blockade. *Anesthesiology* 1981; **55**: 458-61
28. Fuchs-Buder T, Claudius C, Skovgaard LT, Eriksson LI, Mirakhur RK, Viby-Mogensen J. Good clinical research practice in pharmacodynamic studies of neuromuscular blocking agents II: the Stockholm revision. *Acta Anaesthesiol Scand* 2007; **51**: 789-808
29. Tuba ZM, S.;Vizi, E.S. Synthesis and Structure-Activity Relationships of Neuromuscular Blocking Agents. *Current Medicinal Chemistry* 2002; **9**: 1507-36
30. Ramzan IM. Molecular weight of cation as a determinant of speed of onset of neuromuscular blockade. *Anesthesiology* 1982; **57**: 247-8
31. Schmith VD, Fielder-Kelly J, Phillips L, Grasela THJ. Prospective use of population pharmacokinetics-pharmacodynamics in the development of Cisatracurium. *Pharm Res* 1997; **14**: 91-7

Table 1. Physiological parameters during baseline and at onset time in pentobarbital anaesthetized dogs after sequential administration of two doses of cisatracurium. Dogs were randomized for sequence (n=8). Values represent mean \pm SD.

		0.15mg kg ⁻¹	0.6 mg kg ⁻¹		0.15 mg kg ⁻¹	0.6 mg kg ⁻¹	
		Baseline	Baseline	P value	Onset time	Onset time	P value
Heart rate	(bpm)	129 \pm 45	138 \pm 39	0.494	134 \pm 45	144 \pm 35	0.388
Systolic arterial pressure	(mm Hg)	129 \pm 22	131 \pm 32	0.872	127 \pm 24	143 \pm 31	0.164
Diastolic arterial pressure	(mm Hg)	89 \pm 18	98 \pm 24	0.262	93 \pm 21	94 \pm 27	0.880
Muscle blood flow	(ml min ⁻¹ kg ⁻¹)	7.4 \pm 3.4	6.8 \pm 3.9	0.690	8.0 \pm 3.6	7.1 \pm 4.4	0.564
Hind limb vascular resistance	(mmHg min kg ml ⁻¹)	17.7 \pm 11.0	21.8 \pm 12.9	0.332	16.7 \pm 10.4	23.0 \pm 14.8	0.092
Body temperature	(°C)	37.5 \pm 0.6	37.2 \pm 0.6	0.690	37.5 \pm 0.6	37.2 \pm 0.6	0.440

Table 2. Study time flow. Dogs were randomized for sequence (n=8). Values represent mean \pm SD.

During the washout period, neurostimulation was stopped.

Duration (min)	Sequence 1		Sequence 2	
	Dose 1	Dose 2	Dose 1	Dose 2
	0.15 mg kg ⁻¹	0.6 mg kg ⁻¹	0.6 mg kg ⁻¹	0.15 mg kg ⁻¹
Baseline stabilization	10.3 \pm 4.4	7.3 \pm 2.3	8.5 \pm 2.5	4.8 \pm 0.6
Bolus administration	0.033	0.033	0.033	0.033
Recovery time to final T1 value	28.0 \pm 5.3	63.5 \pm 10.9	77.0 \pm 12.2	35.7 \pm 6.7
Recovery time to T1=T4	33.2 \pm 5.2	70.6 \pm 10.8	90.1 \pm 18.7	40.6 \pm 4.9
Stable period of T1=T4	7.7 \pm 4.0	5.5 \pm 0.9	5.5 \pm 3.5	4.3 \pm 2.3
Wash-out period	124.5 \pm 5.8		92.1 \pm 6.1	

Table 3. Pharmacodynamic parameters in pentobarbital anaesthetized dogs after sequential administration of two doses of cisatracurium. Onset: time to maximum neuromuscular block; Max block: magnitude of maximum neuromuscular block. Duration: time to 25% recovery of twitch height; Recovery index: time from 25% to 75% recovery of twitch height. Dogs were randomized for sequence (n=8). Values represent mean \pm SD. *P < 0.05.

	0.15 mg kg ⁻¹	0.6 mg kg ⁻¹	P value
Onset (min)	2.14 \pm 0.48	0.98 \pm 0.17	0.012*
Max block (%)	100 \pm 0	100 \pm 0	1.000
Duration (min)	21.1 \pm 3.0	58.0 \pm 8.9	0.002*
Recovery times (min)			
25%	21.1 \pm 3.0	58.0 \pm 8.9	0.012*
50%	24.0 \pm 4.0	60.7 \pm 9.3	0.012*
75%	27.0 \pm 4.8	64.5 \pm 10.0	0.012*
Recovery index (min)	5.9 \pm 2.0	6.5 \pm 2.0	0.436

Table 4. Pharmacokinetic parameters in pentobarbital anaesthetized dogs after sequential administration of two doses of cisatracurium. C_{max}/D : dose-normalized maximum plasma concentration; T_{max} : time to reach C_{max} ; $AUC_{0-\infty}/D$: dose-normalized area under the curve from 0 to infinite; AUC_{0-1}/D : dose-normalized area under the curve from 0 to 1min; k_{el} : elimination rate constant. Parameters were normalized for a 0.1 mg kg^{-1} dose. Dogs were randomized for sequence (n=8). Values represent mean \pm SD.

		0.15 mg kg^{-1}	0.6 mg kg^{-1}	P value
C_{max}/D	(ng ml^{-1})	4678 ± 1806	4485 ± 767	0.766
T_{max}	(min)	0.26 ± 0.06	0.25 ± 0.11	0.406
$AUC_{0-\infty}/D$	(ng min ml^{-1})	9593 ± 1258	10383 ± 1655	0.294
AUC_{0-1}/D	(ng min ml^{-1})	1448 ± 296	1483 ± 249	0.772
k_{el}	(min^{-1})	0.0402 ± 0.0042	0.0409 ± 0.0096	1.000

Table 5. NONMEM Objective Function Values (-2 log Likelihood) obtained during stepwise exploration of dose impact on PK/PD parameters. k_{e0} : effect compartment equilibration rate constant; EC_{50} : effect compartment concentration at 50% of maximal observed effect; Gamma: slope factor. Obj: NONMEM Objective function value. Symbols (\equiv): One estimation for both doses. Symbols (Δ): Separate estimations for both doses. Values represent mean \pm SD. (n=8) * $P < 0.05$ for model discrimination.

	k_{e0} (min^{-1})	EC_{50} (ng ml^{-1})	Gamma	Obj	P value
Step 1	\equiv	\equiv	\equiv	286 \pm 30	
Step 2	Δ	\equiv	\equiv	239 \pm 33	0.006*
	\equiv	Δ	\equiv	272 \pm 24	0.310
	\equiv	\equiv	Δ	279 \pm 26	0.612
Step 3	Δ	Δ	\equiv	178 \pm 17	0.006*
	Δ	\equiv	Δ	237 \pm 32	0.907
Step 4	Δ	Δ	Δ	173 \pm 19	0.567

Table 6. PK/PD parameters in pentobarbital anaesthetized dogs after sequential administration of two doses of cisatracurium. EC₅₀: effect compartment concentration at 50% of maximal observed effect; T_{ECmax}: time required to reach EC_{max}; EC_{max}/D: dose-normalized maximum concentration in effect compartment; E_{max}: maximum block; k_{e0}: effect compartment equilibration rate constant; Gamma: slope factor. Parameters were normalized for a 0.1 mg kg⁻¹ dose. Dogs were randomized for sequence (n=8). Values represent mean ± SD. * P < 0.05

	0.15 mg kg ⁻¹	0.6 mg kg ⁻¹	P value
EC ₅₀ (ng ml ⁻¹)	235 ± 35	323 ± 57	0.006*
T _{ECmax} (min)	6.13 ± 0.79	10.69 ± 1.39	0.006*
EC _{max} /D (ng ml ⁻¹)	323 ± 30	226 ± 43	0.016*
E _{max} (%)	102 ± 1	102 ± 1	1.000
k _{e0} (min ⁻¹)	0.1278 ± 0.0224	0.0600 ± 0.0072	0.002*
Gamma	7.70 ± 5.44	7.70 ± 5.44	1.000

LIST OF FIGURES

Figure 1. Mean dose-normalized cisatracurium concentrations *versus* time for pentobarbital anaesthetized dogs after a dose of 0.15 mg kg^{-1} (black triangles) and 0.6 mg kg^{-1} (white circles). For illustration purpose, concentrations were normalized for a 0.1 mg kg^{-1} dose.

Figure 2. Individual mean dose-normalized cisatracurium plasma concentrations for the first minute after administration of 0.15 mg kg^{-1} (panel A) and 0.6 mg kg^{-1} (panel B) to pentobarbital anaesthetized dogs. For illustration purpose, concentrations were normalized for a 0.1 mg kg^{-1} dose.

Figure 3. Mean dose-normalized cisatracurium effect compartment concentrations *versus* time after a dose of 0.15 mg kg^{-1} (black triangles) and 0.6 mg kg^{-1} (white circles). For illustration purpose, concentrations were normalized for a 0.1 mg kg^{-1} dose.

Figure 4. Hysteresis curves (panel A) and Sigmoid Emax curves (panel B) derived for dog #1. 0.15 mg kg^{-1} dose (dashed line) and 0.6 mg kg^{-1} dose (solid line)

Figure 5. Collapsed hysteresis curves for a low dose (panel A) and high dose (panel B) for dog #1.

Figure 6. Intraindividual comparison of PK/PD parameters obtained for each dose of cisatracurium.

Figure 7. Temporal profiling of observed (black circles) *vs* simulated effect (solid line) after an i.v. bolus dose of $6 \times \text{ED}_{95}$ of cisatracurium. The dotted line represents the simulated effect obtained using the k_{e0} , EC_{50} and gamma values from the $1.5 \times \text{ED}_{95}$ dose with the same concentration-time profile. Faster onset and recovery times are predicted (dotted line).

Figure 8. Temporal profiling of observed (black circles) *vs* predicted effect (solid line) after an i.v. bolus dose of $1.5 \times \text{ED}_{95}$ of cisatracurium. The dotted line represents the simulated effect obtained using the k_{e0} , EC_{50} and gamma values from the $6 \times \text{ED}_{95}$ dose with the same concentration-time profile. Predicted peak effect (dotted line) is highly underestimated.

Figure 1

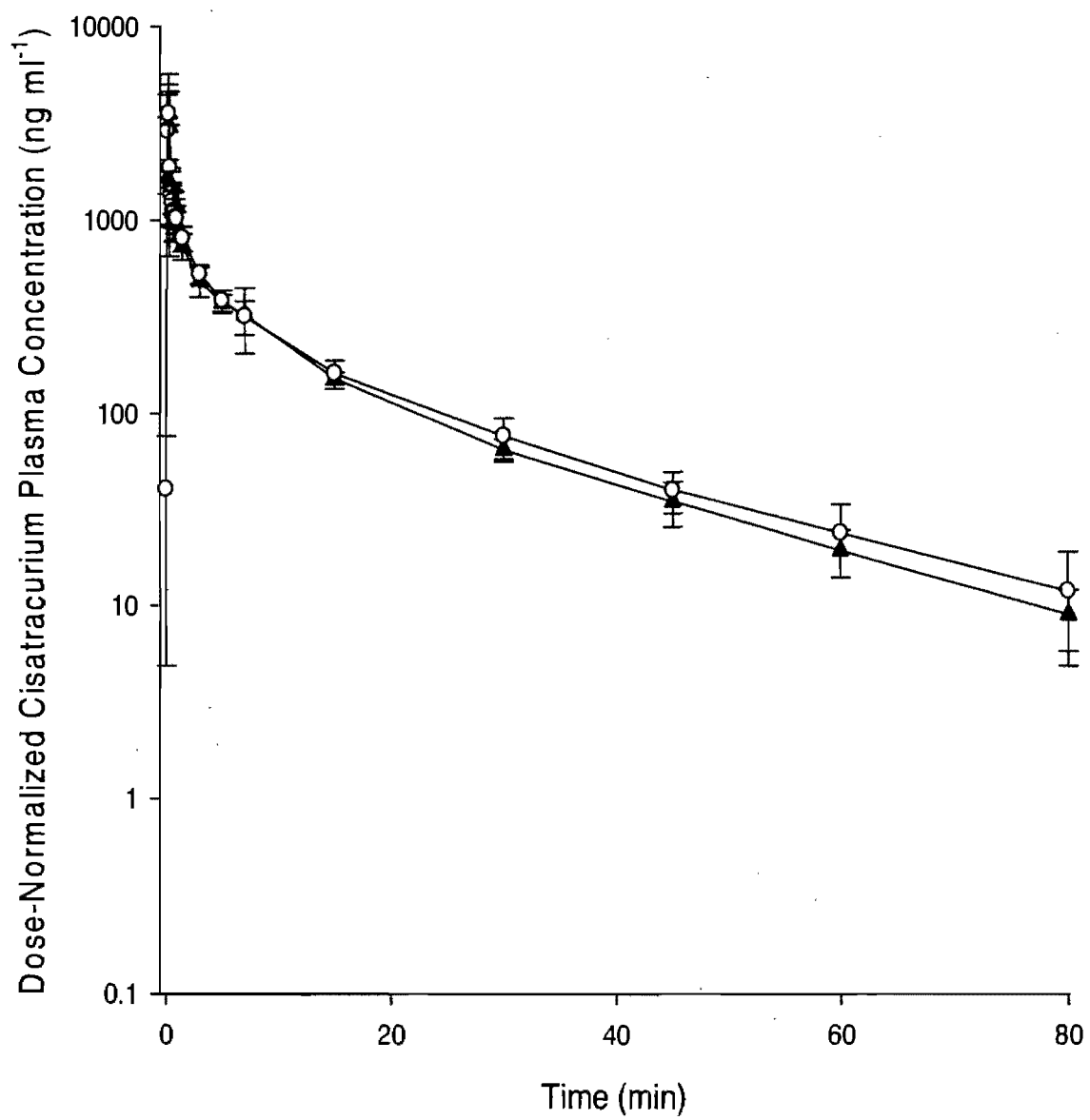


Figure 3

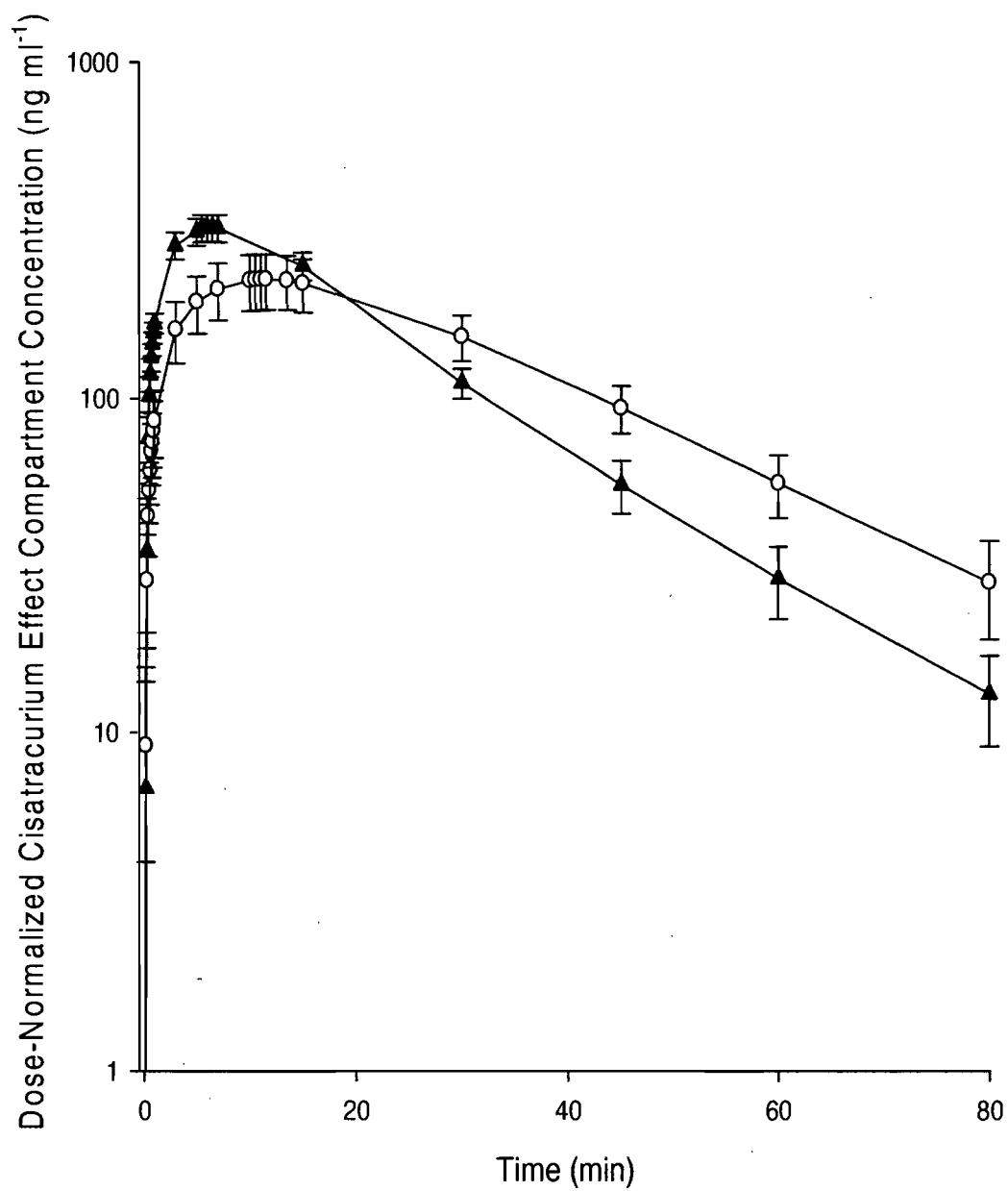


Figure 4

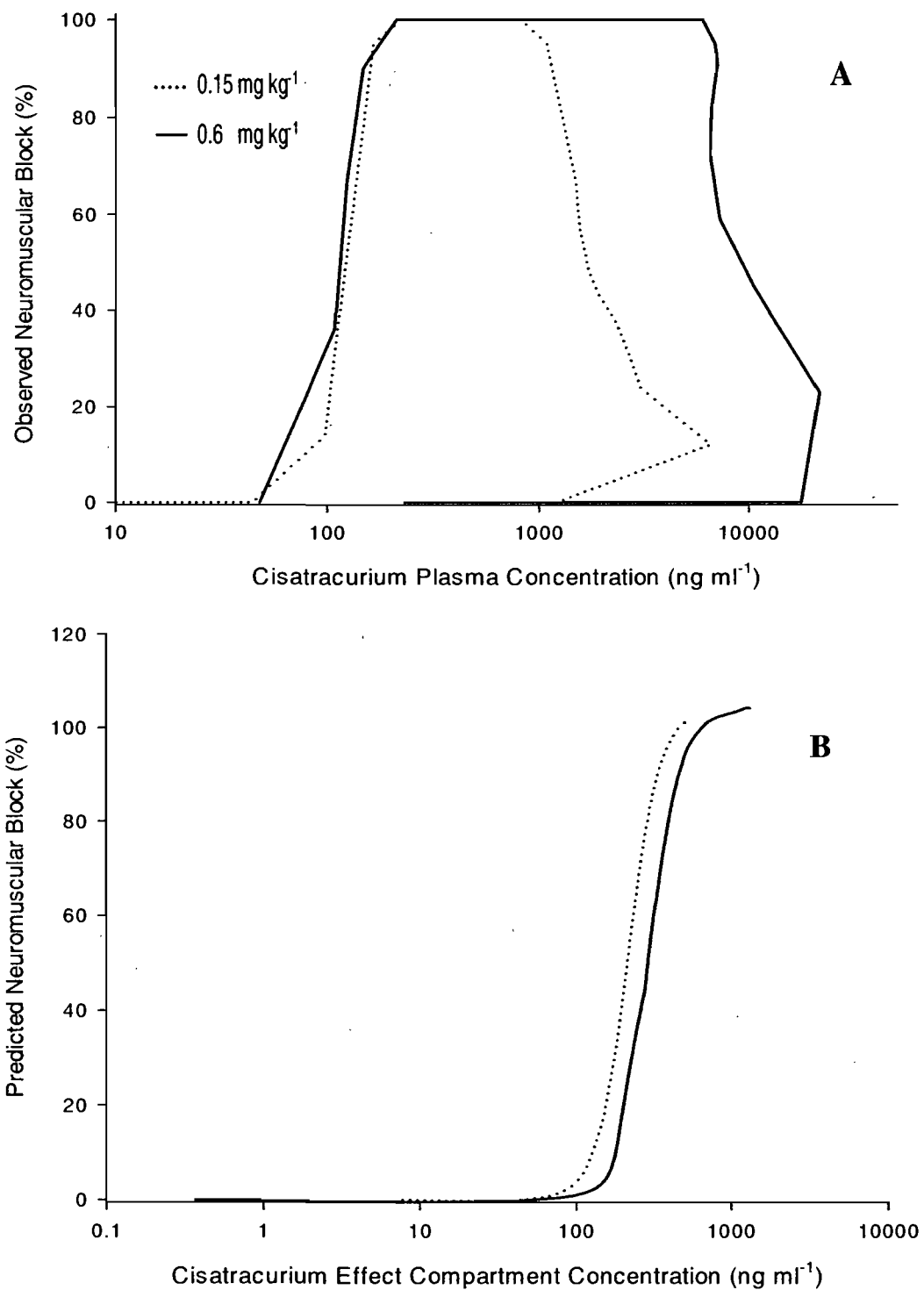


Figure 5

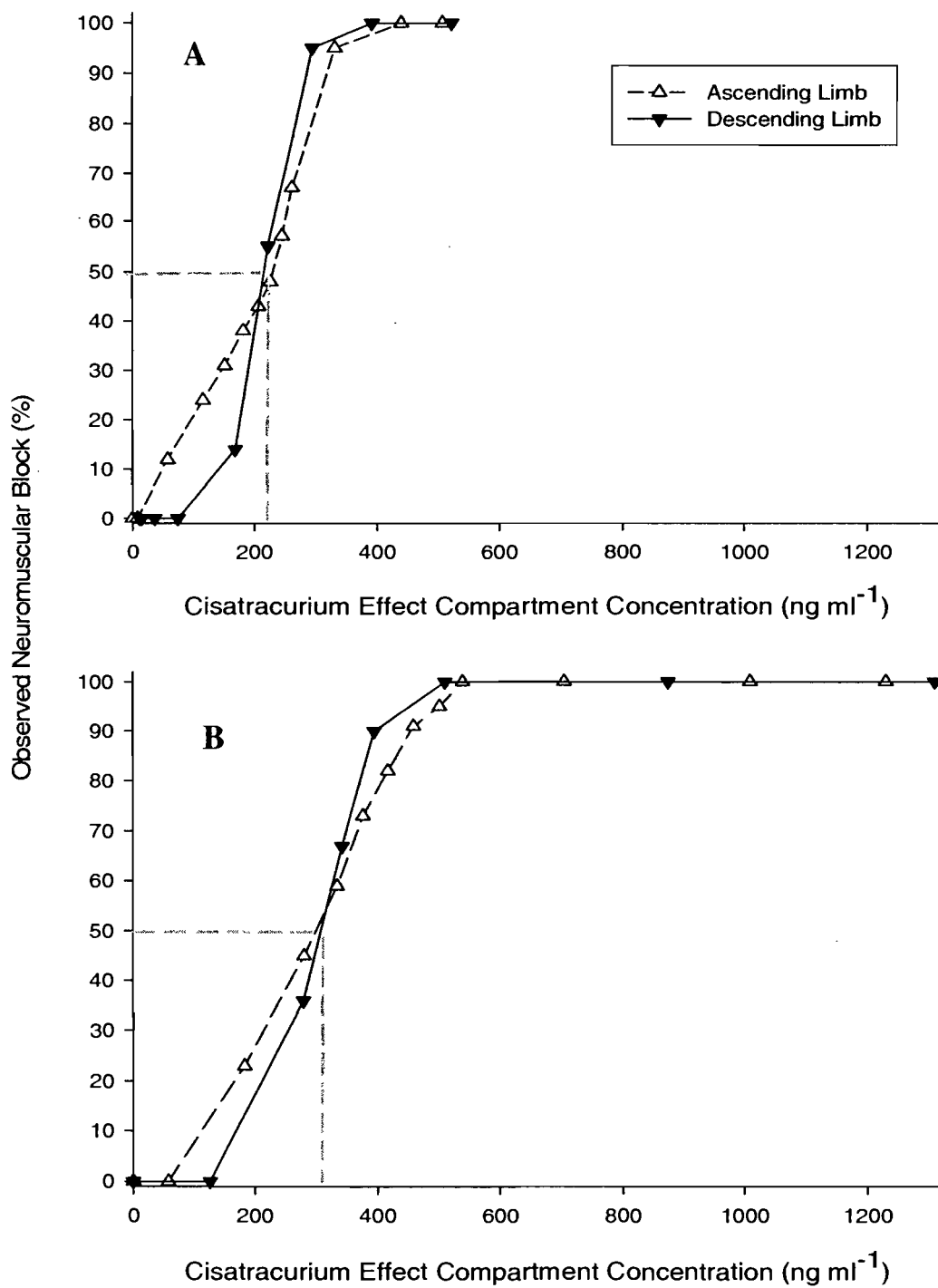


Figure 6

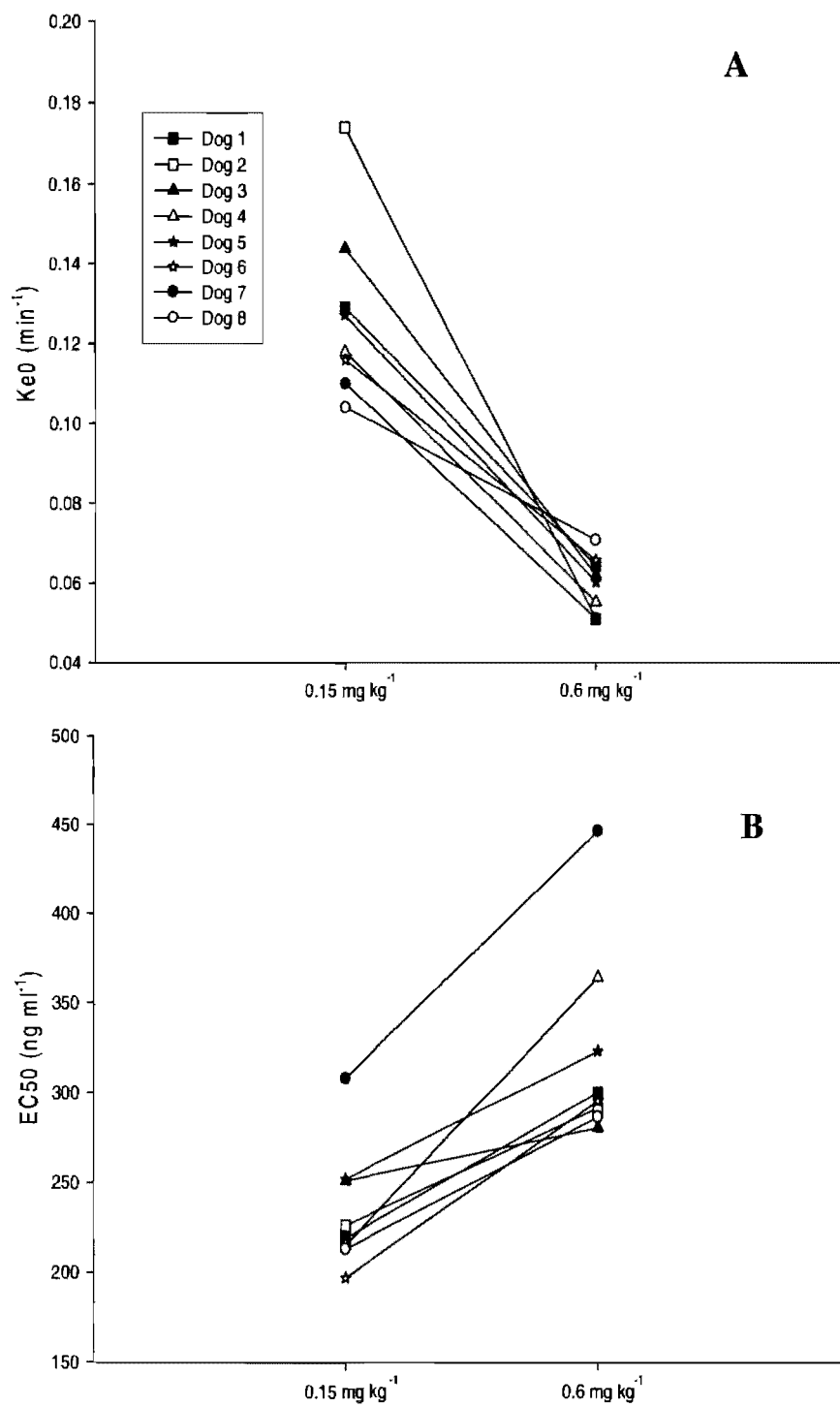


Figure 7

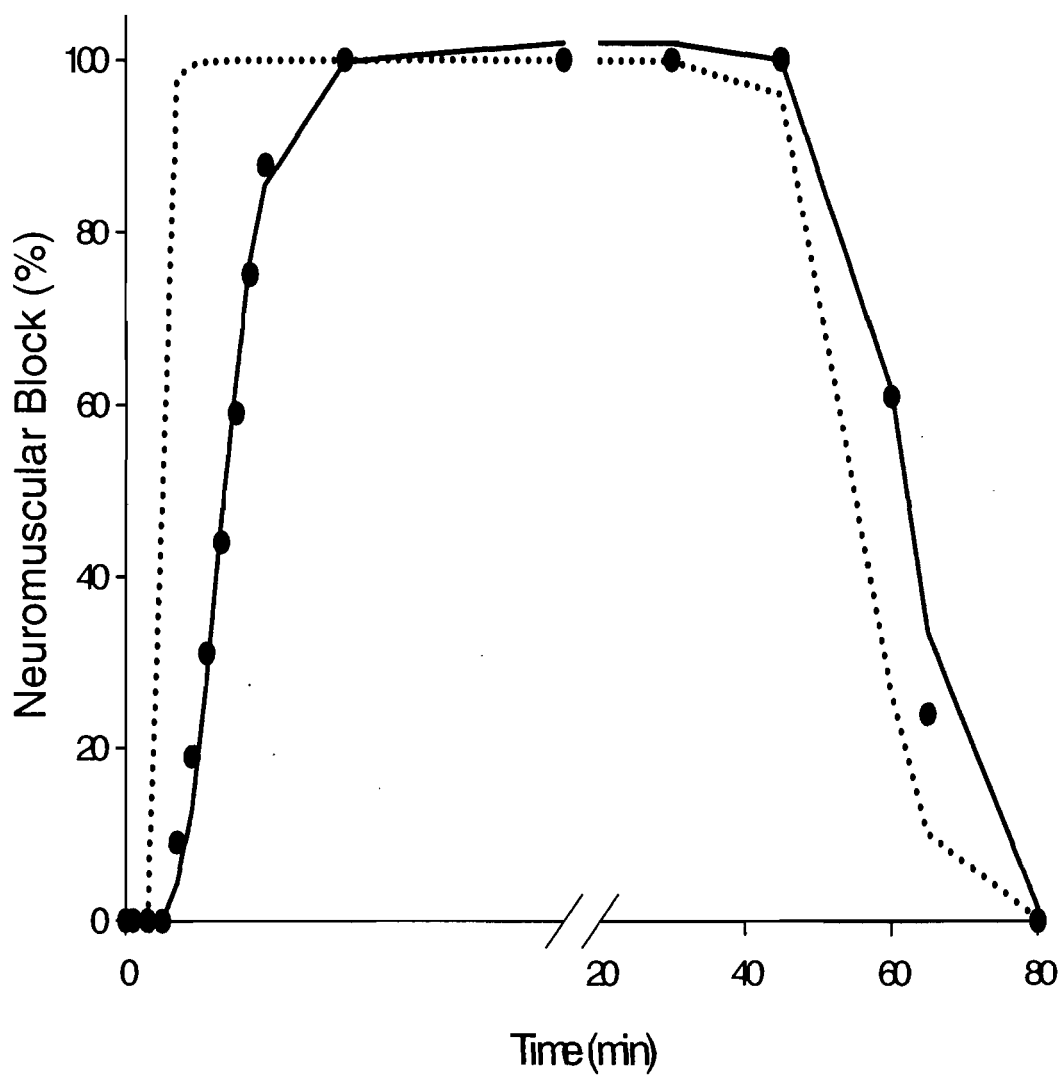
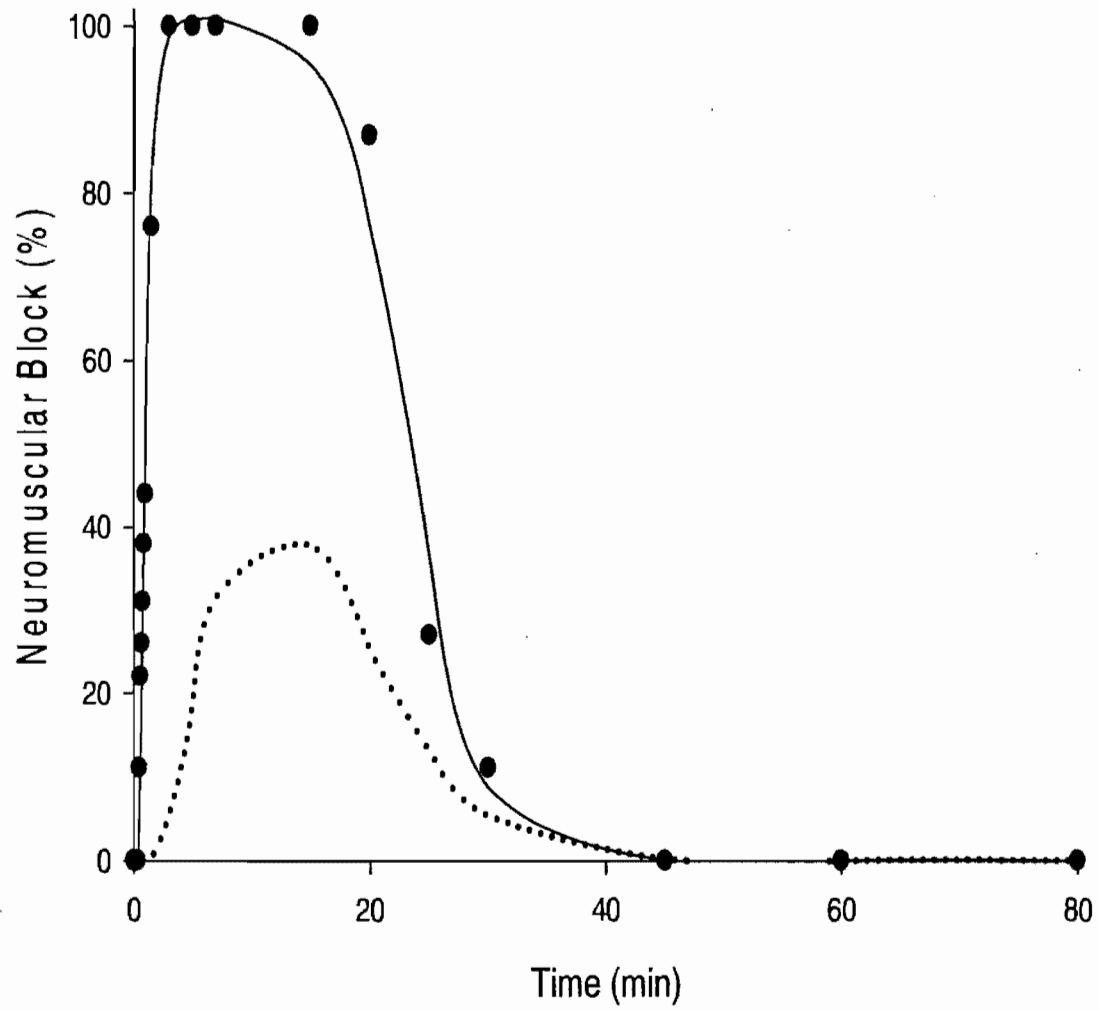


Figure 8



**8. Manuscrit No. 2: Studies on the pharmacokinetics of cisatracurium
in anesthetized dogs: *In vitro- In vivo* correlations**

(Accepted by Journal of Veterinary Pharmacology and Therapeutics)

ChunLin Chen¹, Nobuharu Yamaguchi¹ and France Varin^{1,2}

1. Faculté de pharmacie
Université de Montréal

2. Author to whom correspondence should be addressed :
France Varin
Université de Montréal
Faculté de pharmacie
C.P. 6128, Succursale Centre-ville
Montréal (Québec)
H3C 3J7
Canada
Tel: (514) 343-7016

The authors would like to thank Johanne Couture and Sanae Yamaguchi for their technical support. The contribution of Jean Christian Lepage is acknowledged for the *in vitro* studies.

This research was supported by the Canadian Institutes of Health Research (MA10-274)

Background: Cisatracurium undergoes primarily temperature and pH dependent Hofmann elimination in humans. This study was conducted to describe the pharmacokinetics of cisatracurium in anesthetized dogs and determine whether its in vitro degradation rate in plasma is predictive of its in vivo elimination rate, as this is the case in humans.

Methods: Nine dogs were anesthetized with pentobarbital and administered different bolus doses of cisatracurium in a randomized cross-over design. Arterial blood was drawn at frequent intervals after each bolus injection. In vitro degradation rate ($k_{in\ vitro}$) of cisatracurium was determined in each's dog blank plasma. Plasma concentrations were determined by HPLC. Pharmacokinetic analyses were performed using two compartmental models assuming central or both central and peripheral elimination.

Results: Mean in vivo terminal elimination rate of cisatracurium (16.4 ± 2.7 min) was two-fold faster than mean in vitro degradation rate (32.9 ± 3.7 min) in our dogs. Organ clearance was 6.12 ± 1.69 mL/min-kg and accounted for 56 ± 12 % of the total body clearance. Apparent volume of distribution, an exit site dependent parameter, averaged 212 mL/kg or 184 mL/kg whether or not peripheral elimination was accounted for in the model.

Conclusion: The in vitro rate of degradation in plasma is not of predictive value for the in vivo elimination rate of cisatracurium in anesthetized dogs. Organ clearance plays a more important role in the elimination of cisatracurium in dogs than in humans. Increased biliary excretion and/or presence of renal secretion are potential mechanisms that need to be explored.

Key words: pharmacokinetics, cisatracurium, in vitro degradation, in vitro - in vivo correlations.

Introduction

Cisatracurium besylate is a nondepolarising neuromuscular blocking agent (NMBA) of intermediate duration of action. As for its parent compound atracurium, a chemical process that depends solely on pH and temperature (Hofmann elimination) is an important elimination pathway for cisatracurium in humans. Fisher et al (Fisher, Canfell et al., 1986) proposed a specific two compartment pharmacokinetic model to estimate the clearance of atracurium due to either organ or non-organ elimination; the relative contribution of Hofmann elimination to total body clearance was estimated as 39% in anesthetized patients. When this model was applied to data pooled from three pharmacokinetic studies on cisatracurium (Kisor, Schmith et al., 1996), a relative contribution of 77 % was obtained while as much as 88 % was reported in Bergeron et al's dose-ranging study (Bergeron, Bevan et al., 2001). Thus, organ clearance (e.g., renal or hepatic) plays only a minor role in the elimination of cisatracurium in humans.

The purpose of the present study was to characterize the pharmacokinetics (PK) of cisatracurium in pentobarbital anesthetized dogs and investigate the impact of peripheral elimination on the estimation of its PK parameters. The specific objective was to determine whether the in vitro rate of degradation in plasma is of predictive value for the in vivo elimination rate of cisatracurium, as this proved to be the case in humans.

Materials and Methods

Chemicals and Animals

A commercial preparation of cisatracurium besylate (Nimbex[®], Abbott Canada Ltd. Montréal, Québec, Canada) was used. The internal standard (n-methyl laudanosine) was provided by Glaxo-Wellcome (Stevenage, UK). All solvents were of HPLC grade and purchased from Anachemia (Montréal, Québec, Canada).

The experimental protocol was approved by our institutional Animal Care Committee and was in accordance with the Canadian Council on Animal Care. Veterinary care and housing facilities met Good Animal Practice standards. For the study, nine adult male purpose-bred beagles (7.5 – 10.5 kg) were singly housed and maintained under a 12-h light/dark cycle at 21 ± 0.9 °C and 50 ± 10 % relative humidity. Food was freely available up to 18 h before experiment. There was no restriction for water.

In Vivo Studies

Dogs were anesthetized with an initial injection of 30 mg kg^{-1} sodium pentobarbital (Somnotol[®]; Abbott Laboratories, Montréal, QC, Canada) administered in the cephalic vein of the left leg. Monitoring of the level of anesthesia was based on hemodynamic parameters as well as neurosensory reflexes (hind feet retraction to pinching and cornea response to light touch). Measures were taken every 15 min as well as at predetermined blood sampling times. An adequate level of anesthesia was maintained with supplemental i.v. doses of pentobarbital (3 - 5 mg/kg). Respiration was controlled

mechanically (Model 607, Harvard Apparatus, South Natick, MA) with room air delivered through an endotracheal tube.

When satisfactory level of anesthesia and stability of physiological parameters were achieved, the left femoral vein was cannulated for cisatracurium and pentobarbital administration. The right femoral artery was cannulated for blood sampling. A three-way stopcock was installed on the arterial line for arterial blood pressure monitoring. Hematocrit was measured after administration of each dose and at the end of the experiment. Heart rate was monitored via the arterial pulse. An electromagnetic flow probe (3mm i.d., model FR-030T, Nihon Kohden, Tokyo, Japan) was installed on the left femoral artery and connected to a polygraph system (model RM-6000, Nihon Kohden) for muscle blood flow measurement. The animal was kept warm using a heated surgical table and an insulated sheet. Central body temperature was monitored by means of a rectal probe and kept constant throughout the experiment with a controller. At the end of the experiment, animals were euthanized using an overdose of pentobarbital and saturated KCL.

After stable anesthesia was attained, a blank sample was drawn (10 mL) before the first bolus dose of cisatracurium besylate for in vitro studies. Dogs were randomly assigned to receive either a low or high dose as the first bolus dose. Drug administration was similar for both doses: intravenous tubing was prefilled with the injectable drug solution and flushed completely over 2 sec (approximately 1/4 volume per 0.5 second). Arterial blood samples (2 mL) were drawn directly from the stopcock and transferred into heparinized tubes at 0.5, 1, 1.5, 3, 5, 7, 15, 30, 45, 60 and 80 min. After a washout

period, a blood sample was drawn immediately before the injection of the second bolus (to document any residual plasma concentration) and thereafter, as described above. The volume of blood taken was replaced by saline. To minimize the in vitro degradation of cisatracurium, samples were kept on ice water bath and centrifuged within 2 minutes at 4°C. Plasma was then transferred into pre-acidified tubes (30 µl of 2M H₂SO₄) to obtain a final pH between 3 and 4 and frozen immediately on dry ice. Samples were stored at –70°C until analysis.

Plasma concentrations of cisatracurium were determined using a high performance liquid chromatograph coupled to a fluorescence detector set at 280 nm (excitation) and 320 nm (emission). Bond-Elut® phenyl solid-phase extraction cartridges (Varian, Harbor City, CA) were used for extraction of cisatracurium from plasma. The method published by Bryant et al (Bryant BJ, 1997) for urine samples was slightly modified and validated for plasma in our laboratory. Cisatracurium was separated from its major metabolites on a Spherisorb SCX column (150 X 4.6 mm i.d., 5 µm; Phenomenex®, Torrance, CA, USA), using a stepwise gradient (Thermo Separation Products, Riviera Beach, FL, USA). The mobile phase changed from a first phase (14 mM Na₂SO₄ in 0.5 mM H₂SO₄: Acetonitrile: H₂O 40:60:6) during 5 min to a second phase (70 mM Na₂SO₄ in 0.5 mM H₂SO₄: Acetonitrile 40:60) during 6 min. The solvent flow rate was 2 mL/min and the column maintained at 50°C. This assay proved to be sensitive (lower limit of quantification, 6.5 ng/mL), precise (mean coefficient of variation, 11%), and linear up to 2500 ng/mL (r^2 : 0.995).

In Vitro Studies

Dog plasma (6 mL) was transferred into polypropylene tubes and placed uncapped into a water bath incubator. A pH meter electrode (Orion Research Inc, Beverly, MA) was put into plasma and an automatic feedback thermometer in the water bath. This system provided accurate pH and temperature recordings during the incubation period. The pH of plasma was maintained between 7.39 and 7.42 by the periodic addition of small volumes (1 to 8 ul) of HEPES buffer. Water bath temperature was adjusted to each dog's mean in vivo temperature recorded during the in vivo study. Zero time for incubation corresponded to the addition of cisatracurium to plasma. Aliquots were drawn at 20, 40, 60, 80, 100, 120 minutes. Plasma samples were processed and analyzed as for in vivo studies.

The rate of in vitro disappearance of cisatracurium from dog plasma was estimated by fitting the data to a non-compartmental model with bolus input that applied linear regression to all data points (WinNonlin 5.2 software, Scientific Consulting Inc, Cary, NC). The in vitro elimination half-life ($T_{1/2 \text{ in vitro}}$) was calculated using $0.693 \times k_{\text{in vitro}}^{-1}$.

Pharmacokinetic Analysis of In Vivo Data

The pharmacokinetics of a bolus dose of cisatracurium was best described by a two-compartment model. A weighting function of $1/y(\text{predicted})^2$ was applied. Parameters were estimated using a standard minimization method (Gauss-Newton, Levenberg, and Hartley). Goodness of fit was verified by the precision of the parameter estimates (CV %), the Akaike's Information Criterion (Yamaoka, Nakagawa et al., 1978), and visual

inspection of the plots of observed and model-predicted concentrations vs time as well as those of residuals (%) vs time.

Descriptive curve parameters (distribution (α) and elimination (β) rate constants and their corresponding dose-normalized A and B coefficients) as well as exit-site independent PK parameters such as the volume of the central compartment (V_1), total body clearance (CL_T) and dose-normalized area under the curve (AUC/D) were obtained. The following exit-site dependent PK parameters were also derived: first-order rate constant of elimination from the central compartment (k_{10}), first-order rate constants associated with drug transfer from compartment 1 to compartment 2 (k_{12}) and from compartment 2 to compartment 1 (k_{21}), volume of distribution at steady state (V_{ss}) and intercompartmental clearance (CL_{12}).

Each dog's plasma concentration-time profile was analyzed using two approaches: when assuming central elimination only and when assuming elimination from both the central (k_{10}) and peripheral (k_{20}) compartments as previously described by Nakashima and Benet.(Nakashima & Benet, 1988) Since the rate of elimination from the peripheral compartment (k_{20}) cannot be independently estimated, its value was fixed to the mean in vitro degradation rate ($k_{in\ vitro}$) determined in each dog's plasma. A similar approach was carried out for human studies (Kisor, Schmith et al., 1996; Bergeron, Bevan et al., 2001) using the in vitro degradation rate of cisatracurium in human plasma reported by Welch et al.(Welch, Brown et al., 1995).

The following parameters were derived:

$$V_{ss} = V_1 \cdot (1 + (k_{12} / (k_{20} + k_{21}))) \quad (1) \quad (\text{Nakashima \& Benet, 1988})$$

Organ (CL_{ORG}) and Hofmann (CL_{HOF}) clearances were calculated as:

$$CL_{ORG} = V_1 \cdot k_{ORG} = V_1 \cdot (k_{10} - k_{20}) \quad (2) \quad (\text{Fisher, Canfell et al., 1986})$$

$$CL_{HOF} = CL_T - CL_{ORG} \quad (3) \quad (\text{Fisher, Canfell et al., 1986})$$

Metabolic clearance associated with the central and peripheral compartments were also calculated as follows.

$$CL_{10} = k_{10} \times V_1 \quad (4) \quad (\text{Fisher, Canfell et al., 1986})$$

$$CL_{20} = k_{in\ vitro} \times V_2 \quad (5) \quad (\text{Fisher, Canfell et al., 1986})$$

Statistical Analysis

Results were expressed as mean values \pm standard deviation (SD). Before pooling data, an analysis of variance (ANOVA) test was carried out to exclude the presence of sequence effect or period effect for PK parameters (R 2.6.2 Software, the R Foundation for Statistical Computing). The factors included in the ANOVA were sequence, period (first vs second administration), treatment (high or low dose) and subjects nested within sequence. Student's paired t test was used to compare, for each dog, the pharmacokinetic parameters obtained with/without peripheral elimination. When the normality test failed, Wilcoxon signed rank test was applied. The threshold for statistical significance (α) was set at $p < 0.05$.

Results

Arterial blood pressure and heart rate were stable throughout the experiment. Femoral artery blood flow during installation of neuromuscular block (7.48 ± 3.67 vs 6.88 ± 4.20 mL/min·kg) and hematocrit ($38.2\% \pm 4.4\%$ vs $37.9\% \pm 4.3\%$) were similar during the first and second period. Throughout the study, each dog's body temperature was maintained to its baseline value which averaged 37.3 ± 0.6 °C (range: 36.3 - 38.2). Individual body temperatures did not vary by more than 1 °C for the two consecutive doses. During in vitro studies, water bath temperature was adjusted to be similar to the in vivo dog's temperature (mean: 37.3 ± 0.05 °C; range: 36.7 - 38.1) and pH (mean: 7.40 ± 0.01 ; range: 7.39 - 7.41). The stability of pH was well documented throughout in vitro studies (pH never deviated more than 0.05 pH units from the initial measurement).

The results of the ANOVA showed no evidence of a statistically significant treatment, sequence or period effects on the total clearance, the dose-normalized area under the curve, the terminal half-life and the apparent volume of distribution at steady-state. Therefore, results from the high and low dose were pooled in the summary table. No dose dependency in any PK parameters was observed.

Individual dose-normalized cisatracurium plasma concentration-time curves are displayed in Figure 1. Exit-site-independent and exit-site dependent pharmacokinetic parameters of cisatracurium are shown in Tables 1 and 2, respectively. The apparent volume of distribution at steady state was underestimated by approximately 15% when central elimination only was assumed (Table 2). The mean half-lives for $k_{in\ vitro}$ and $k_{in\ vivo}$ value in dogs were 32.5 and 16.4 min, respectively (Table 3). Mean CL_{HOF} was 4.68

mL/min·kg and accounted for 44% of mean CL_T . Mean CL_{ORG} was 6.12 mL/min·kg and accounted for 56% of mean CL_T .

Simple linear regression analysis of the relationship between temperature (set at in vivo temperature) and $k_{in\ vitro}$ revealed a positive correlation with an R^2 value of 0.54 (Fig.2). The slope of the regression line was significantly different from zero ($P < 0.05$).

Discussion

To our best knowledge, this is the first report on the pharmacokinetics of cisatracurium in pentobarbital anesthetized dogs. An almost twofold higher total body clearance and shorter terminal elimination half-life was observed in dogs when compared to humans. This apparent discrepancy between human and canine data would result mostly from a difference in the relative contribution of organ clearance. This finding was unexpected given the acknowledged organ-independent elimination of cisatracurium.

The pharmacokinetics of cisatracurium has been well characterized in healthy adults (Lien, Schmith et al., 1996) (Schmith, Fiedler-Kelly et al., 1997; Bergeron, Bevan et al., 2001). The structure of the PK model usually accounts for peripheral elimination by substituting the value of $k_{in\ vitro}$ for k_{20} . This is why we performed *in vitro* studies where each dog's plasma was incubated under pH and temperature controlled conditions. The mean half-life for the *in vitro* degradation of cisatracurium in dog plasma (32.9 min) was found similar to that reported (Welch, Brown et al., 1995) in Sorensen phosphate buffer (34.1 min) and in human plasma (29.2 min) maintained at the same range of pH and temperature. Despite the small range of temperatures that were studied during our *in vitro* studies, we observed a positive correlation between temperature and $k_{in\ vitro}$, a finding consistent with previous *in vitro* studies on atracurium (Merrett, Thompson et al., 1983).

In the current study, cisatracurium *in vivo* elimination rate constant was almost twofold faster than its corresponding *in vitro* rate of degradation in plasma. In contrast to

humans, the *in vitro* rate of degradation in plasma is therefore not of predictive value for the *in vivo* elimination rate of cisatracurium in dogs. Consequently, the mean *in vivo* elimination half-life (17 minutes) of cisatracurium in dogs was significantly lower than that observed in healthy adult surgical patients, which ranged from 22 to 30 minutes (Ornstein, Lien et al., 1996; Sorooshian, Stafford et al., 1996; Schmith, Fiedler-Kelly et al., 1997) (Bergeron, Bevan et al., 2001).

Exit-site dependent parameters are expected to differ when both central and peripheral elimination are accounted for in a PK model. Indeed, the transfer of drug into the peripheral compartment (CL_{12}) becomes greater than the transfer back into the central compartment (CL_{21}); a finding consistent with the increased amount of drug drained into the peripheral compartment (Laurin, Nekka et al., 1999). For cisatracurium, the impact of peripheral elimination on distributive equilibrium was significant, as it resulted in a 25% increase in CL_{12} and a 15 % increase in V_{ss} .

The contribution of the metabolic clearance associated with the peripheral compartment was 2.95 mL/min·kg, which amounts to approximately 30 % of the total body clearance of cisatracurium in our dogs. This value is relatively low when compared to that observed in humans (55 %) (Bergeron, Bevan et al., 2001). Accordingly, the percentage of total clearance attributable to Hofmann elimination in dogs (44%) is approximately half those reported in two clinical studies (77%) (Kisor, Schmith et al., 1996) and (88 %) (Bergeron, Bevan et al., 2001).

In our dogs, total body clearance was twofold higher than that observed in humans. Hofmann clearance was similar in both species; a finding compatible with the lack of interspecies differences of both the *in vitro* rates of degradation in plasma and apparent volume of distribution of cisatracurium. As a result, the interspecies difference in total body clearance would mostly be due to organ clearance. In dogs, CL_{ORG} of cisatracurium would represent approximately 56 % of total body clearance, indicating that eliminating organs play a more important role than in humans.

Glomerular filtration rate (GFR) is a major determinant of renal clearance for most drugs. Cisatracurium renal clearance accounted for approximately 71 % of CL_{ORG} in humans (Kisor, Schmith et al., 1996). In dogs, renal clearance is expected to be faster than in humans (Lin, 1995) (Davies & Morris, 1993; MAHMOOD, 2005), since GFR is twofold faster in dogs than in humans (4.0 vs 1.8 mL/min·kg) (Davies & Morris, 1993; Lin, 1995; MAHMOOD, 2005). From a rate limiting step in humans, GFR becomes a competing pathway to Hofman elimination in dogs. Another potential contributing mechanism to the elimination of neuromuscular blocking agents is biliary excretion (Appiah-Ankam, 2004). There is a general agreement that the nonrenal clearance of cisatracurium (0.35 mL/min·kg) in humans is mostly due to biliary excretion (Kisor, Schmith et al., 1996). Biliary excretion was also documented in dogs, although not in a quantitative manner (Dear, Harrelson et al., 1995). Renal secretion of quaternary ammoniums has been reported in other animal species (Rennick, 1981) and its contribution remains a potential mechanism too, in absence of urinary data for cisatracurium in our dogs.

Conclusions

Large interspecies differences in the body disposition of cisatracurium exist between human and dogs. Increased biliary excretion and/or presence of renal secretion are potential mechanisms that need to be explored.

References

Bergeron, L., Bevan, D.R., Berrill, A., Kahwaji, R. & Varin, F. (2001). Concentration-effect relationship of cisatracurium at three different dose levels in the anesthetized patient. *Anesthesiology*, **95**(2), 314-323.

Bryant BJ, J.C., Cook DR, Harrelson JC (1997). High performance liquid chromatography assay for cisatracurium and its metabolites in human urine. *J Liq Chrom Rel Technol* **20**, 2041-2051
Davies, B. & Morris, T. (1993). Physiological parameters in laboratory animals and humans. *Pharm Res*, **10**(7), 1093-1095.

Dear, G.J., Harrelson, J.C., Jones, A.E., Johnson, T.E. & Pleasance, S. (1995). Identification of urinary and biliary conjugated metabolites of the neuromuscular blocker 51W89 by liquid chromatography/mass spectrometry. *Rapid Commun Mass Spectrom*, **9**(14), 1457-1464.

Fisher, D.M., Canfell, P.C., Fahey, M.R., Rosen, J.I., Rupp, S.M., Sheiner, L.B. & Miller, R.D. (1986). Elimination of atracurium in humans: contribution of Hofmann elimination and ester hydrolysis versus organ-based elimination. *Anesthesiology*, **65**(1), 6-12.

Jonas Appiah-Ankam, M.C.F., Honorary Lecturer (2004). Pharmacology of neuromuscular blocking drugs. *Continuing Education in Anaesthesia Critical Care and Pain*, **4**, 2-7.
Kisor, D.F., Schmith, V.D., Wargin, W.A., Lien, C.A., Ornstein, E. & Cook, D.R. (1996). Importance of the organ-independent elimination of cisatracurium. *Anesth Analg*, **83**(5), 1065-1071.

Laurin, J., Nekka, F., Donati, F. & Varin, F. (1999). Assuming peripheral elimination: its impact on the estimation of pharmacokinetic parameters of muscle relaxants. *J Pharmacokinet Biopharm*, **27**(5), 491-512.

Lien, C.A., Schmith, V.D., Belmont, M.R., Abalos, A., Kisor, D.F. & Savarese, J.J. (1996). Pharmacokinetics of cisatracurium in patients receiving nitrous oxide/opioid/barbiturate anesthesia. *Anesthesiology*, **84**(2), 300-308.

Lin, J.H. (1995). Species similarities and differences in pharmacokinetics. *Drug Metab Dispos*, **23**(10), 1008-1021.

MAHMOOD, I. (2005). Interspecies Pharmacokinetic Scaling: Principles And Application of Allometric Scaling Pine House Publishers; First edition

Merrett, R.A., Thompson, C.W. & Webb, F.W. (1983). In vitro degradation of atracurium in human plasma. *Br J Anaesth*, **55**(1), 61-66.

Nakashima, E. & Benet, L.Z. (1988). General treatment of mean residence time, clearance, and volume parameters in linear mammillary models with elimination from any compartment. *J Pharmacokinetic Biopharm*, **16**(5), 475-492.

Ornstein, E., Lien, C.A., Matteo, R.S., Ostapovich, N.D., Diaz, J. & Wolf, K.B. (1996). Pharmacodynamics and pharmacokinetics of cisatracurium in geriatric surgical patients. *Anesthesiology*, **84**(3), 520-525.

Rennick, B.R. (1981). Renal tubule transport of organic cations. *Am J Physiol Renal Physiol* **240**, F83-F89.

Schmith, V.D., Fiedler-Kelly, J., Phillips, L. & Grasela, T.H., Jr. (1997). Dose proportionality of cisatracurium. *J Clin Pharmacol*, **37**(7), 625-629.

Sorooshian, S.S., Stafford, M.A., Eastwood, N.B., Boyd, A.H., Hull, C.J. & Wright, P.M. (1996). Pharmacokinetics and pharmacodynamics of cisatracurium in young and elderly adult patients. *Anesthesiology*, **84**(5), 1083-1091.

Welch, R.M., Brown, A., Ravitch, J. & Dahl, R. (1995). The in vitro degradation of cisatracurium, the R, cis-R'-isomer of atracurium, in human and rat plasma. *Clin Pharmacol Ther*, **58**(2), 132- 142.

Yamaoka, K., Nakagawa, T. & Uno, T. (1978). Application of Akaike's information criterion (AIC) in the evaluation of linear pharmacokinetic equations. *J Pharmacokinetic Biopharm*, **6**(2),165-175.

Table 1. Exit-site-independent pharmacokinetic parameters of cisatracurium in pentobarbital anesthetized dogs

α (min^{-1})	β (min^{-1})	A/D (ng/mL)	B/D (ng/mL)	V_1 (mL/kg)	AUC/D (ng·min/mL)	CL_T (mL/min·kg)
0.3744 ± 0.0708	0.0427 ± 0.0057	1109 ± 231	270 ± 41	75 ± 13	9434 ± 1407	10.80 ± 1.52

Data are presented as mean \pm SD (range), n=18

α =initial distribution rate constant; β =terminal elimination rate constant; A/D= time zero corresponding dose-normalized coefficient; B/D= time zero corresponding dose-normalized coefficient; V_1 = apparent volume of distribution in the central compartment; AUC/D=dose-normalized area under the curve; CL_T =total clearance.

Table 2. Exit-site-dependent pharmacokinetic parameters of cisatracurium in pentobarbital anesthetized dogs

	V_{ss} (mL/kg)	k_{10} (min ⁻¹)	k_{12} (min ⁻¹)	k_{21} (min ⁻¹)	CL_{12} (mL/min·kg)
Central elimination only	184 ± 29	0.1476 ± 0.0268	0.1611 ± 0.0390	0.1083 ± 0.0170	11.85 ± 2.64
Central and peripheral elimination	212 ± 36*	0.1077 ± 0.0264*	0.2010 ± 0.0446*	0.0870 ± 0.0170*	14.76 ± 3.15*

Data are presented as mean ±SD (range), n=18

*p<0.001(pooled data) between the two models (paired t test)

V_{ss} : apparent volume of distribution at steady state; k_{10} : elimination rate constant for the first compartment; k_{12} : transfer rate constant from the first to the second compartment; k_{21} : transfer rate constant from the second to the first compartment; CL_{12} : intercompartment clearance.

Table 3. Comparison of cisatracurium pharmacokinetic parameters in humans and dogs

	Humans	Dogs
$k_{in\ vitro}$ (min ⁻¹)	0.0237 ^a	0.0213 ± 0.0023
$k_{in\ vivo}$ (min ⁻¹)	0.0282 ^b	0.0427 ± 0.0057
CL ₁₀ /CL ₂₀	0.84 ^b	2.92 ± 1.99
CL _T (mL/min·kg)	5.13 ^b ;5.20 ^c	10.80 ± 1.52
CL _{HOF} (mL/min·kg)	4.13 ^b ;4.00 ^c	4.68 ± 1.13
CL _{ORG} (mL/min·kg)	1.00 ^b ;1.20 ^c	6.12 ± 1.69
CL _R (mL/min·kg)	0.85 ^c	-
CL _{NR} (mL/min·kg)	0.35 ^c	-

Data are presented as mean ±SD (range), n=18

$k_{in\ vitro}$:the rate of in vitro disappearance in plasma; $k_{in\ vivo}$: the rate of in vivo elimination; CL₁₀/CL₂₀:ratio of metabolic clearance central compartment with the peripheral compartment. CL_T:total clearance; CL_{HOF}:Hofmann clearance; CL_{ORG}:organ clearance; CL_R:renal clearance; CL_{NR}: nonrenal clearance. Data obtained from: ^a (Welch, Brown et al., 1995); ^b (Bergeron, Bevan et al., 2001); ^c(Kisor, Schmith et al., 1996).

LIST OF FIGURES

Figure 1. Individual dose-normalized cisatracurium plasma concentration-time curves.

For illustration purpose, concentrations were normalized for a 0.1 mg/kg dose.

Figure 2. Linear regression of the temperature versus the *in vitro* speed of degradation ($K_{in\ vitro}$) for 9 dogs. There is a positive relationship between variable; $R^2=0.54$, $P<0.05$.

Figure 1

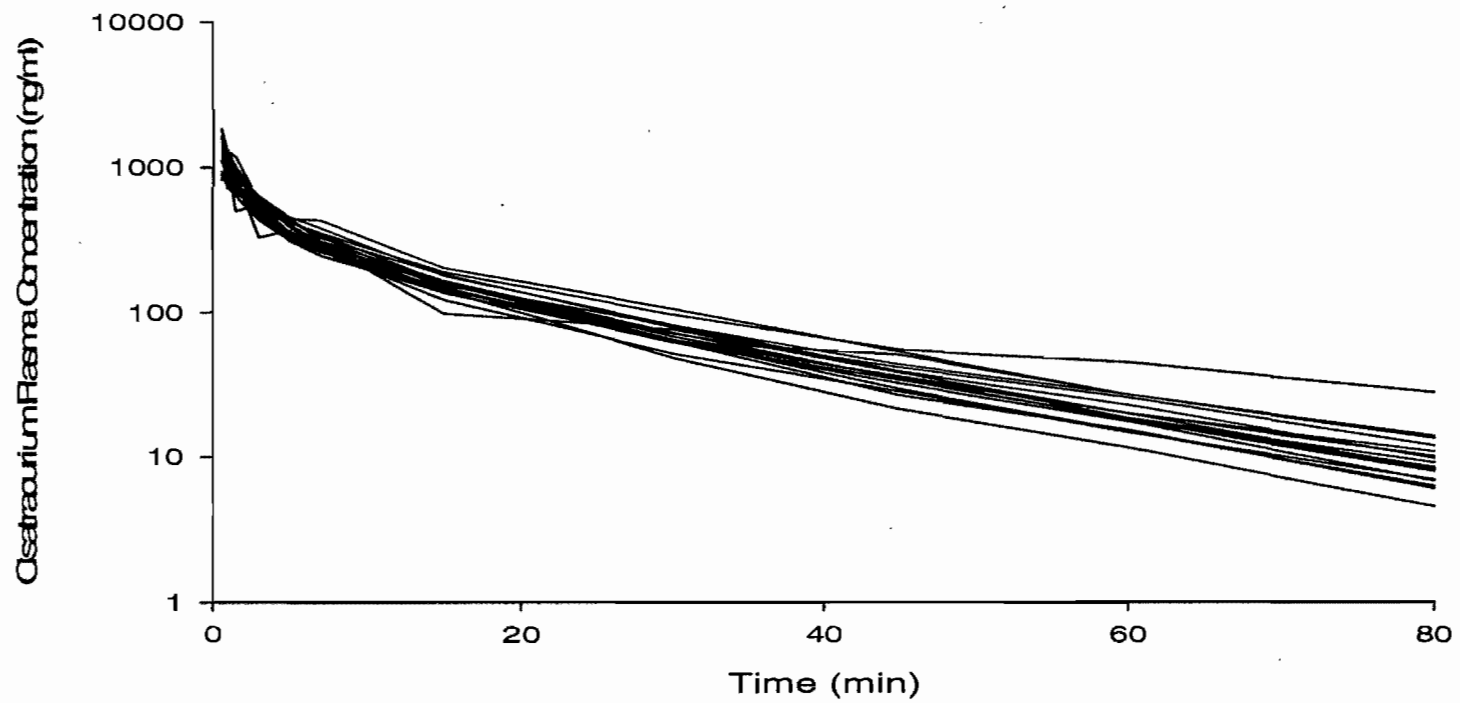
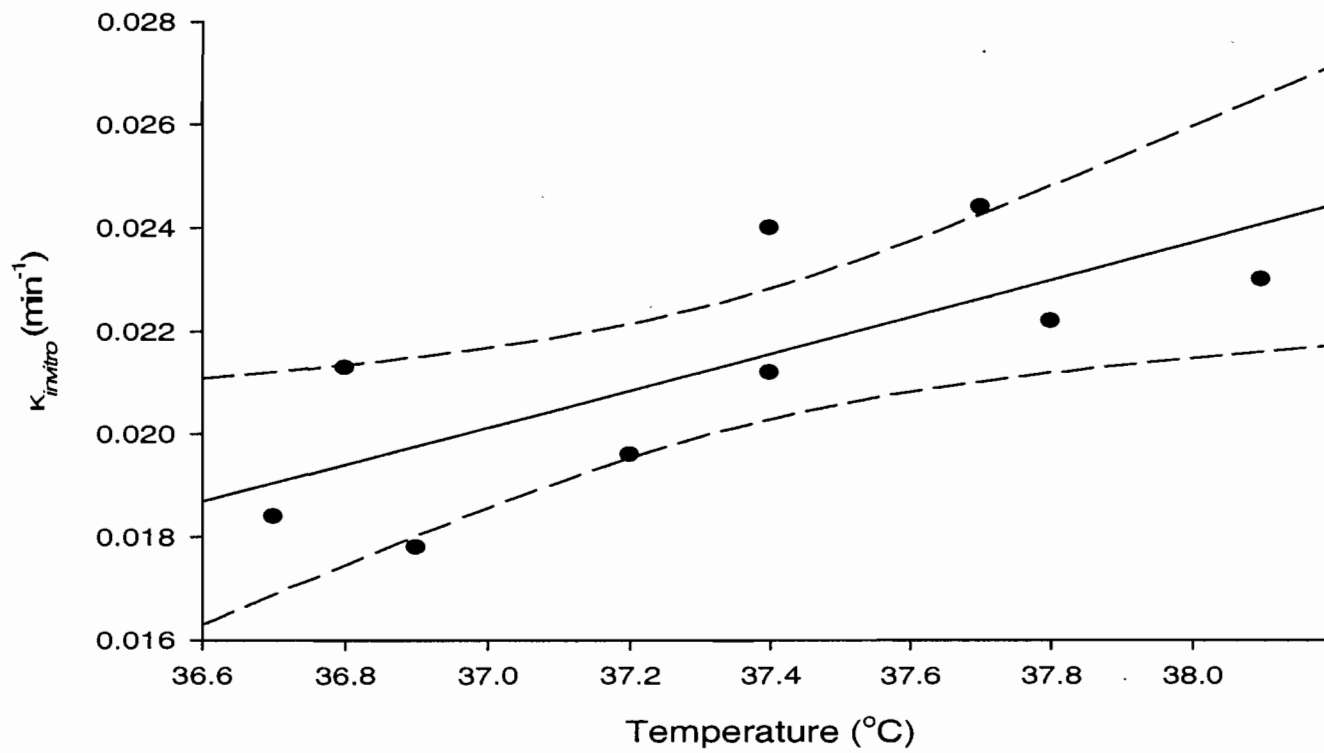


Figure 2



**9. Manuscrit No. 3: Modeling of the Intravascular Mixing Phase of
Neuromuscular Blocking Agents Following Intravenous Bolus Injection**

(Submitted to Anesthesiology)

ChunLin Chen, M.D., B.Sc.*

François Donati, M.D., Ph.D., F.R.C.P.C. §

France Varin, B.Pharm., Ph.D. #,1

* Ph.D. Candidate,

Full Professor, Faculté de pharmacie,

§ Full Professor, Faculté de médecine, Département

d'anesthésiologie, Hôpital Maisonneuve-Rosemont, Université de
Montréal

Abbreviated title: A new model for describing the intravascular mixing phase

¹ Author to whom correspondence should be addressed:

France Varin

Université de Montréal

Faculté de pharmacie

C.P. 6128, Succursale Centre-ville

Montréal (Québec)

H3C 3J7

Canada

Tel (514) 343-7016

FAX: (514) 343-5735



Background: For drugs having a very rapid onset of action, early plasma concentrations after a bolus injection are crucial for an accurate estimation of their pharmacokinetic/pharmacodynamic relationship. The objective of this study was to develop a unified pharmacokinetic (PK) model that would adequately fit the data collected during the intravascular mixing (IVM) phase in four studies where neuromuscular blocking agents (NMBAs) were administered as a $1.5 \times ED_{95}$ bolus dose in anesthetized patients. **Methods:** The IVM phases of doxacurium, vecuronium, atracurium and succinylcholine were characterized by collecting arterial blood every 10 sec for the first 2 min after injection; samples were drawn at frequent times thereafter for at least 4 half-lives. The Inverse Gaussian (IG) density input function combined with compartmental models was implemented in NONMEM VI for PK analysis of individual data sets. For each NMBA, this approach was compared with a non compartmental analysis. **Results:** Satisfactory fit of data sets (including the IVM phase) was achieved with the IG model for each NMBA. A good agreement between pharmacokinetic parameters derived with both approaches was also observed. Time to peak concentrations (T_{max}) did not differ significantly between NMBAs ($P = 0.279$). For all NMBAs, mean estimates of central volume of distribution closely approximated the intravascular volume while apparent total body distribution did not exceed the extracellular space. **Conclusions:** The early pharmacokinetic profile after NMBA injection does not depend on which specific drug is given, but probably is a function of circulatory factors. The IG model is flexible enough to provide a good simulation of the IVM phase for most NMBAs.

Introduction

In pharmacokinetic studies (PK) where the first blood sample (arterial or venous) is obtained one minute after intravenous bolus administration of a drug, the traditional mammillary compartmental model is well accepted and sufficient for fitting the concentration-time data. It is well recognized that a poor characterization of the early kinetics will ensue if an instantaneous input in the central compartment is assumed in the model¹⁻³. Indeed, samples obtained frequently during the first minute would reveal that, after a brief delay, drug levels rapidly rise to a peak, followed by oscillations that will eventually be followed by the expected monotonic decrease.⁴ Depending on the terminal half-life of the drug, assuming an instantaneous input may result in subtle^{1,5} or large^{6,7} errors on the estimation of major PK parameters. This limitation of the compartmental approach is almost impossible to overcome when one attempts to fit the concentration-effect data of anesthetic drugs having an onset of action within the very first two minutes.⁷⁻¹⁰ The intravascular mixing (IVM) phase plays a large part in determining the rate and extent of drug distribution to the site of drug effect and this early distribution kinetics should be most accurately characterized.¹¹ In the past years, physiologically-based¹², stochastic¹³ and other types¹⁴ of models have been proposed for this purpose.

In this paper, we present an alternate approach which incorporates an Inverse Gaussian density (IG) input function to predict the intravascular mixing phase and subsequent distribution of neuromuscular blocking agents in the body. This probability density function was tested because, at first glance, its shape was visually compatible with our data but also because it had previously been used to describe oral absorption¹⁵. The IG

model was applied to data gathered in anesthetized patients following administration of a bolus dose of either doxacurium⁵, vecuronium², atracurium¹, and succinylcholine⁷.

Methods

Subjects and protocol

These clinical studies received approval from Institutional Review Boards. And patients were enrolled after signing the informed consent form.

Study group A consisted of eight American Society of Anesthesiologists (ASA) physical status I or II patients, aged between 20 and 62 years, who received a 25 ug/kg iv bolus dose of doxacurium chloride (Nuromax®, Glaxo Wellcome). Anesthesia was induced with alfentanil (20-30 µg/kg) and propofol (1.5-3 mg/kg) and maintained with nitrous oxide (70%) in oxygen and by continuous infusion of propofol (10-15 mg/kg/hr). Arterial blood samples were obtained every 10 sec for the first 2 min and then frequent intervals for 300 min. Doxacurium plasma concentrations were determined using an HPLC assay.¹⁶

Study group B consisted of nine ASA physical status I or II patients, aged between 26 and 69 years, who received a 0.1 mg/kg iv bolus dose of vecuronium bromide (Norcuron®, Organon, Ontario, Canada). Anesthesia was induced with thiopental (5-7 mg/kg) and fentanyl (1-5 µg/kg) and maintained with nitrous oxide (70%) in oxygen and isoflurane 0.5 % end-tidal and supplemented with fentanyl if necessary. Arterial blood

samples were obtained every 10 sec for the first 2 min and then at frequent intervals for 240 min. Vecuronium plasma concentrations were determined using an HPLC assay.¹⁷

Study group C consisted of six ASA physical status I or II patients, aged between 20 and 61 years, who received a 0.5 mg/kg *iv* bolus dose of atracurium besylate (Tracrium®, Glaxo Wellcome). Anesthesia was induced with thiopental (5-7 mg/kg) and fentanyl (1-5 µg/kg) and maintained with isoflurane 0.5% end-tidal and nitrous oxide 70% in oxygen, with supplementary doses of fentanyl if necessary. Arterial blood samples were collected every 10 sec for the first 2 min and then at frequent intervals for 90 min. The elimination phase was simulated using second dose parameters. Atracurium plasma concentrations were determined using an HPLC assay.¹⁸

Study group D consisted of seven ASA physical status I or II patients, aged between 36 and 56 years, who received a 1 mg/kg *iv* bolus dose of succinylcholine chloride (Nuromax®, Glaxo Wellcome). Anesthesia was induced with remifentanyl and propofol and maintained with nitrous oxide in oxygen and by continuous infusion of propofol. Arterial blood samples were obtained every 5 sec for the first 2 min and then at frequent intervals for 10 min. Succinylcholine plasma concentrations were determined using an HPLC assay.⁷

Data analysis

As different doses were given, plasma concentrations were normalized to dose to allow comparisons between drugs. Dose-normalized concentrations were then converted to nmol/ml to take into account the molecular weight of these NMBA. For consistency,

plasma concentrations were averaged to obtain 10 sec intervals during the IVM phase for succinylcholine.

Model-independent pharmacokinetic analysis was performed using a commercial nonlinear regression software (WinNonlinPro 5.2, Pharsight Corp., Cary, NC). The terminal half-life was derived from the equation $t_{1/2 \text{ in vivo}} = 0.693/\lambda_z$, where λ_z is the terminal elimination constant determined by log linear regression. The area under the plasma concentration-time curve ($AUC_{0-\infty}$) was calculated using trapezoidal integration with extrapolation to time infinity. Systemic clearance was estimated as $\text{dose}/AUC_{0-\infty}$. The apparent volume of distribution at steady state (V_{ss}) was calculated as the product of clearance and mean residence time. The maximum plasma concentration (C_{max}) and time to reach a C_{max} (T_{max}) were read directly from the experimental data.

Model-dependent pharmacokinetic analysis was based on descriptions of the intravascular mixing phase and subsequent distribution of injected NMBAs in the body. It is assumed that, immediately after injection, the drug travels from the injection site to a small lag compartment, as described by an Inverse Gaussian probability density function that is subsequently linked with an open compartment model with first-order elimination from the central compartment. A distinguished feature of this model is this hypothetical lag compartment that enables to take into account the time between drug's entry into the blood stream and drug's appearance at the site of blood sampling. As such, this lag time also depends on the sensitivity of the analytical assay. The addition of this compartment, though virtual, proved to be necessary to achieve a good fit of the IVM phase kinetics.

The basic model is illustrated in Figure 1 and specified by the following differential equations:

$$\frac{dA_1}{dt} = -IG_j(t) \quad (1)$$

$$\frac{dA_2}{dt} = K_{32}A_3 - K_{23}A_2 + IG_j(t) \quad (2)$$

$$\frac{dA_3}{dt} = K_{23}A_2 + K_{43}A_4 + K_{53}A_5 - (K_{32} + K_{34} + K_{35} + K_{30})A_3 \quad (3)$$

$$\frac{dA_4}{dt} = K_{34}A_3 - K_{43}A_4 \quad (4)$$

$$\frac{dA_5}{dt} = K_{35}A_3 - K_{53}A_5 \quad (5)$$

where A represents the amount of drug in the respective compartments, j , the number of input function and K_{xy} the transfer rate constants from compartment x to compartment y.

The Inverse Gaussian density function, $IG_j(t)$, is expressed by the following equation:^{19,20}

$$IG_j(t) = Dose \cdot F \cdot \sqrt{\frac{MAT}{2\pi \cdot NV^2 \cdot t^3}} \exp\left[-\frac{(t - MAT)^2}{2 \cdot NV^2 \cdot MAT \cdot t}\right] \quad (6)$$

In which Dose is the administered dose, F is the fraction absorbed, MAT is the mean input time, t is the time after dosing. The normalized variance of the input time

distribution, NV^2 , represents the relative dispersion of MAT by way of the squared coefficient of variation:

$$NV^2 = \text{Var}MAT / MAT^2 \quad (7)$$

In addition, the time ($T_{\text{max-rate}}$) at which the input rate reaches its maximum value ($\text{input}_{\text{max}}$) is calculated by use of the following equation:

$$T_{\text{max-rate}} = MAT \left[\sqrt{1 + \frac{9}{4} \cdot NV^4} - \frac{3}{2} \cdot NV^2 \right] \quad (8)$$

The input function can be represented using a sum of Inverse Gaussian functions as follows:

$$I(t) = D \sum_{j=1}^n f_i IG_j(t) \quad (9)$$

$$\text{where } 0 \leq \sum_{j=1}^n f_i \leq 1, \text{ and the bioavailability is derived as } F = \sum_{j=1}^n f_i .$$

The structural models were fitted to each individual data set and parameters were estimated using an iterative nonlinear modeling program, NONMEM VI,²¹ with a proportional plus additive error model/proportional error model. Each estimate was derived from repeated run starting from several initial estimates or use of constraints to ensure that the estimation converged to a global minimum of the objective function. The selection of the best model was based on the physiological perspective and goodness of fit criteria, including visual inspection of plots of predicted versus observed values as well as those of residuals (%) vs time, the Akaike's Information Criterion.²²

Statistical Analysis

Data are presented as mean \pm SD. The paired t test was used to compare the pharmacokinetic parameters obtained with both non compartment and IG models. Within each model, between drugs comparisons of pharmacokinetic parameters were made using One-way analysis of variance or One-way analysis of variance on ranks when normality or homoscedasticity test failed. The threshold for statistical significance (α) was set to 0.05.

Results

Figure 2 shows the individual dose-normalized doxacurium, vecuronium, atracurium and succinylcholine plasma concentration-time profiles after iv bolus injection. Mean peak plasma concentration was 9.89 nmol/ml (CV: 41%) for doxacurium, 9.41 nmol/ml (CV: 30%) for vecuronium, 6.12 nmol/ml (CV: 23%) for atracurium, and 17.44 nmol/ml (CV: 17%) for succinylcholine. Time to reach peak plasma concentration ranged from 0.42 to 0.92 min for doxacurium, 0.42 to 0.58 min for both vecuronium and atracurium, and 0.42 to 0.75 min for succinylcholine.

Table 1 summarizes patient demographic data and anesthetic procedure for NMBAs. Table 2 summarizes the mean pharmacokinetic parameters derived for the combined non compartmental and IG models. Pair-wise comparisons did not show any significant difference for V_{ss} , AUC, C_{max} and T_{max} . Estimated values for total body clearance were in agreement.

Figure 3 showed individual predicted (solid line) and observed (closed circle) dose-normalized doxacurium (A), vecuronium (B), atracurium (C) and succinylcholine (D) plasma concentrations versus time curves in anesthetized patients. Predicted (solid line) and observed (closed circle) mean dose-normalized doxacurium (A), vecuronium (B), atracurium (C) and succinylcholine (D) plasma concentrations versus time curves in anesthetized patients are shown in Figure 4. Inserts represent weighted residuals vs time plots.

Discussion

Our objective was to develop a unified pharmacokinetic model that would adequately fit the plasma concentrations of NMBAs data previously measured during the IVM phase of four NMBAs in anesthetized patients. Although each muscle relaxant has its own pharmacokinetic parameters that may influence the initial distribution and mixing, the underlying mixing and dilutional processes are most likely common to all muscle relaxants. In the structural model-building process, the first, zero order or the Weibull functions were not satisfactory input functions that would adequately characterize the IVM phase. Judged against the observed data that informed the model, the Inverse Gaussian density function not only adequately described the early peaks in the plasma concentrations of NMBAs but also proved to be of predictive value for midazolam.

Our pharmacokinetic studies were designed to characterize the concentration-time profile during the very first 2 min after a bolus administration in anesthetized patients. These studies required an intensive blood sampling and were meant to investigate the variability in the kinetics of the initial intravascular mixing (IVM) phase for a series of NMBAs. These highly hydrosoluble compounds were expected to be distributed to a similar extent in the extracellular fluid.

The inability of conventional compartmental models to adequately describe the initial mixing of drugs was first pointed out by Chiou in 1979.²³ Back-extrapolation to zero assumes that following drug administration instantaneous and complete mixing of drug throughout the central volume of distribution occurs.^{24,25} However, this is physiologically impossible since drugs initially mix with only a part of the central

volume, which explains the very high concentrations observed.^{12,25,26} Back-extrapolation may therefore result in a gross underestimation of peak concentrations. Also, the result of extrapolation may depend heavily on a single plasma concentration measurement, which makes extrapolation less reliable. Finally, the size of the central compartment calculated on the basis of the extrapolated plasma concentrations at time zero varies greatly with the sampling site²⁴ or schedule.²⁷ Although the polyexponential model is well accepted, and probably sufficient for most drugs, we now recognize its limitation when applied to bolus administration of anesthetic drugs, particularly those that attain maximum effect within the very first 2 min.^{2,3}

Physiologically-based pharmacokinetic (PBPK) models are able to accurately describe the early kinetics of drug distribution. Indeed, PBPK models²⁸ or hybrids of physiological and compartmental models^{29,30} have been successfully applied to intravenous anesthetics. However, PBPK modeling requires the input of countless data such as anatomical tissue weights and blood flows as well as drug tissue/blood partition ratio to enable prediction of blood and tissue concentrations. As regional blood flows reported in healthy humans may not apply to anesthetized patients undergoing surgical procedures, a PBPK model for NMBAs would have required actual measurements of organ blood flows and tissue drug concentrations.

Recirculatory models were elaborated to overcome this difficulty.³¹ It is simpler than PBPK because it estimates blood flow to tissue compartments on the basis of the calculated intercompartmental clearance of a flow-limited tissue distribution marker (for example indocyanine green ICG for intravascular volume).¹¹ It has the advantage to

incorporate the influence of cardiac output on the distribution kinetics. In a PK/PD study on rocuronium in anesthetized patients, a better correlation between the plasma - effect compartment equilibration rate constant and the cardiac output was observed with the recirculatory model compared to the compartmental analysis.³² However, these models require appropriate markers for at least the intravascular volume (generally ICG) which renders the clinical protocol more complex and invasive. Also, the recirculatory approach splits the compartment playing the role of plasma into two parts and then attempts to fit the ensuing model piecewise.²⁶

For all four NMBAs peak arterial concentrations were not reached until approximately 30 sec post injection. Interpatient variability in C_{max} ranged from 17% to 41% while that for T_{max} ranged from 12% to 30 %. This variability is consistent with processes such as mixing, flow (circulatory factors) and diffusion (physicochemical properties) that govern initial drug distribution. There was generally a good correlation between MAT, the mean input time and observed T_{max} for all NMBAs. When comparing the input function for the four NMBAs, a slightly longer MAT was predicted for doxacurium but was in agreement with the observed T_{max} . There are no clear explanations for this longer delay before reaching C_{max} in this group of patients, circulatory factors are most probably responsible.

If we assume that the ideal V_c includes only the central circulation and nondistributive peripheral pathways of the recirculatory pharmacokinetic model,³³ then the corresponding volume estimated for rocuronium would be 37 ml/kg. This value is identical to that published earlier for rocuronium using a three compartment model.³⁴

Our estimate of V_c ranges 25 to 40 ml/kg for all NMBA, which is in good agreement with published data. Finally, the estimated V_{ss} with our model are not different from those obtained with the noncompartmental approach.

Our model is quite versatile as it can include more than one input function. This was tested for succinylcholine where one data set that displayed an obvious second peak of distribution that could be associated with recirculation.⁷ This data set was better characterized by a sum of two Inverse Gaussian functions, as shown in Figure 5. The Inverse Gaussian density function can also be easily implemented into available softwares for modeling and simulation of pharmacokinetic data that are based on the parametric approach. This constitutes a definite advantage for our model.

We wanted to challenge the general predictive capacity of the IGD model using a drug that would distribute more readily into tissues, midazolam.³⁵ Three compartment PK parameters were derived using plasma concentrations drawn after 1 min (thus avoiding the ascending portion of the IVM phase) and fixed into the IG model. Two approaches were evaluated for predicting midazolam IVM concentrations: (1) using the mean values for V_{lag} , V_c , MAT and NV derived for NMBAs (Figure 6, A and B) or, (2) using iterative adjustments of these parameters (Figure 6, C and D). Although the first approach provided a fairly good approximation, an excellent fit was obtained using optimized values with the later approach.

To our knowledge, this is the first application of Inverse Gaussian density function to describe the IVM phase of a drug after its intravenous bolus administration. We have

shown that addition of this input function to classical compartmental models can adequately describe the whole plasma concentration-time profile of several NMBAs after a bolus dose and that this model may be applicable to other anesthetic drugs.

References

1. Ducharme J, Varin F, Bevan DR, Donati F: Importance of early blood sampling on vecuronium pharmacokinetic and pharmacodynamic parameters. *Clin Pharmacokinet* 1993; 24: 507-518
2. Ducharme J, Varin F, Donati F: Pharmacokinetics and pharmacodynamics of a second dose of atracurium in anaesthetised patients. *Clin Drug Invest* 1995; 9: 98-110
3. Fisher DM: (Almost) everything you learned about pharmacokinetics was (somewhat) wrong! *Anesth Analg* 1996; 83: 901-3
4. Bissinger U, Nigrovic V: Simulation of the onset of neuromuscular block based on the early oscillations in the arterial plasma concentrations. *Eur J Clin Pharmacol* 1997; 52: 71-5
5. Zhu Y, Audibert G, Donati F, Varin F: Pharmacokinetic-pharmacodynamic modeling of doxacurium: effect of input rate. *J Pharmacokinet Biopharm* 1997; 25: 23-37
6. Lacroix M, Donati F, Varin F: Pharmacokinetics of mivacurium isomers and their metabolites in healthy volunteers after intravenous bolus administration. *Anesthesiology* 1997; 86: 322-330
7. Roy JJ, Donati F, Boismenu D, Varin F: Concentration-effect relation of succinylcholine chloride during propofol anesthesia. *Anesthesiology* 2002; 97: 1082-92
8. Bergeron L, Bevan DR, Berrill A, Kahwaji R, Varin F: Concentration-effect relationship of cisatracurium at three different dose levels in the anesthetized patient. *Anesthesiology* 2001; 95: 314-23
9. Matthias P, Fisher DM: Pharmacodynamic modeling of muscle relaxants. Effects of design issues on results. *Anesthesiology* 2002; 96: 711-7
10. Struys MM, Coppens MJ, De Neve N, Mortier EP, Doufas AG, Van Bocxlaer JF, Shafer SL: Influence of administration rate on propofol plasma-effect site equilibration. *Anesthesiology* 2007; 107: 386-96
11. Minto CF, Schnider TW: Contributions of PK/PD modeling to intravenous anesthesia. *Clin Pharmacol Ther* 2008; 84: 27-38

12. Upton RN: A model of the first pass passage of drugs from i.v. injection site to the heart-parameter estimates for lignocaine in the sheep. *Br J Anaesth* 1996; 77: 764-772
13. Krejcie TC, Avram MJ, Brooks Gentry W, Niemann CU, Janowski MP, Henthorn TK: A recirculatory model for the pulmonary uptake and pharmacokinetics of lidocaine based on analysis of arterial and mixed venous data from dogs. *J Pharmacokinet Biopharm* 1997; 25: 169-190
14. Lafrance P, Lemaire V, Varin, Donati F, Belair J, Nekka F: Spatial effects in modelling pharmacokinetics of rapid action drugs. *Bulletin of mathematical biology* 2002
15. Zhou H: Pharmacokinetic strategies in deciphering atypical drug absorption profiles. *J Clin Pharmacol* 2003; 43: 211-27
16. Garipey LP, Varin F, Donati F, Salib Y, Bevan DR: Influence of aging on the pharmacokinetics and pharmacodynamics of doxacurium. *Clin Pharmacol Ther* 1993; 53: 340-347
17. Ducharme J, Varin F, Bevan DR, Donati F, Theoret Y: High-performance liquid chromatography-electrochemical detection of vecuronium and its metabolites in human plasma. *J Chromatogr* 1992; 573: 79-86
18. Varin F, Ducharme J, Besner JG, Theoret Y: Determination of atracurium and laudanosine in human plasma by high-performance liquid chromatography. *J Chromatogr* 1990; 529: 319-27
19. Weiss M: A novel extravascular input function for the assessment of drug absorption in bioavailability studies. *Pharm Res* 1996; 13: 1547-53
20. Csajka C, Drover D, Verotta D: The use of a sum of inverse Gaussian functions to describe the absorption profile of drugs exhibiting complex absorption. *Pharm Res* 2005; 22: 1227-35
21. Beal S, LB S: *NONMEM User's Guide*. San Francisco, 1992
22. Yamaoka K, Nakagawa T, Uno T: Application of Akaike's information criterion (AIC) in the evaluation of linear pharmacokinetic equations. *J Pharmacokinet Biopharm* 1978; 6(2): 165-175

23. Chiou WL: Potential pitfalls in the conventional pharmacokinetic studies: effects of the initial mixing of drug in blood and pulmonary first-pass elimination. *J Pharmacokinet Biopharm* 1979; 7(5): 527-536
24. Chiou WL: The phenomenon and rationale of marked dependence of drug concentration on blood sampling site. Implications in pharmacokinetics, pharmacodynamics, toxicology and therapeutics (Part I). *Clin Pharmacokinet* 1989; 17: 175-199
25. Chiou WL: The phenomenon and rationale of marked dependence of drug concentration on blood sampling site. Implications in pharmacokinetics, pharmacodynamics, toxicology and therapeutics (Part II). *Clin Pharmacokinet* 1989; 17: 275-90
26. Henthorn TK, Avram MJ, Krejcie TC, Shanks CA, Asada A, Kaczynski DA: Minimal compartmental model of circulatory mixing of indocyanine green. *Am.J Physiol.* 1992; 262: H903-H910
27. Donati F, Gill SS, Bevan DR, Ducharme J, Theoret Y, Varin F: Pharmacokinetics and pharmacodynamics of atracurium with and without previous suxamethonium administration [see comments]. *Br J Anaesth* 1991; 66: 557-561
28. Wada DR, Stanski DR, Ebling WF: A PC-based graphical simulator for physiological pharmacokinetic models. *Comput Methods Programs Biomed* 1995; 46: 245-55
29. Upton RN, Ludbrook GL, Gray EC, Grant C: The cerebral Pharmacokinetics of Meperidine and Alfentanil in Conscious Sheep. *Anesthesiology* 1997; 86: 1317-1325
30. Ludbrook GL, Upton RN: A physiological model of induction of anaesthesia with propofol in sheep. 2. Model analysis and implications for dose requirements. *Br J Anaesth* 1997; 79: 505-13
31. Krejcie TC, Jacquez JA, Avram MJ, Niemann CU, Shanks CA, Henthorn TK: Use of parallel Erlang density functions to analyze first-pass pulmonary uptake of multiple indicators in dogs. *J Pharmacokinet Biopharm* 1996; 24: 569-588

32. Kuipers JA, Boer F, E. O, J. B, A.G.L. B: Recirculatory pharmacokinetics and pharmacodynamics of rocuronium in patients. The influence of cardiac output. *Anesthesiology* 2001; 94: 47-55
33. Avram MJ, Krejcie TC: Using front-end kinetics to optimize target-controlled drug infusions. *Anesthesiology* 2003; 99: 1078-86
34. Dragne A, Varin F, Plaud B, Donati F: Rocuronium pharmacokinetic-pharmacodynamic relationship under stable propofol or isoflurane anesthesia. *Can J Anaesth* 2002; 49: 353-60
35. Mastey V, Donati F, Varin F: Early pharmacokinetics of Midazolam. Sampling site and schedule considerations. *Clin Drug Invest* 1995; 9(3): 131-140

Table 1. Patient demographic data and anesthetic procedure for doxacurium, vecuronium, atracurium and succinylcholine.

Characteristic	Doxacurium ⁵	Vecuronium ¹	Atracurium ²	Succinylcholine ⁷
ASA physical status (I/II)	4 / 4	6 / 3	3 / 3	4 / 3
Sex (F/M)	3 / 5	5 / 4	0 / 6	2 / 5
Age (y)	46 ± 5	47 ± 9	48 ± 5	48 ± 7
Weight (kg)	71 ± 3	52 ± 6	80 ± 4	74 ± 10
Anesthesia				
Induction	alfentanil and propofol	thiopental and fentanyl	thiopental and fentanyl	remifentanil and propofol

ASA: American Society of Anesthesiologists; F: female; M=male;

Table 2. Mean doxacurium, vecuronium, atracurium and succinylcholine pharmacokinetic parameters

		doxacurium (n=8)	vecuronium (n=9)	atracurium (n=6)	succinylcholine (n=7)
Noncompartment analysis					
C_{max}	(nmol·ml ⁻¹)	9.89 ± 4.05 ^{\$}	9.42 ± 2.84 ^{\$}	6.12 ± 1.42 ^{\$}	17.44 ± 3.03 ^{\$}
T_{max}	(min)	0.67 ± 0.20	0.51 ± 0.08	0.55 ± 0.07	0.58 ± 0.14
$AUC_{0-\infty}$	(nmol·min·ml ⁻¹)	91.12 ± 37.53 ^{\$#}	52.75 ± 7.83 ^{\$#}	20.04 ± 4.73 ^{\$#}	9.63 ± 2.21 ^{\$#}
V_{ss}	(ml·kg ⁻¹)	139.4 ± 41.8 ^{\$}	159.9 ± 38.8 ^{\$}	116.1 ± 19.2 ^{\$}	41.3 ± 9.7 ^{\$}
CL	(ml·min·kg ⁻¹)	1.19 ± 0.37 ^{\$#}	3.45 ± 0.47 ^{\$#}	5.64 ± 1.40 ^{\$#}	37.16 ± 7.35 ^{\$#}
IG model analysis					
C_{max} predicted	(nmol·ml ⁻¹)	9.32 ± 3.68 ^{\$}	8.99 ± 2.51 ^{\$}	5.98 ± 1.30 ^{\$}	17.77 ± 3.94 ^{\$}
T_{max} predicted	(min)	0.67 ± 0.25	0.51 ± 0.08	0.58 ± 0.10	0.58 ± 0.14
MAT1	(min)	0.76 ± 0.23	0.57 ± 0.06	0.63 ± 0.10	0.68 ± 0.14
NV1		0.27 ± 0.14 ^{\$#}	0.30 ± 0.04 ^{\$#}	0.20 ± 0.05 ^{\$#}	0.21 ± 0.04 ^{\$}
$T_{max-rate1}$	(min)	0.69 ± 0.26	0.50 ± 0.07	0.59 ± 0.10	0.63 ± 0.12

MAT2	(min)	-	-	-	0.35
NV2		-	-	-	0.13
T _{max-rate2}	(min)	-	-	-	0.34
AUC _{0-∞predicted}	(nmol · min · ml ⁻¹)	88.95 ± 35.93 ^{§#}	50.36 ± 9.58 ^{§#}	19.93 ± 4.78 ^{§#}	9.40 ± 2.48 ^{§#}
V _{Lag}	(ml · kg ⁻¹)	0.0004 ± 0.0003 [§]	0.0005 ± 0.0000 [§]	0.0003 ± 0.0003 [§]	0.0001 ± 0.0002 [§]
V _{Central}	(ml · kg ⁻¹)	24.3 ± 6.7 [§]	30.2 ± 6.1 [§]	29.5 ± 8.6 [§]	40.8 ± 13.2 [§]
V _{Fast Peripheral}	(ml · kg ⁻¹)	45.2 ± 11.8	48.2 ± 20.9	34.9 ± 15.1	-
V _{Slow Peripheral}	(ml · kg ⁻¹)	67.1 ± 33.5 [#]	86.8 ± 17.8 [#]	36.0 ± 1.1 [#]	-
V _{ss}	(ml · kg ⁻¹)	137.3 ± 38.0 ^{§#}	165.2 ± 18.0 ^{§#}	100.4 ± 21.1 ^{§#}	40.8 ± 13.2 ^{§#}
CL	(ml · min · kg ⁻¹)	0.85 ± 0.30 ^{§##}	2.53 ± 0.37 ^{§##}	4.04 ± 1.11 ^{§##}	47.40 ± 16.87 ^{§#}
CL _L	(ml · min · kg ⁻¹)	19.06 ± 11.08 ^{§#}	42.79 ± 12.99 ^{§#}	43.05 ± 8.50 ^{§#}	37.7 ± 12.2 ^{§#}
CL _F	(ml · min · kg ⁻¹)	4.71 ± 4.31	4.08 ± 1.04	9.25 ± 10.39	-
CL _S	(ml · min · kg ⁻¹)	0.41 ± 0.60	0.17 ± 0.31	1.22 ± 1.47	-

Data are presented mean ± SD

* p<0.05 between the two models (paired t test)

§ p<0.05 between all drugs within each model (one way ANOVA)

p<0.05 between drugs excluding succinylcholine within each model (one way ANOVA)

C_{max}: maximum observed plasma concentration; T_{max}: time to reach C_{max}; AUC_{0-∞}: area under the plasma concentration-time curve extrapolated to infinity; CL: systemic clearance; V_{ss}: apparent volume of distribution at steady state. V_{lag}: volume of distribution for the hypothetical lag compartment; V_{central}: volume of distribution for the central compartment; V_{peripheral}: volume of distribution for the peripheral compartment; CL_L: intercompartment clearance between lag and central compartment; CL_F: intercompartment clearance between central and fast compartment; CL_S: intercompartment clearance between central and slow compartment; MAT: mean input time; NV: the coefficient of variation of the inverse gaussian density function; T_{max-rate}: the time at which the input rate reached its maximum value.

LIST OF FIGURES

Figure 1. Schematic presentation of the proposed pharmacokinetic model.

Figure 2. Individual dose-normalized doxacurium, vecuronium, atracurium and succinylcholine plasma concentrations versus time curves in anesthetized patients.

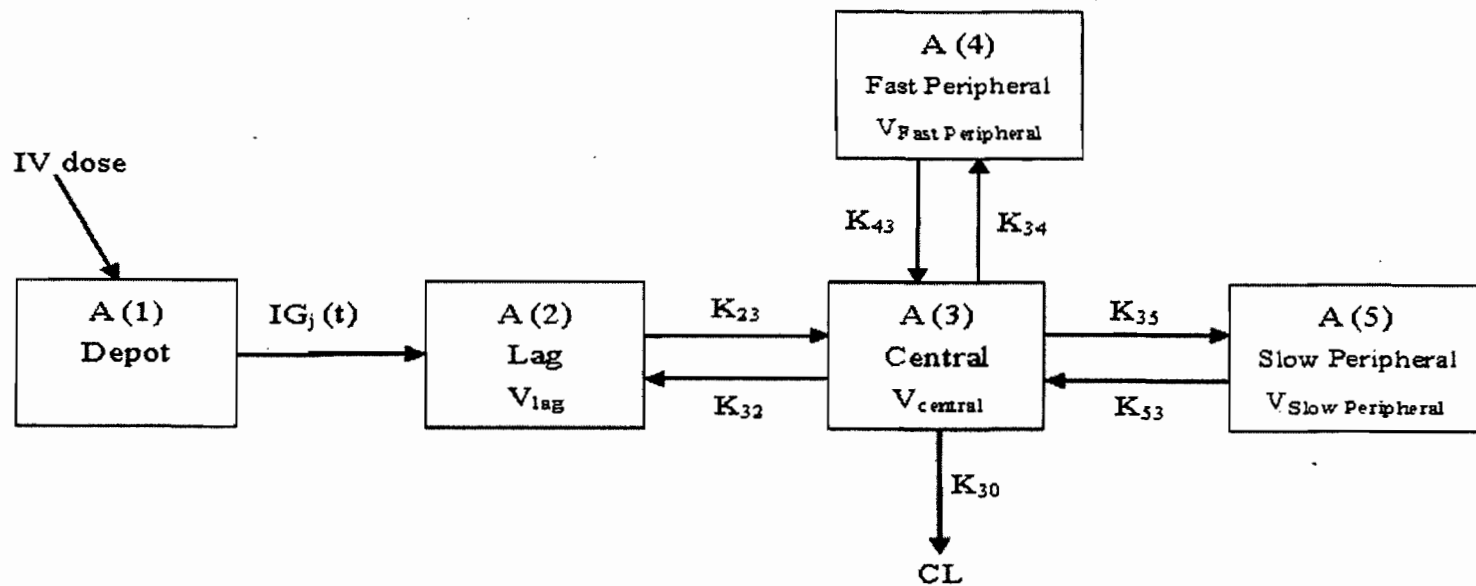
Figure 3. Individual predicted (solid line) and observed (closed circle) dose-normalized doxacurium (A), vecuronium (B), atracurium (C) and succinylcholine (D) plasma concentrations versus time curves in anesthetized patients. Inserts represent their respective plasma concentration-time curves for 2 min.

Figure 4. Predicted (solid line) and observed (closed circle) mean dose-normalized doxacurium (A), vecuronium (B), atracurium (C) and succinylcholine (D) plasma concentrations versus time curves in anesthetized patients. Inserts represent their respective weighted residuals versus time plots.

Figure 5. Predicted (solid line) and observed (closed circle) individual dose-normalized succinylcholine plasma concentrations versus time curves in anesthetized patients using single (A) or two (B) IG density functions.

Figure 6. Simulated (solid line) and observed (closed circle) midazolam dose-normalized plasma concentration versus time curves obtained in two patients using mean NMBAs parameters (A and B) or optimized values (C and D) for the IG input function.

Figure 1



IV, intravenous; V_{lag} , volume of distribution for the hypothetical lag compartment; $V_{central}$, volume of distribution for the central compartment; $V_{peripheral}$, volume of distribution for the peripheral compartment; CL, total clearance from the central compartment; K_{xy} , transfer rate constants from compartment x to compartment y.

Figure 2

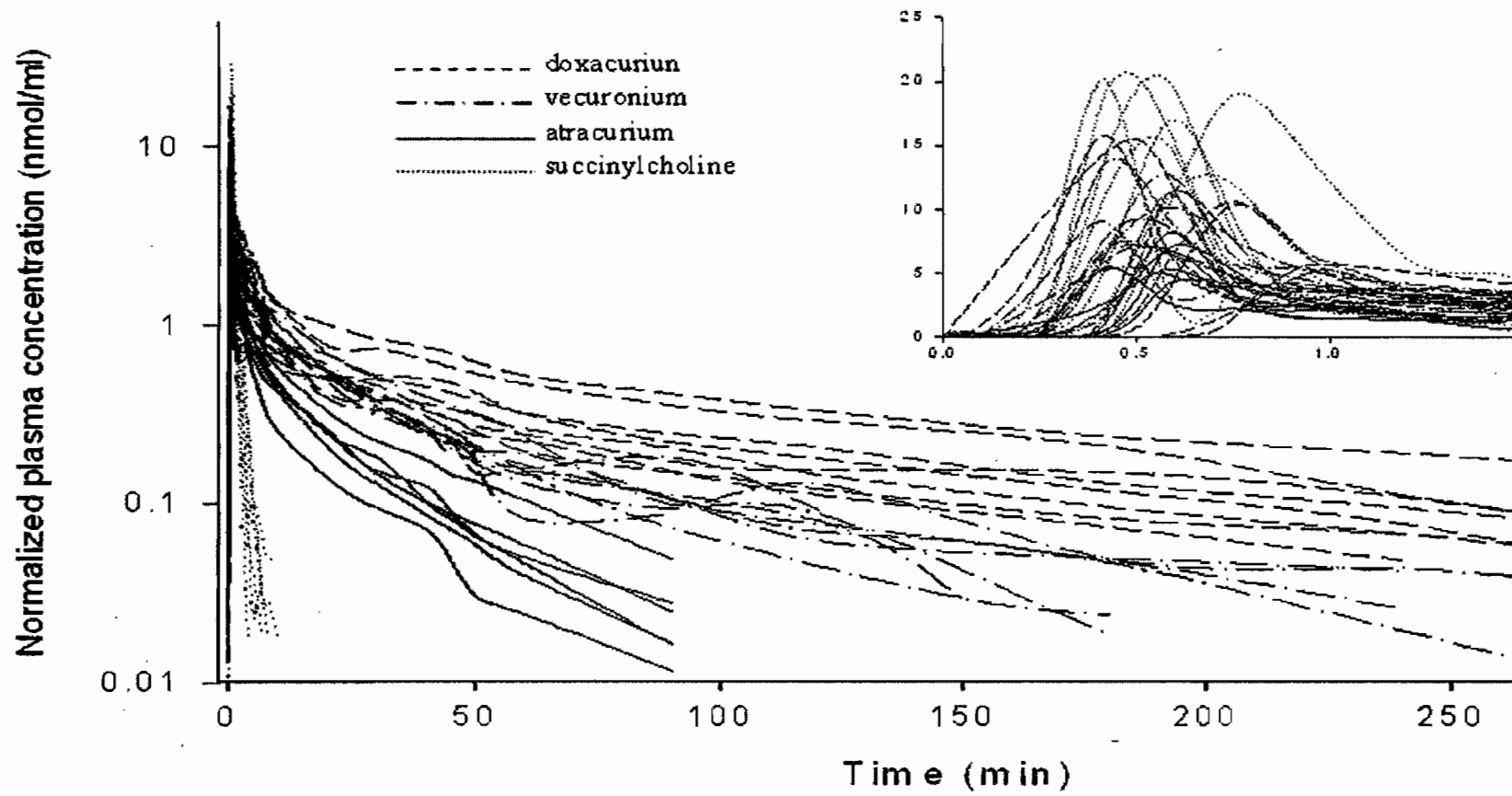


Figure 3

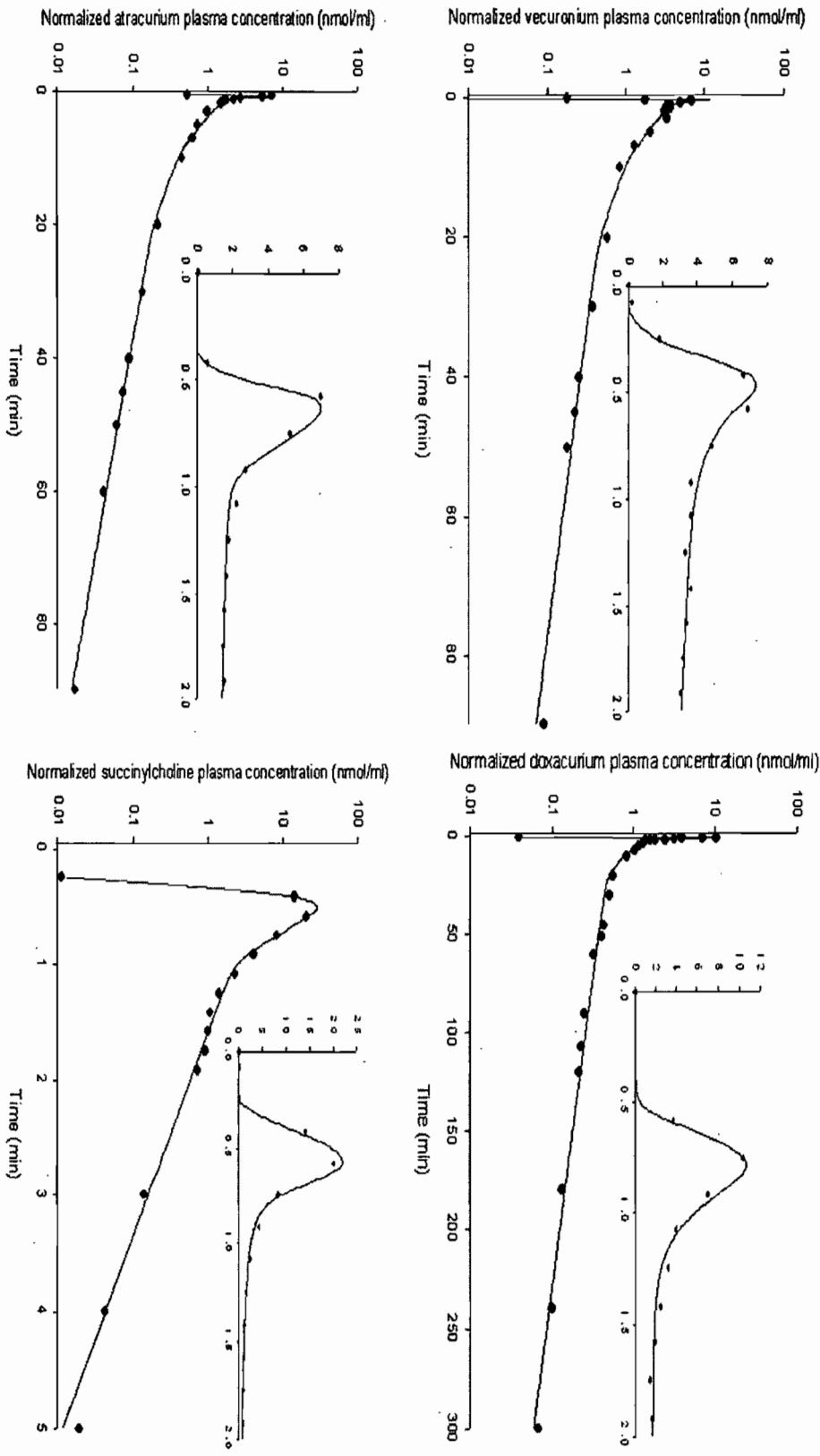


Figure 4

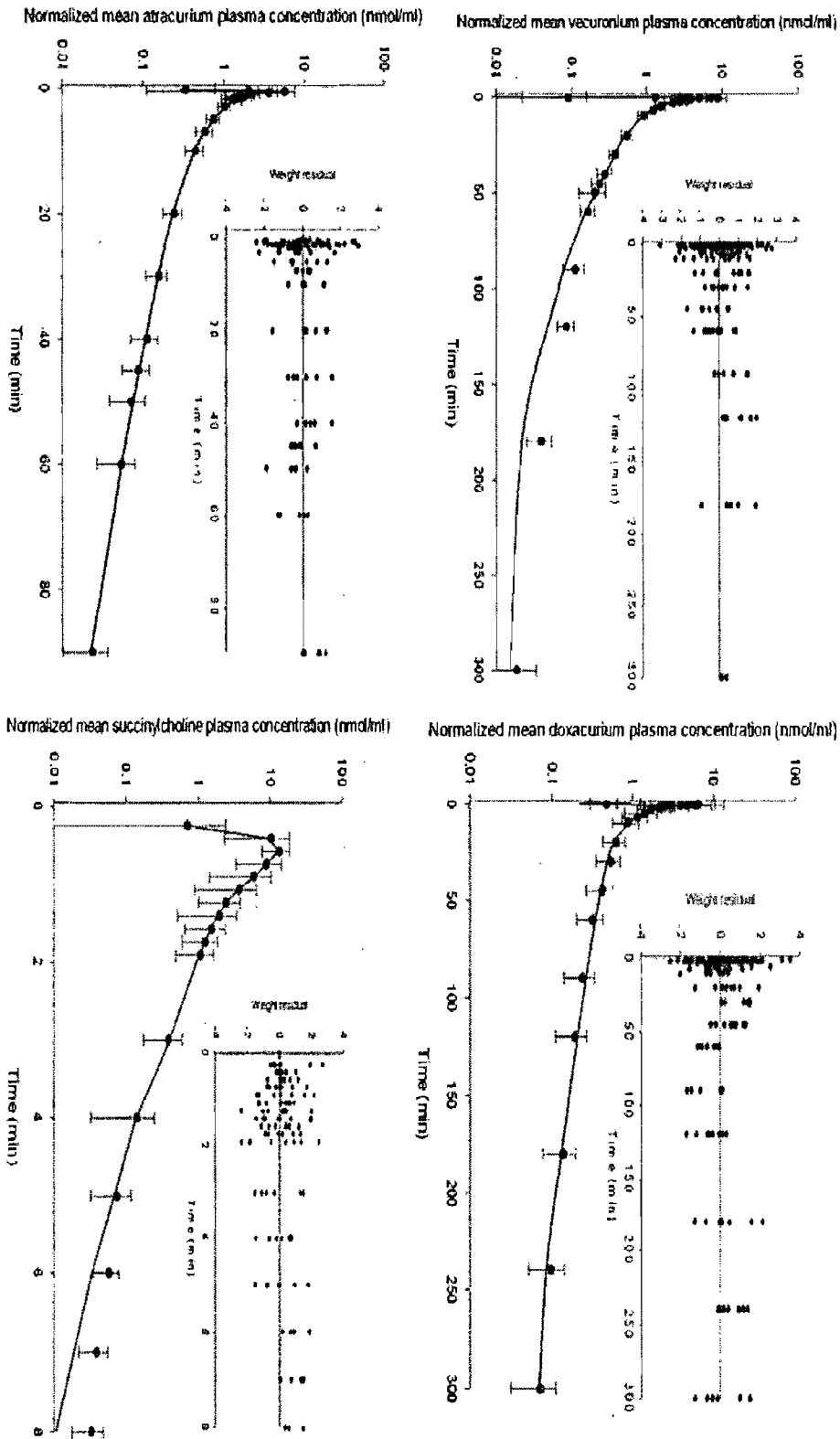


Figure 5

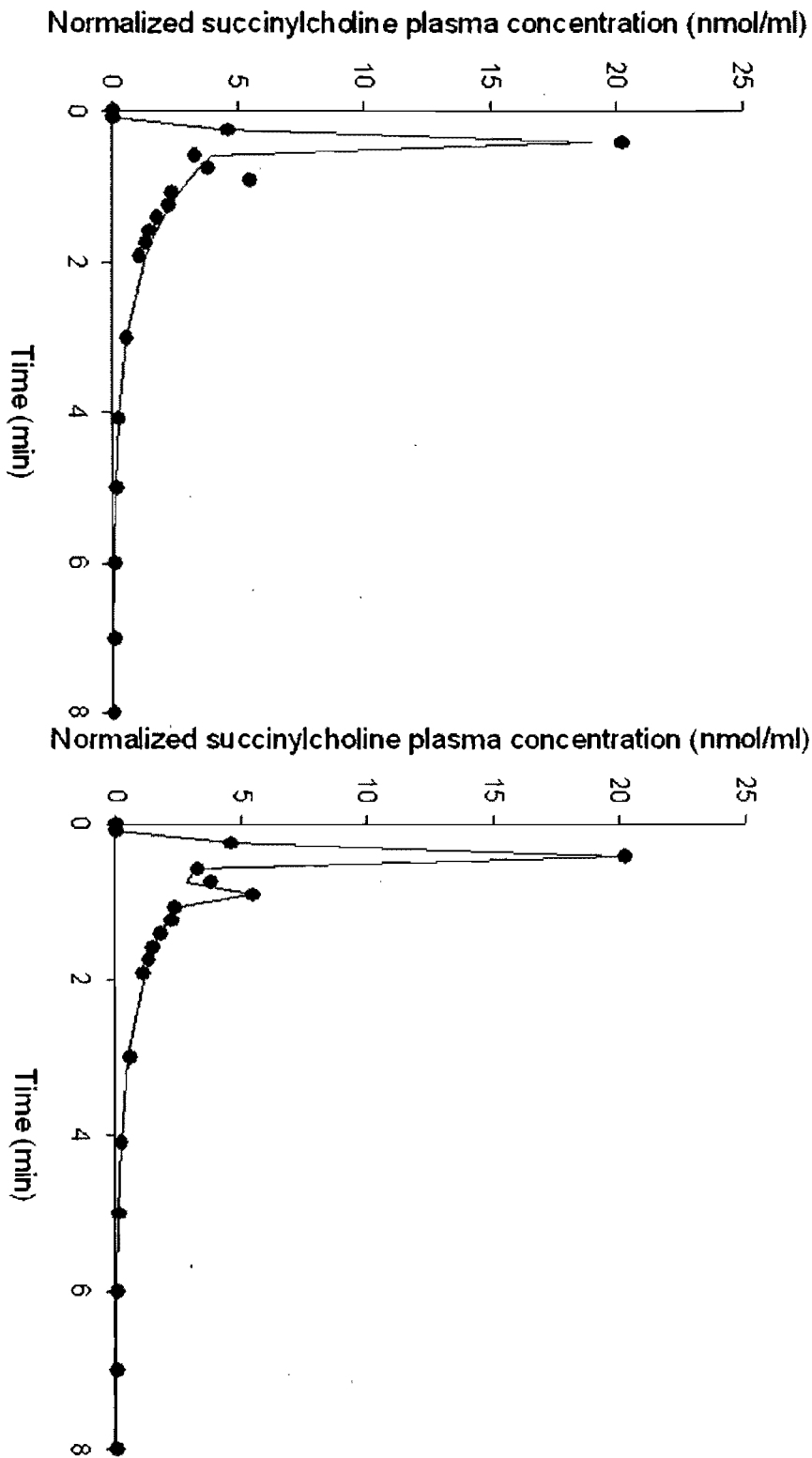
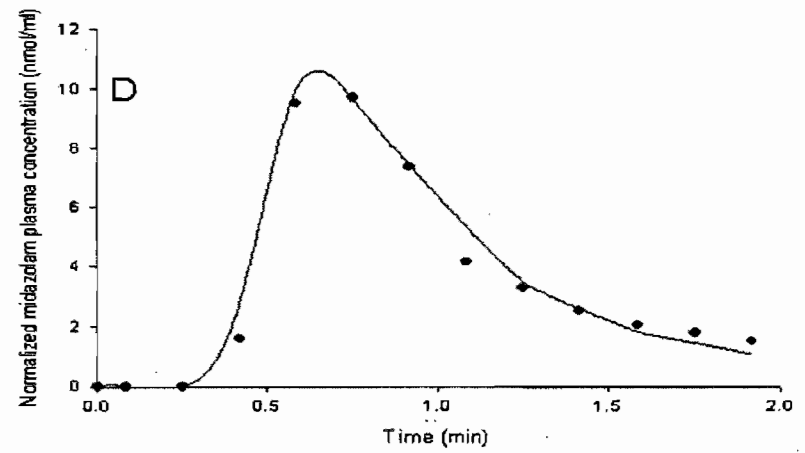
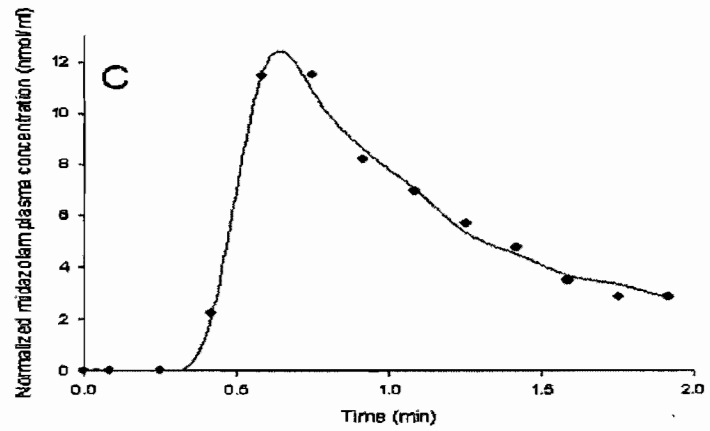
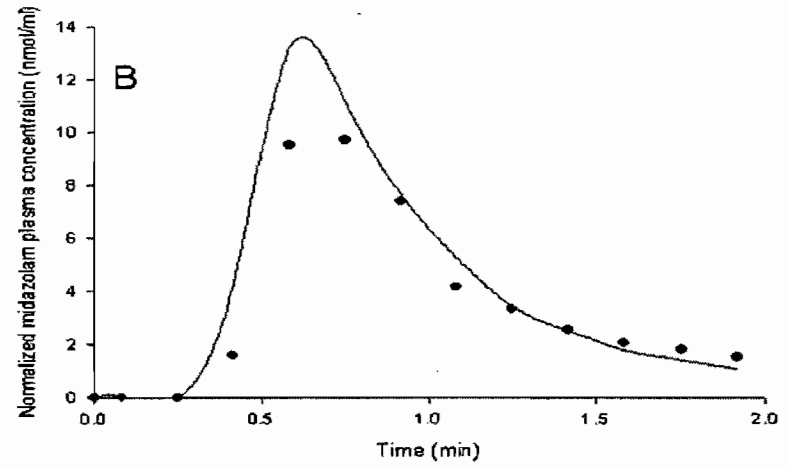
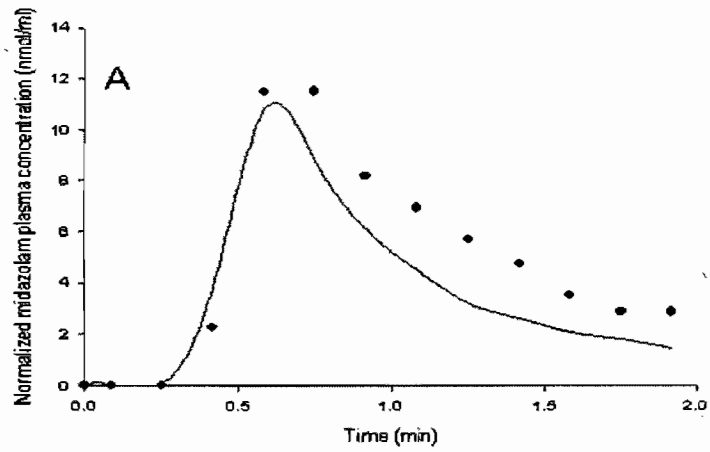


Figure 6



10. Discussion

10.1 Dose-dependency of PK/PD parameters after intravenous bolus doses of cisatracurium

It is well recognized that methodological issues such as the sampling schedule during the intravascular mixing phase have a significant impact on the estimation of PK as well as PK/PD parameters.(Beaufort et al. 1999; Ducharme et al. 1993; Lacroix et al. 1997) This project was intended to validate previous controversial findings of a dose-related change in the PK/PD parameters of cisatracurium, as reported in patients by Bergeron et al.(Bergeron et al. 2001) Indeed, some authors argued that a systemic error in the recording of twitch data might have impacted on the accuracy of PK/PD parameters estimation.(Paul and Fisher 2002) Using simulations, Paul et al. showed that estimated EC_{50} resulting from a systematic shift of pharmacodynamic data of -6, -3, +3, and +6 s vary more after a higher dose (300 ug/kg) than after a low dose (75 ug/kg). Similarly, shifting the time base of the pharmacodynamic data by ± 6 s affected k_{e0} more with the large dose than with the small dose. In contrast to Bergeron et al's study. (Bergeron et al. 2001) where plasma concentrations were not determined during the intravascular mixing phase, the latter was characterized during the protocol conducted in anesthetized dogs and experimental conditions were rigorously controlled to avoid any systematic bias. Regarding the importance of the exact timing of blood samples, all our attention was focused on ensuring that samples were drawn exactly on time. There were four persons involved in the collection of data and each of them had its own role. After proper stabilization, dose was administered in the middle of a 12s TOF interval. Thereafter, the

response was recorded automatically by the mechanograph without intervention of the investigators. All procedures were carried out exactly the same way for both doses.

In our initial data analysis, we used a two-stage approach in which the values for each animal and each occasion were determined independently. The Sigmoid Emax model was used since our primary objective was to confirm a dose-dependency using the most commonly used model for PK/PD analysis of NMBAs. Nonlinear mixed effect modeling based on this traditional compartmental approach was also used in the past to analyze dose-ranging data during the clinical development of cisatracurium.(Schmith et al. 1997) This was another reason for choosing this descriptive model.

The limitation of the two-stage approach is that it does not account for the standard errors of the individual parameter estimates. However, these point estimates are associated with standard errors and might, in fact, not differ statistically. There were two approaches that could have been used to solve this issue. First, using a Bayesian approach, we could have analyzed the two periods simultaneously twice - once assuming identical k_{e0} values for the two occasions, the other time allowing different k_{e0} values. If a statistically significant improvement in the objective function was shown with the additional parameter, the issue would be addressed. The second approach would have been a likelihood profile. Having determined the point estimates, we would have fixed k_{e0} to a range of values, and then determined the true confidence range based on the change in the objective function. However, this probably would have worked only if the loss function is indeed likelihood. Of these two approaches, the former method was preferred because it allows a true assessment, in a step-wise manner, of what

combination of parameters is actually affected by dose - k_{e0} , $k_{e0} + EC_{50}$, or $k_{e0} + EC_{50} +$

There was another issue that we wanted to verify with the animal experiment: can the input function be responsible of the dose-dependency. For this purpose, we reproduced Bergeron et al's experimental design where the front-end kinetics of cisatracurium was not characterized (first blood sample drawn at 1 min). Thus, we started the datasets for the parametric analysis 6 or 12 sec after peak plasma concentrations. (Results are shown in Appendix I). To verify whether a bias was indeed introduced by the input function (instantaneous) of the parametric PK model, cisatracurium PK/PD modeling was compared to results obtained using nonparametric analysis of the full data set based on Unadkat'al. (Unadkat et al. 1986) Such a method was previously validated for bolus doses of vecuronium and atracurium. (Ducharme et al. 1993; Ducharme. et al. 1995) For the nonparametric analysis, mean EC_{50} values increased and mean k_{e0} values decreased by almost 50% after the high bolus dose. A similar but less pronounced trend was observed with the parametric analysis. Therefore, mean dose-related changes in EC_{50} and k_{e0} are found using both empirical modeling approaches.

Thus, the input function does not appear to be responsible for the dose-dependency. However, a potential modeling misspecification cannot be excluded. Indeed, when using Sheiner's effect compartment model,(Sheiner et al. 1979) we usually assume a first order diffusion coefficient between the central and effect compartment. This might not always be true, in particular after a very high bolus dose. A distorsion in the equilibrium

between the effect and central compartment concentrations could result if the mass transfer via diffusion becomes saturable or hindered then the diffusion coefficient may vary with concentration. In this case, diffusion processes (and saturation) should be considered using a concentration-dependent diffusion coefficient during mathematical modeling.

As mentioned previously, our study was not designed to be mechanistic. However, during preparation of this manuscript, we considered two mechanistic models despite the fact that they required too many assumptions. The mechanism underlying the first model, the unbound receptor model (URM), is receptor occupancy. (De Haes et al. 2003) Using this model, PK/PD parameters of another NMBA (rocuronium) were quite similar to those derived with Sheiner's model, the approach we used for cisatracurium. Therefore, we did not investigate further with this approach. The second model, the R_{tot} model published by Donati and Meistelman (Donati and Meistelman 1991), is characterized by a finite number of receptors in the effect compartment. Our laboratory previously used this type of mechanistic model to provide an explanation for the difference between the PK/PD parameters derived during onset and recovery after a therapeutic dose of vecuronium, a potent drug. (Ducharme. et al. 1994) Compared to Sheiner's model, the k_{e0} value derived with the R_{tot} model will be faster only if the drug is potent. This mechanistic model highly depends on the potency of the drug (thus the administered dose). Assuming a finite number of receptors would predict a faster k_{e0} after a therapeutic dose of cisatracurium (0.075 mg/kg) but would have no impact on k_{e0} after the high bolus dose (0.3 mg/kg). When compared to Sheiner's model, the gap

between k_{e0} values for the high and low doses for cisatracurium would even be larger with the R_{tot} model.

In conclusion, our findings clearly indicate that PK/PD data obtained after i.v. bolus doses that are beyond those used in clinical practice should be tested for linearity of PK/PD estimates before including them in the general model. These results bear important clinical implication as an accurate estimate of the EC_{50} is desirable for target-controlled infusion systems. Also potency is an important parameter during the drug development because it can be scaled from animal models to human and can be used to discriminate between compounds, saving considerable time and money. Further studies on the rate of transfer into the interstitial fluid may provide valuable insight into mechanisms responsible for the dose-dependency. Although, it is not certain that these studies would translate changes observed at the NMBA receptor level.

10.2 Pharmacokinetics of cisatracurium in anesthetized dogs: In vitro-In vivo correlations

This study was conducted to describe the pharmacokinetics of cisatracurium in anesthetized dogs and determine whether its in vitro degradation rate in plasma is predictive of its in vivo elimination rate, as this proved to be the case in humans.

In 1986, Fisher proposed a pharmacokinetic model which includes elimination from both central and peripheral compartments.(Fisher et al. 1986) In this model, the $k_{in\ vitro}$ rate determined after incubation is substituted for $K_{non\ organ}$; the latter is thus assumed to

be the same in both central and peripheral compartments. However, elimination from the peripheral compartment might differ from that in plasma. In an effort to delineate the potential effect of peripheral elimination on PK parameter estimation, an explanatory model(Laurin et al. 1999) was applied to data previously gathered for a series of model drugs, e.g. mivacurium isomers (cis-cis, cis-trans and trans-trans), atracurium and doxacurium (as a negative control). When the relative importance of peripheral elimination was varied arbitrarily from 0 (no peripheral elimination) to 1000 (negligible central elimination), the rate of transfer from the central compartment was increased resulting in a higher V_{dss} . Indeed, although the physiological processes that determine drug distribution and those affecting peripheral elimination are independent, the two are mathematically tied together in the two-compartment model with both central and peripheral elimination.

Two specific applications were discussed. In the first one, k_{20} is fixed to a predetermined $k_{in\ vitro}$ value obtained from plasma incubations, ideally from the same patient. In the second one, the primary assumption is that $k_{20} = \beta$ when empirical evidence has confirmed that the in vivo rate of elimination (β) is similar to $k_{in\ vitro}$ in the same patient. This proved to be the case for atracurium (unpublished data) and succinylcholine. (Roy et al. 2002)

These explanatory models clearly demonstrated that the choice of k_{20} value will have a direct impact on exit-site dependent parameter estimation and that the effect will be more pronounced for shorting-acting drugs such as succinylcholine and mivacurium's

active isomers. Even a slow rate of peripheral elimination could contribute significantly to the overall elimination of the NMBAs since the volume of the peripheral compartment is larger than that of the central compartment. Recently, our laboratory determined the $k_{in\ vitro}$ values for mivacurium's isomers in plasma from volunteers. For the active isomers, the $k_{in\ vitro}$ was almost twofold greater than the terminal elimination rate constant observed previously in other patients. In this case, the peripheral compartment would serve as a reservoir that delays overall elimination. (Laurin et al. 1999)

In dogs, cisatracurium *in vivo* elimination rate constant was almost twofold faster than its corresponding *in vitro* rate of degradation in plasma. Therefore, in contrast to humans, the $k_{in\ vitro}$ is not of predictive value for β when cisatracurium is administered in dogs. However, in our dogs, the impact of peripheral elimination on distributive equilibrium is still significant as it will result in a 25% increase in Cl_{12} and a 15 % increase in Vd_{ss} . Hence, our studies revealed large interspecies differences in the body disposition of cisatracurium between human and dogs. Scaling of human data to dogs was therefore undertaken to support potential mechanisms that would explain this relative increase in organ clearance.

First, we had to predict the unbound fraction of cisatracurium in dogs. The unbound fraction of cisatracurium (0.62) measured in humans (Barbato et al. 1997) was scaled to dogs (0.71) according to Equation 1 (Appendix II). This scaling approach was validated using data previously obtained for rocuronium. When scaling human data (Dragne et al.

2002) to dogs, the predicted unbound fraction (0.51) for rocuronium was similar to the median value (0.54) measured in a previous study.(Ezzine and Varin 2005)

Taking into account differences in GFR and unbound fraction in the scaling of human renal clearance (0.85 mL/min·kg) to dogs, the estimate of CL_R for cisatracurium was 2.16 mL/min·kg (Equation 2, Appendix II). This predicted renal clearance is quite close to the theoretical value of 2.84 mL/min·kg expected for a compound having an unbound fraction of 0.71 and that is neither reabsorbed nor actively secreted in the kidney. (Mahmood 2005)

Another potential contributing mechanism to the elimination of neuromuscular blocking agents is biliary excretion. (Appiah-Ankam 2004) There is a general agreement that the nonrenal clearance of cisatracurium (0.35 mL/min·kg) in humans is mostly due to biliary excretion. (Kisor et al. 1996) Biliary excretion was also documented in dogs, although not in a quantitative manner.(Dear et al. 1995) After applying a correction factor of 2.4 for bile flow (Mahmood 2005), the human value of CL_{NR} (0.35 mL/min·kg) was scaled to dogs (0.84 mL/min·kg). After adding the contribution of biliary excretion to that of renal clearance, the organ clearance would now totalize to 3.00 mL/min·kg. This estimation is quite similar to that obtained for dogs (2.92 mL/min·kg) after applying the one species-based scaling method described by Tang et al (Tang. et al. 2007)

Using these animal scaling methods, almost 50% of organ clearance in dogs remains unexplained. It is worth mentioning that, during interspecies scaling, the relative contribution of biliary excretion to the total body clearance of cisatracurium in dogs is

assumed equal to that in humans (7%). Also, because human data do not support the presence of renal secretion for cisatracurium, this potential mechanism was not taken into account in the scaling of human renal clearance to dogs. Renal secretion of quaternary ammoniums has been reported in other animal species (Rennick 1981) and its contribution remains a potential mechanism, in absence of urinary data for cisatracurium in our dogs. Overlooking these two mechanisms may explain why organ clearance was underestimated. However, the predictive error is less when we compare the predicted (7.68 mL/min•kg) and observed (10.80 mL/min•kg) values for total clearance in dogs. This estimate is acceptable since animal scaling of clearance is considered to be successful when the predictive error is 30 % or less. (Mahmood 2005)

10.3 Modeling of the intravascular mixing phase of neuromuscular blocking agents following intravenous bolus injection

In this paper, we developed a unified pharmacokinetic (PK) model that adequately fits the plasma concentrations of NMBAs data previously measured during the IVM phase of four NMBAs in anesthetized patients. Adequate fitting of the intravascular mixing phase proved to be quite a challenge.

The concentration-time profile of the IVM phase is similar, exception made of the time-scale, to that observed during oral absorption. Using compartmental modeling, oral absorption is often represented by a first-order absorption rate constant, k_a (per time unit). Inclusion of a lag-time is often needed to better describe the absorption process. Although the assumption of first-order absorption is satisfactory for many drugs, the

absorption of certain drugs is better described by assuming zero-order (constant rate) absorption. It became evident that none of the above absorption models allowed an adequate or appropriate description of the plasma concentration-time profiles during the IVM phase.

During preparation of this manuscript, different models were tested to provide an improved description of the data: Weibull function(s), non linear absorption, time dependent adsorption, gamma distribution. (Debord et al. 2001) or Erlang frequency distribution, which describes asymmetric S-shape absorption profiles, (Rousseau et al. 2004). However, these models gave poor fitting or unreasonable parameter estimates with large uncertainty.

Finally, the Inverse Gaussian (IG) density input function (Weiss 1996) combined with compartmental models was implemented in NONMEM VI for PK analysis of individual data sets. For carrying out the IVM phase, intensive sampling was collected during the first 2 minutes. Therefore the two-stage method was used to analyze the data set instead of using the population approach. The IG density absorption model has been used in many areas of pharmacokinetics. Zhang et al (Zhang et al. 2002) used the IG density function input model to describe the complex enfuvirtide absorption profiles following its subcutaneous administration in patients with HIV infection. Csajka et al. (Csajka et al. 2005) used a sum of IG density functions to characterize the absorption of hydromorphone and veralipride. This approach offers the advantage of being parametric and results can be directly related to the absorption process, that is, F , MAT_j , t_{maxj} , the mean absorption times or times of maximal input rate; the parameter CV can be related

to the dispersion of the shape of the concentration-time profile. This approach also offers a simpler and more easily interpretable implementation in a population context.

The capacity of each model parameter value to influence the predicted AUC₀₋₁ (first-pass. of vecuronium) was also tested. The mean model parameter values, obtained from individual fits, were separately varied as far as $\pm 50\%$. The sensitivity tests were based on the following normalized sensitivity coefficient:

$$R = \frac{(O_2 - O_1)/O_1}{(I_2 - I_1)/I_1} \quad \text{Equation 24}$$

Where I_1 is the default value of the parameter analyzed for sensitivity, I_2 its modified value and where O_1 is the predicted AUC₀₋₁ using default parameter values, O_2 its predicted value with the modified parameter values.

For vecuronium, MAT was the main parameters governing the AUC₀₋₁. The peripheral compartment parameters have little impact. The optimal sampling times (3 data points) that would adequately predict the IVM phase of NMBAs will be the object of further studies.

11. Conclusion

NMBAs have routinely been used as model drugs since the very beginning of PK/PD modeling. Pharmacometrics is now widely used during drug development to accelerate its process. Estimates of PK/PD parameters, usually obtained during phase II dose-ranging studies, should be as accurate as possible. Our results indicate that, after high bolus doses of NMBAs, classic compartmental models are not adequate because PK/PD parameters become dose-dependent. Therefore, PK/PD estimates should rather be obtained after doses given in clinical practice.

Anesthesiology relies on drugs having a rapid onset of effect (1-2 min), in contrast to most therapeutic classes where focus is primarily on duration of action. Often, onset of effect of intravenous anesthetics happens before the IVM phase is completed. This peculiarity is a problem when one attempts PK/PD modeling of these drugs. The instantaneous input assumed in classic mammillary models is an obvious misspecification with respect to the first 2 min after an intravenous bolus dose of NMBAs. Development of an IG model proved to solve this issue. In our opinion, this may prove to be a major contribution in this field.

For NMBAs undergoing nonorgan-based elimination, *in vitro* studies are often carried out to provide an estimate of the *in vivo* elimination rate occurring in either the central and peripheral compartment. Our results have shown that a PK model may be appropriate in humans but not in another animal specie and emphasize the limits of animal scaling in absence of experimental data.

The work presented in this thesis thus bring to light the need to develop new PK/PD approaches that are closer to the physiological reality, thereby helping the clinician in understanding and predicting the response to anesthetic drugs.

Reference

- Evers, A. S. and Mervyn. M. (2004). Anesthetic Pharmacology: Physiologic Principles and Clinical Practice, hurchill Livingstone, Philadelphia.
- Aitkenhead, A. R., Smith, G., Rowbotham, D.J. (2007). "TEXTbook of Anaesthesia. Fifth edition."
- Avram, M. J., Krejcie T.C., Niemann, C. U., Klein, C., Gentry, W. B., Shanks C. A and Henthorn, T.K. (1997). "The effect of halothane on the recirculatory pharmacokinetics of physiologic markers [see comments]." Anesthesiology **87**(6): 1381-1393.
- Barbato, F., La Rotonda, M. I. and Quaglia, F. (1997). "Interactions of nonsteroidal antiinflammatory drugs with phospholipids: comparison between octanol/buffer partition coefficients and chromatographic indexes on immobilized artificial membranes." J Pharm Sci **86**(2): 225-9.
- Beal, S., Sheiner, L.B. (1992). "NONMEM User's Guide. NONMEM Project Group, UCSF San Francisco."
- Beaufort, T. M., Proost, J. H., Houwertjes, M. C., Roggeveld J.,and Wierda , J. M. (1999). "The pulmonary first-pass uptake of five nondepolarizing muscle relaxants in the pig." Anesthesiology **90**(2): 477-483.
- Beaufort, T. M., Proost, J. H., Kuizenga, K., Houwertjes, M. C., Kleef U. W.and Wierda J. M. (1999). "Do plasma concentrations obtained from early arterial blood sampling improve pharmacokinetic/pharmacodynamic modeling?" J Pharmacokinet Biopharm **27**(2): 173-90.
- Belmont, M. R., Lien, C. A., Quessy, S., Abou-Donia, M. M., Abalos, A., Eppich L. and Savarese J. J. (1995). "The clinical neuromuscular pharmacology of 51W89 in patients receiving nitrous oxide/opioid/barbiturate anesthesia." Anesthesiology **82**(5): 1139-45.
- Bergeron, L., Bevan, D. R., Berrill, A., Kahwaji,R.and Varin, F. (2001). "Concentration-effect relationship of cisatracurium at three different dose levels in the anesthetized patient." Anesthesiology **95**(2): 314-23.
- Bevan, D.R, Bevan, J.C and Donati, F (1988). "Muscle Relaxants in Clinical Anesthesia. Chicago, London, Boca Raton: Year Book Medical Publishers, Inc."
- Bevan, J. C., Donati, F. and Bevan, D. R. (1985). "Attempted acceleration of the onset of action of pancuronium. Effects of divided doses in infants and children." Br J Anaesth **57**(12): 1204-8.
- Bissinger, U. and Nigrovic, V. (1997). "Simulation of the onset of neuromuscular block based on the early oscillations in the arterial plasma concentrations." Eur J Clin Pharmacol **52**(1): 71-5.
- Bluestein, L. S., L. W. Stinson, Jr., Lennon, R. L., Quessy, S. N. and Wilson, R. M. (1996). "Evaluation of cisatracurium, a new neuromuscular blocking agent, for tracheal intubation." Can J Anaesth **43**(9): 925-31.
- Bonate, P. (2005). Pharmacokinetic-Pharmacodynamic Modeling and Simulation, Springer.
- Booij., L. (1997). "Neuromuscular transmission and its pharmacological blockade. Part 1: Neuromuscular transmission and general aspects of its blockade." Pharm World Sci. **19**(1): 1-12.

- Bowman, W. C. (1980). "Prejunctional and postjunctional cholinergic receptors at the neuromuscular junction." Anesth Analg **59**(12): 935-43.
- Bowman, W. C., Rodger, I. W., Houston, J., Marshall, R. J. and McIndewar, I. (1988). "Structure:action relationships among some desacetoxylated analogues of pancuronium and vecuronium in the anesthetized cat." Anesthesiology **69**(1): 57-62.
- Boxenbaum, H. (1982). "Interspecies scaling, allometry, physiological time, and the ground plan of pharmacokinetics." J Pharmacokinet Biopharm **10**(2): 201-27.
- Boyd, A. H., Eastwood, N. B., Parker, C. J. and Hunter J. M. (1996). "Comparison of the pharmacodynamics and pharmacokinetics of an infusion of cis-atracurium (51W89) or atracurium in critically ill patients undergoing mechanical ventilation in an intensive therapy unit." Br J Anaesth **76**(3): 382-8.
- Buzello, W., Noeldge, G., Krieg, N., and Brobmann, G. F.(1986). "Vecuronium for muscle relaxation in patients with myasthenia gravis." Anesthesiology **64**(4): 507-9.
- Ceccarelli, B. and Hurlbut, W. P. (1980). "Vesicle hypothesis of the release of quanta of acetylcholine." Physiol Rev **60**(2): 396-441.
- Chiou, W. L. (1989). "The phenomenon and rationale of marked dependence of drug concentration on blood sampling site. Implications in pharmacokinetics, pharmacodynamics, toxicology and therapeutics (Part I)." Clin Pharmacokinet **17**(3): 175-199.
- Cohen, E., Paulson, W. and Elbert, B. (1957). "Studies of d-Tubocurarine with measurements of concentration in human blood." Anesthesiology **18**(2): 300-309.
- Csajka, C., Drover, D. and Verotta, D. (2005). "The use of a sum of inverse Gaussian functions to describe the absorption profile of drugs exhibiting complex absorption." Pharm Res **22**(8): 1227-35.
- Cutler, D. J. (1979). "A linear recirculation model for drug disposition." J Pharmacokinet Biopharm **7**(1): 101-116.
- David, E., Longnecker and Frank, L., Murphy (1997). Introduction to Anesthesia. Philadelphia, Pennsylvania, W.B.Saunders Company.
- Davidian, M. and Gallant, A. R. (1992). "Smooth nonparametric maximum likelihood estimation for population pharmacokinetics, with application to quinidine." J Pharmacokinet Biopharm **20**(5): 529-56.
- De Haes, A., Proost, J. H., De Baets, M. H., Stassen, M. H., Houwertjes, M. C. and Wierda, J.M (2003). "Pharmacokinetic-pharmacodynamic modeling of rocuronium in case of a decreased number of acetylcholine receptors: a study in myasthenic pigs." Anesthesiology **98**(1): 133-42.
- De Haes, A., Proost, J. H., Kuks, J. B., van den Tol, D. C. and Wierda, J. M. (2002). "Pharmacokinetic/pharmacodynamic modeling of rocuronium in myasthenic patients is improved by taking into account the number of unbound acetylcholine receptors." Anesth Analg **95**(3): 588-96, table of contents.
- De Wolf, A. M., Freeman, J. A., Scott, V. L., Tullock, W., Smith, D. A., Kisor, D. F., Kerls, S. and Cook, D. R. (1996). "Pharmacokinetics and pharmacodynamics of cisatracurium in patients with end-stage liver disease undergoing liver transplantation." Br J Anaesth **76**(5): 624-8.

- Dear, G. J., Harrelson, J. C., Jones, A. E., Johnson, T. E. and Pleasance, S. (1995). "Identification of urinary and biliary conjugated metabolites of the neuromuscular blocker 51W89 by liquid chromatography/mass spectrometry." Rapid Commun Mass Spectrom **9**(14): 1457-64.
- Debord, J., Risco, E., Harel, M., Le Meur, Y., Buchler, M., Lachatre, G., Le Guellec, C. and Marquet, P.(2001). "Application of a gamma model of absorption to oral cyclosporin." Clin Pharmacokinet **40**(5): 375-82.
- Donati, F. and Meistelman, C.(1991). "A kinetic-dynamic model to explain the relationship between high potency and slow onset time for neuromuscular blocking drugs." J Pharmacokinet Biopharm **19**(5): 537-52.
- Donati, F., Meistelman, C. and Plaud, B. (1990). "Vecuronium neuromuscular blockade at the diaphragm, the orbicularis oculi, and adductor pollicis muscles." Anesthesiology **73**(5): 870-5.
- Donati, F., Varin, F., Ducharme, J., Gill, S. S., Theoret, Y. and Bevan, D. R. (1991). "Pharmacokinetics and pharmacodynamics of atracurium obtained with arterial and venous blood samples." Clin Pharmacol Ther **49**(5): 515-522.
- Dragne, A., Varin, F., Plaud, B. and Donati, F. (2002). "Rocuronium pharmacokinetic-pharmacodynamic relationship under stable propofol or isoflurane anesthesia." Can J Anaesth **49**(4): 353-60.
- Ducharme, J., Varin, F., Bevan, D. R. and Donati F. (1993). "Importance of early blood sampling on vecuronium pharmacokinetic and pharmacodynamic parameters." Clin Pharmacokinet **24**(6): 507-18.
- Ducharme., J., Varin, F. and Donati., F. (1994). "Vecuronium pharmacokinetics-pharmacodynamics modeling with and without a receptor concentration in the effect compartment in anaesthetised patient." Drug investigation **7**(2): 74-83.
- Ducharme., J., Varin, F. and Donati, F. (1995). "Pharmacokinetics and pharmacodynamics of a second dose of atracurium in anaesthetised patients." Clin Drug Invest **9**: 95-110.
- Renkin, E. M. and Gilmore., J. P. (1973.). Glomerular filtration. In "Handbook of Physiology-Renal Physiology" (J. Orlogg and R. W. Berliner, eds.),chap. 9, pp. 185-248., Williams & Wilkins, Baltimore, MD. .
- Eastwood, N. B., Boyd, A. H., Parker, C. J. and Hunter, J. M.(1995). "Pharmacokinetics of 1R-cis 1'R-cis atracurium besylate (51W89) and plasma laudanosine concentrations in health and chronic renal failure." Br J Anaesth **75**(4): 431-5.
- Engbaek, J. and Roed, J. (1992). "Differential effect of pancuronium at the adductor pollicis, the first dorsal interosseous and the hypothenar muscles. An electromyographic and mechanomyographic dose-response study." Acta Anaesthesiol Scand **36**(7): 664-9.
- Ezzine, S. and Varin, F. (2005). "Interstitial muscle concentrations of rocuronium under steady-state conditions in anaesthetized dogs: actual versus predicted values." Br J Anaesth **94**(1): 49-56.
- Fahey, M. R., Rupp, S. M., Fisher, D. M., Miller, R. D., Sharma, M., Canfell, C., Castagnoli, K. and Hennis, P. J. (1984). "The pharmacokinetics and pharmacodynamics of atracurium in patients with and without renal failure." Anesthesiology **61**(6): 699-702.

- Feng MR, Lou, X., Brown, R.R. and Hutchaleelaha, A. (2000). "Allometric pharmacokinetic scaling: towards the prediction of human oral pharmacokinetics." Pharm Res **17**: 410-418.
- Fisher, D. M., Canfell, P. C., Fahey, M. R., Rosen, J. I., Rupp, S. M., Sheiner, L. B. and Miller, R. D. (1986). "Elimination of atracurium in humans: contribution of Hofmann elimination and ester hydrolysis versus organ-based elimination." Anesthesiology **65**(1): 6-12.
- Fuseau, E. and Sheiner, L. B. (1984). "Simultaneous modeling of pharmacokinetics and pharmacodynamics with a nonparametric pharmacodynamic model." Clin Pharmacol Ther **35**(6): 733-41.
- Gambus, P. L. and Troconiz, I. F. (2001). "Pharmacokinetic-pharmacodynamic modeling in anesthesia." International Congress Series **1220**: 89-97.
- Garipey, L. P., Varin, F., Donati, F., Salib, Y. and Bevan, D. R. (1993). "Influence of aging on the pharmacokinetics and pharmacodynamics of doxacurium." Clin Pharmacol Ther **53**(3): 340-7.
- Guy, H. R. (1984). "A structure model of the acetylcholine receptor channel based on partition energy and helix packing calculations." Biophysical Journal **45**: 249-261.
- Harper, N. J., Bradshaw, E. G. and Healy, T. E. (1986). "Evoked electromyographic and mechanical responses of the adductor pollicis compared during the onset of neuromuscular blockade by atracurium or alcuronium, and during antagonism by neostigmine." Br J Anaesth **58**(11): 1278-84.
- Harper, N. J., Martlew, R., Strang, T. and Wallace, M. (1994). "Monitoring neuromuscular block by acceleromyography: comparison of the Mini-Accelograph with the Myograph 2000." Br J Anaesth **72**(4): 411-4.
- Harrison, G. A. and Junius, F. (1972). "The effect of circulation time on the neuromuscular action of suxamethonium." Anaesth Intensive Care **1**(1): 33-40.
- Hayes, A.W. (2001). Principles and Methods of Toxicology, Taylor and Francis. Philadelphia, PA. Reserve copy.
- Healy, T. E., Pugh, N. D., Kay, B., Sivalingam T. and Petts H. V. (1986). "Atracurium and vecuronium: effect of dose on the time of onset." Br J Anaesth **58**(6): 620-4.
- Hennis, P and Stanski, D.R. (1985). "Pharmacokinetic and Pharmacodynamic factors that govern the clinical use of muscle relaxants." Seminars in Anesthesia **4**(1): 21-30.
- Henthorn, T. K., Avram, M. J., Krejcie, T. C., Shanks, C. A., Asada, A. and Kaczynski, D. A. (1992). "Minimal compartmental model of circulatory mixing of indocyanine green." Am.J Physiol. **262**(3 Pt 2): H903-H910.
- Hoshi, K, Hashimoto, Y. and Matsukawa, S (1993). "Pharmacokinetics of succinylcholine in man." Tohoku J Exp Med **170**: 245-50.
- Hughes, B. W., Kusner, L. L. and Kaminski, H. J. (2006). "Molecular architecture of the neuromuscular junction." Muscle Nerve **33**(4): 445-61.
- Imbeault, K., Withington, D. E. and Varin, F. (2006). "Pharmacokinetics and pharmacodynamics of a 0.1 mg/kg dose of cisatracurium besylate in children during N2O/O2/propofol anesthesia." Anesth Analg **102**(3): 738-43.
- Ings, R. M. J. (1990). "Interspecies scaling and comparisons in drug development and toxicokinetics." Xenobiotica **20**: 1201-31.
- Jahn, R. and Sudhof, T. C. (1994). "Synaptic vesicles and exocytosis." Annu Rev Neurosci **17**: 219-46.

- Mahmood, I. and Balian, J.D. (1996b). "Interspecies scaling: predicting pharmacokinetic parameters of antiepileptic drugs in humans from animals with special emphasis on clearance." J Pharm Sci **85**: 411-414.
- Appiah-Ankam, J., Honorary Lecturer (2004). "Pharmacology of neuromuscular blocking drugs." Continuing Education in Anaesthesia Critical Care and Pain **4**: 2-7.
- Jonsson, E. N. and Karlsson, M. O. (1998). "Automated covariate model building within NONMEM." Pharm Res **15**(9): 1463-8.
- Karlsson, M. O., Beal, S. L. and Sheiner, L. B. (1995). "Three new residual error models for population PK/PD analyses." J Pharmacokinet Biopharm **23**(6): 651-72.
- Karlsson, M. O. and Sheiner, L. B. (1993). "The importance of modeling interoccasion variability in population pharmacokinetic analyses." J Pharmacokinet Biopharm **21**(6): 735-50.
- Katz, R. L. (1973). "Electromyographic and mechanical effects of suxamethonium and tubocurarine on twitch, tetanic and post-tetanic responses." Br J Anaesth **45**(8): 849-59.
- Kisor, D. F., Schmith, V. D., Wargin, W. A., Lien, C. A., Ornstein, E. and Cook, D. R. (1996). "Importance of the organ-independent elimination of cisatracurium." Anesth Analg **83**(5): 1065-71.
- Kistler, J., Stroud, R. and Klymkowsky, M.W. (1982). "Structure and function of an acetylcholine receptor." Biophysical Journal **37**: 371-383.
- Kopman, A. F. (1985). "The relationship of evoked electromyographic and mechanical responses following atracurium in humans." Anesthesiology **63**(2): 208-11.
- Krejcie, T. C., Avram, M. J., Brooks Gentry, W., Niemann, C. U., Janowski, M. P. and Henthorn, T. K. (1997). "A recirculatory model for the pulmonary uptake and pharmacokinetics of lidocaine based on analysis of arterial and mixed venous data from dogs." J Pharmacokinet Biopharm **25**(2): 169-190.
- Krejcie, T. C., Jacques, J. A., Avram, M. J., Niemann, C. U., Shanks, C. A. and Henthorn, T. K. (1996). "Use of parallel Erlang density functions to analyze first-pass pulmonary uptake of multiple indicators in dogs." J Pharmacokinet Biopharm **24**(6): 569-588.
- Lacroix, M., Donati, F. and Varin, F. (1997). "Pharmacokinetics of mivacurium isomers and their metabolites in healthy volunteers after intravenous bolus administration." Anesthesiology **86**(2): 322-30.
- Lafrance, P., Lemaire, V., Varin, F., Donati, F., Belair, J. and Nekka, F. (2002). "Spatial effects in modelling pharmacokinetics of rapid action drugs." Bulletin of mathematical biology.
- Laurin, J., Nekka, F., Donati, F. and Varin, F. (1999). "Assuming peripheral elimination: its impact on the estimation of pharmacokinetic parameters of muscle relaxants." J Pharmacokinet Biopharm **27**(5): 491-512.
- Lave, T., Coassolo, P., Ubeaud, G., Brandt, R., Schmitt, C., Dupin, S., Jaeck, D. and Chou, R.C. (1996). "Interspecies scaling of bosentan, a new endothelin receptor antagonist and integration of in vitro data into allometric scaling." Pharm Res **13**: 97-101.
- Lee, C. (1972). "Chemistry and pharmacology of polypeptide toxins in snake venoms." Annual Review of Pharmacology **12**: 265-286.

- Lepage, J.Y., Malinge J.M., Malinge, M, Cozian, A and Pinaud, M. (1994). "Comparison of equipotent doses of 51W89 and atracurium." Anesthesiology: 81: A1090 (abstract).
- Lien, C. A., Schmith, V. D., Belmont, M. R., Abalos, A., Kisor, D. F. and Savarese, J. J. (1996). "Pharmacokinetics of cisatracurium in patients receiving nitrous oxide/opioid/barbiturate anesthesia." Anesthesiology **84**(2): 300-8.
- Lin, J. H. (1995). "Species similarities and differences in pharmacokinetics." Drug Metab Dispos **23**(10): 1008-21.
- Mahmood, I. (2005). Interspecies Pharmacokinetic Scaling: Principles And Application of Allometric Scaling Pine House Publishers; 1st edition.
- Mahmood, I. (2005). "Interspecies scaling of biliary excreted drugs: a comparison of several methods." J Pharm Sci **94**(4): 883-92.
- Mahmood, I. and Balian, J. D. (1996). "Interspecies scaling: predicting clearance of drugs in humans. Three different approaches." Xenobiotica **26**(9): 887-95.
- Mallet, A. (1986). "A maximum likelihood estimation method for random coefficient regression models." Biometrika **73**: 645-656.
- Mastey, V., Donati, F. and Varin, F. (1995). "Early pharmacokinetics of Midazolam Sampling site and schedule considerations." Clin Drug Invest **9**(3): 131-140.
- Meriggioli, M. N., Howard, J. E. and Michel Harper, Jr. C. (2004). "Neuromuscular Junction Disorders: Diagnosis and Treatment. Marcel Dekker. Inc."
- Minto, C. F., Schnider, T. W., Gregg, K. M., Henthorn, T. K. and Shafer, S. L. (2003). "Using the time of maximum effect site concentration to combine pharmacokinetics and pharmacodynamics." Anesthesiology **99**(2): 324-33.
- Mishina M, Takai, T., Imoto, K, Noda, M, Takahashi, T, Numa, S, Methfessel, C. and Sakmann, B. (1986). "Molecular distinction between fetal and adult forms of muscle acetylcholine receptor." Nature. **321**: 406-11.
- Mordenti, J. (1986). "Man versus beast: pharmacokinetic scaling in mammals." J Pharm Sci **75**(11): 1028-40.
- Daniel, M.P. and Voge, Z. (1975). "Immunoperoxidase staining of alpha-bungarotoxin binding sites in muscle endplates shows distribution of acetylcholine receptors." Nature **254**: 339-341.
- Nakashima, E. and Benet, L. Z. (1988). "General treatment of mean residence time, clearance, and volume parameters in linear mammillary models with elimination from any compartment." J Pharmacokinet Biopharm **16**(5): 475-92.
- O'Neill, R. and Wetherill, G.B. (1971). "The Present State of Multiple Comparison Methods." Journal of the Royal Statistical Society. Series B (Methodological) **33**(2): 218-250.
- Ornstein, E., Lien, C. A., Matteo, R. S., Ostapkovich, N. D., Diaz, J. and Wolf, K. B. (1996). "Pharmacodynamics and pharmacokinetics of cisatracurium in geriatric surgical patients." Anesthesiology **84**(3): 520-5.
- Park, K., Verotta, D., Gupta, S. K. and Sheiner, L. B. (1998). "Use of a pharmacokinetic/pharmacodynamic model to design an optimal dose input profile." J Pharmacokinet Biopharm **26**(4): 471-92.
- Parke, J., Holford, N. H. and Charles, B. G. (1999). "A procedure for generating bootstrap samples for the validation of nonlinear mixed-effects population models." Comput Methods Programs Biomed **59**(1): 19-29.

- Parker, C. J. and Hunter, J. M. (1989). "Pharmacokinetics of atracurium and laudanosine in patients with hepatic cirrhosis." Br J Anaesth **62**(2): 177-83.
- Paton, W.D. and Waud, D.R. (1967). "The margin of safety of neuromuscular transmission." J Physiol **191**(1): 59-90.
- Paul, M. and Fisher, D. M. (2002). "Pharmacodynamic modeling of muscle relaxants: effect of design issues on results." Anesthesiology **96**(3): 711-7.
- Protti, D. A., Reisin, R., Mackinley, T. A. and Uchitel, O. D. (1996). "Calcium channel blockers and transmitter release at the normal human neuromuscular junction." Neurology **46**(5): 1391-6.
- Rakesh., N. and Keith, W. (2004). "A comprehensive analysis of the role of correction factors in the allometric predictivity of clearance from rat, dog, and monkey to humans." J Pharm Sci **93**: 2522-2534.
- Rakesh., N. and Keith, W. (2005). "Extrapolation of human pharmacokinetic parameters from rat, dog, and monkey data: molecular properties associated with extrapolative success or failure." J Pharm Sci **94**: 1467-1483.
- Rang, H. P., Dale, M.M., Ritter, J.M., and Moore, P.K. (2003). Pharmacology, Churchill Livingstone/Elsevier Science, Edinburgh.
- Rennick, B. R. (1981). "Renal tubule transport of organic cations." Am J Physiol Renal Physiol **240**: F83-F89.
- Rousseau, A., Leger, F., Le Meur, Y., Saint-Marcoux, F., Paintaud, G., Buchler, M. and Marquet, P. (2004). "Population pharmacokinetic modeling of oral cyclosporin using NONMEM: comparison of absorption pharmacokinetic models and design of a Bayesian estimator." Ther Drug Monit **26**(1): 23-30.
- Rowland, N. and Tozer, T. (1995). Clinical pharmacokinetics: Concepts and Applications, Baltimore, Williams & Wilkins.
- Roy, J. J., Donati, F., Boismenu, D. and Varin, F. (2002). "Concentration-effect relation of succinylcholine chloride during propofol anesthesia." Anesthesiology **97**(5): 1082-92.
- Rubin, D. (1996). "Multiple Imputation After 18+ Years." Journal of the american statistical association **96**: 473-489.
- Schmith, V. D., Fiedler-Kelly, J., Phillips, L. and Grasela, T. H. (1997). "Prospective use of population pharmacokinetics/pharmacodynamics in the development of cisatracurium." Pharm Res **14**(1): 91-7.
- Schmith, V.D, Phillips, L. and Kisor, D.F (1996). "Pharmacokinetics/pharmacodynamics of cisatracurium in healthy adult patients." Current Opinion in Anesthesiology **9** Suppl. 1: S9-15.
- Schnider, T. W. and Minto, C. F. (2001). "Predictors of onset and offset of drug effect." Eur J Anaesthesiol Suppl **23**: 26-31.
- Scott, R. P. and Goat, V. A. (1982). "Atracurium: its speed of onset. A comparison with suxamethonium." Br J Anaesth **54**(9): 909-11.
- Shafer, S. L., Varvel, J. R. and Gronert, G. A. (1989). "A comparison of parametric with semiparametric analysis of the concentration versus effect relationship of metocurine in dogs and pigs." J Pharmacokinet Biopharm **17**(3): 291-304.
- Sheiner, L.B. and Wakefield, J. (1999). "Population modelling in drug development." Stat Methods Med Res **8**(3): 183-93.

- Sheiner, L. B., Stanski, D. R., Vozech, S., Miller, R. D. and Ham, J. (1979). "Simultaneous modeling of pharmacokinetics and pharmacodynamics: application to d-tubocurarine." Clin Pharmacol Ther **25**(3): 358-71.
- Smith, C. E., Baxter, M., Bevan, J. C., Donati, F. and Bevan, D. R. (1987). "Accelerated onset and delayed recovery of d-tubocurarine blockade with pancuronium in infants and children." Can J Anaesth **34**(6): 555-9.
- Smith, C. E., Donati, F. and Bevan, D. R. (1988). "Dose-response curves for succinylcholine: single versus cumulative techniques." Anesthesiology **69**(3): 338-42.
- Smith, D. C. and Booth, J. V. (1994). "Influence of muscle temperature and forearm position on evoked electromyography in the hand." Br J Anaesth **72**(4): 407-10.
- Smith, R. L. (1971). Excretion of drugs in bile. In "Handbook of Experimental Pharmacology. Volume XXVIII: Concepts in Biochemical Pharmacology", pp. 354-389., Springer-Verlag, Berlin, Germany.
- Smith, R. L. (1973.). The Excretory Function of Bile: The Elimination of Drugs and Toxic Substances in Bile., Chapman and Hall, London, UK.
- Sorooshian, S. S., Stafford, M. A., Eastwood, N. B., Boyd, A. H., Hull, C. J. and Wright, P. M. (1996). "Pharmacokinetics and pharmacodynamics of cisatracurium in young and elderly adult patients." Anesthesiology **84**(5): 1083-91.
- Stanski, D. R., Ham, J., Miller, R. D. and Sheiner, L. B. (1979). "Pharmacokinetics and pharmacodynamics of d-tubocurarine during nitrous oxide-narcotic and halothane anesthesia in man." Anesthesiology **51**(3): 235-41.
- Stoelting, R. K. and Hillier, A. C. (2006). Pharmacology & Physiology in Anesthetic Practice. Philadelphia, PA 19106 USA, Lippincott Williams & Wilkins.
- Swen, J., Rashkovsky, O. M., Ket, J. M., Koot, H. W., Hermans, J. and Agoston, S. (1989). "Interaction between nondepolarizing neuromuscular blocking agents and inhalational anesthetics." Anesth Analg **69**(6): 752-755.
- Swerdlow, B. N. and Holley, F. O. (1987). "Intravenous anaesthetic agents. Pharmacokinetic-pharmacodynamic relationships." Clin Pharmacokinet **12**(2): 79-110.
- Szalados, J. E., Donati, F. and Bevan, D. R. (1990). "Effect of d-tubocurarine pretreatment on succinylcholine twitch augmentation and neuromuscular blockade." Anesth Analg **71**(1): 55-9.
- Tang, H. and Mayersohn, M. (2005). "A novel model for prediction of human drug clearance by allometric scaling." Drug Metab Dispos **33**(9): 1297-303.
- Tang, H., Hussain, A., Leal, M., Mayersohn, M. and Fluhler, E. (2007). "Interspecies Prediction of Human Drug Clearance Based on Scaling Data from One or Two Animal Species." Drug Metab Dispos **35**: 1886-1893.
- Tang, H. and Mayersohn, M. (2005a). "Accuracy of allometrically predicted pharmacokinetic parameters in humans: role of species selection." Drug Metab Dispos **33**: 1288-1293.
- Tucek, S. (1984). "Problems in the organization and control of acetylcholine synthesis in brain neurons." Prog. Biophys. Mol. Biol. **44**: 1-46.
- Tran, T.V., Fiset, P and Varin, F. (1998). "Pharmacokinetics and pharmacodynamics of cisatracurium after a short infusion in patients under propofol anesthesia." Anesthesia & Analgesia **87**: 1158-1163.

- Unadkat, J. D., Bartha, F. and Sheiner, L. B. (1986). "Simultaneous modeling of pharmacokinetics and pharmacodynamics with nonparametric kinetic and dynamic models." Clin Pharmacol Ther **40**(1): 86-93.
- Upton, R. N. (2004). "The two-compartment recirculatory pharmacokinetic model--an introduction to recirculatory pharmacokinetic concepts." Br J Anaesth **92**(4): 475-84.
- Vincent, A., Beeson, D. and Lang, B. (2000). "Molecular targets for autoimmune and genetic disorders of neuromuscular transmission." Eur J Biochem **267**(23): 6717-28.
- Vincent, A. and Wray D. (1992). " Neuromuscular transmission: basic and applied aspects. Pergammon Press, Oxford."
- Wade, J. R., Beal, S. L. and Sambol, N. C. (1994). "Interaction between structural, statistical, and covariate models in population pharmacokinetic analysis." J Pharmacokinet Biopharm **22**(2): 165-77.
- Weiss, M. (1997). "Errors in clearance estimation after bolus injection and arterial sampling: nonexistence of a central compartment." J Pharmacokinet Biopharm **25**(2): 255-260.
- Weiss, M. (1996). "A novel extravascular input function for the assessment of drug absorption in bioavailability studies." Pharm Res **13**(10): 1547-53.
- Welch, R. M., Brown, A., Ravitch, J. and Dahl, R. (1995). "The in vitro degradation of cisatracurium, the R, cis-R'-isomer of atracurium, in human and rat plasma." Clin Pharmacol Ther **58**(2): 132-42.
- Wierda, J.M., Proost, J.H., Muir, A.W. and Marshall, R.J. (1993). "Design of drugs of rapid onset." Anaesthetic Pharmacology Review. **1**: 57-68.
- Yamaoka, K., Nakagawa, T. and Uno, T. (1978). "Application of Akaike's Information Criterion (AIC) in the evaluation of linear pharmacokinetic equations. ." J Pharmacokinetics Biopharm **6**: 165-75
- Yano, Y., Beal, S. L. and Sheiner, L. B. (2001). "Evaluating pharmacokinetic/pharmacodynamic models using the posterior predictive check." J Pharmacokinet Pharmacodyn **28**(2): 171-92.
- Zhang, X., Nieforth, K., Lang, J. M., Rouzier-Panis, R., Reynès, J., Dorr, A., Kolis, S., Stiles, M. R., Kinchelov, T. and Patel, I. H. (2002). "Pharmacokinetics of plasma enfuvirtide after subcutaneous administration to patients with human immunodeficiency virus: Inverse Gaussian density absorption and 2-compartment disposition." Clin Pharmacol Ther **72**(1): 10-9.
- Zhu, Y., Audibert, G., Donati, F. and Varin, F. (1997). "Pharmacokinetic-pharmacodynamic modeling of doxacurium: effect of input rate." J Pharmacokinet Biopharm **25**(1): 23-37.

APPENDIX I

Table 1. Parametric PK/PD parameters in pentobarbital anaesthetized dogs after sequential administration of two doses of cisatracurium. EC₅₀: effect compartment concentration at 50% of maximal observed effect; T_{ECmax}: time required to reach EC_{max}; EC_{max}/D: dose-normalized maximum concentration in effect compartment; E_{max}: maximum block; k_{e0}: effect compartment equilibration rate constant; Gamma: slope factor. Parameters were normalized for a 0.1 mg kg⁻¹ dose. Dogs were randomized for sequence (n=8). Values represent mean ± SD. * P < 0.05

		0.15 mg kg ⁻¹	0.6 mg kg ⁻¹	P value
EC ₅₀	(ng ml ⁻¹)	219 ± 32	293 ± 63	0.003*
T _{ECmax}	(min)	5.39 ± 0.71	8.95 ± 1.24	<0.001*
EC _{max} /D	(ng ml ⁻¹)	0.0033 ± 0.0005	0.0024 ± 0.0004	0.011*
K _{e0}	(min ⁻¹)	0.1437 ± 0.0253	0.0756 ± 0.0099	<0.001*
Gamma		7.50 ± 4.34	8.67 ± 5.22	0.124

APPENDIX II

The unbound fraction in dogs was estimated as:

$$f_{u(dog)} = (f_{u(human)} \times V_{SS(dog)}) / V_{SS(human)} \quad (1) \text{ (Mahmood 2005)}$$

Renal clearance (CL_R) in dogs was estimated as:

$$CL_{R(dog)} = CL_{R(human)} \times (GFR_{(dog)} / GFR_{(human)}) \times (f_{u(dog)} / f_{u(human)}) \quad (2) \text{ (Mahmood 2005)}$$